Developing a fresh core neutronic model at 300K for a VVER-1000 reactor type using MCNP6

GP Nyalunga

25449753

Dissertation submitted in partial fulfilment of the requirements for the degree *Magister Scientiae in* Nuclear Engineering at the Potchefstroom Campus of the North-West University

Supervisor : Dr VV Naicker

Co-supervisor: Miss MH du Toit

May 2016

Declaration of Author

I, Gezekile Nyalunga, declare that the work provided in the following dissertation is my own work. I hereby confirm that where I have consulted the published work of others, this is always clearly acknowledged, and where I have quoted from the work of others, the source is always given.

_____

Gezekile Portia Nyalunga

Date: 13 November 2015

NWU - Potchefstroom

Abstract

A steady state neutronics model for a fresh core Voda Voda Energo Reaktor (VVER)-1000 reactor type is developed using an internationally recognised code, Monte Carlo N-Particle, version 6 (MCNP6). This research study is based on a VVER type of pressurized water reactor (PWR), which is of Russian design. The neutronics model is done at 300 K, assuming the use of fresh fuel. Major core operational parameters including the k_{eff} , power profiles, reactivity coefficients and control rod worth were evaluated for the reactor core. The present study looks at the ability of the VVER-1000 reactor system to provide appropriate neutronics behaviour of the fresh core at the start of the initial cycle from cold zero power.

A convergence study on the MCNP6 results is the most crucial part of MCNP6 simulation in the study, hence a convergence study of the MCNP6 results was initially done to ensure accuracy. The primary objective of the study is to develop an MCNP input model for the VVER-1000 reactor core using the North-West University Reactor Code suite (NWURCS) developed at the North-West University, School of Mechanical and Nuclear Engineering. The verification of the NWURCS code also forms part of the study.

The steady state results obtained from the different models for all the investigated cases are presented and compared to previous research. The calculated values support safe start-up of a reactor and also assist in predicting the behaviour of the system.

Keywords: MCNP6, Neutronics, Convergence, Criticality, Reactivity coefficients, Verification, NWURCS

Acknowledgements

- To the SARChi Chair in Nuclear Engineering, I would love to show my appreciation for financially supporting my studies for the two years of the programme.
- A million times thank you would go to my two supervisors, Dr Naicker and Miss du Toit for their massive assistance and the guidance they provided me throughout the study.
- To my parents (Mr TK and Mrs DK Nyalunga), son Khayalethu, and siblings (Nomcebo, Fortune, and Nontokozo), I would love to show my appreciation for the support I received from all of you when I decided to pursue master's studies. Without your support and patience, I could not have done it.
- A special thanks to my half-sister (Zakhele Nyalunga) for looking after my son when my mom was at work; for the love, she gave my son while I was not there.
- To my colleagues, Tannie Francina and the professors at the department, a special thank you goes to all of you for the nice times we had together when we were taking a break from studying and the catching up we used to do during birthday celebration.
- I would like to give gratitude to the HPC at the NWU for allowing me to use their cluster computers for the MCNP calculations.
- I would like to give a special thanks to Mr Eric Chinaka for assisting me with the MCNP6 code.
- Last but not least, I would like to thank my God, the Almighty for giving me strength and always holding my head high.

Table of Contents

List of Tables

List of figures

List of Acronyms

Abbreviation	Meaning
BC	Boron Concentration
BOC	Beginning of Cycle
CZP	Cold Zero Power
DC	Doppler Coefficient
DOE	Department of Energy
ENDF	Evaluated Nuclear Data Files
EOC	End of Cycle
EPR	European Pressurized Reactor
FA	Fuel Assembly
FC	Full Core
FOM	Figure of Merit
FSAR	Final Safety Analysis Report
HFP	Hot Full Power
HPC	High Performance Computing
H_{src}	Shannon Entropy
HZP	Hot Zero Power
INP file	MCNP Input file
IRP	Integrated Resource Plan
K	Kelvin
k_{∞}	Infinity Multiplication Factor
KCODE	Criticality Code
k_{eff}	Effective Multiplication Factor
KSRC	Criticality Source
MCNP6	Monte Carlo N-Particle, version 6
MCNPX	Monte Carlo N-Particle Extended
MTC	Moderator Temperature Coefficient
NWURCS	North-West University Reactor Code Suite
^{o}C	Degrees Celsius
PCM	Per Cent Million
PDF	Probability Density Function
Ppm	Parts Per Million
PWR	Pressurised Water Reactor
RPV	Reactor Pressure Vessel
SDEF	Source Definition
VISED	Visual Editor
VVER/WWER	Voda Voda Energo Reaktor/Water-cooled Water-moderated Power Reactor
β_{eff}	Effective Delayed Neutrons Beta Coefficient

1. Background and Overview

1.1. Introduction

The growing demand for energy and the effects of greenhouse emissions caused by the current major energy source (coal) have led to the South African (SA) interest in expanding nuclear energy as part of the country's total energy mix. Nuclear energy is a vital option for SA, since it is a source of clean-air, carbon-free electricity, producing no greenhouse gases or air pollutants. Nuclear energy can supply base-load electricity with limited effects on the environment compared to other energy sources listed in the Integrated Resource Plan (IRP) (DOE, 2013).

Operations evidence over six decades demonstrates that nuclear power is a safe means of generating electricity. The risk of accidents in nuclear power plants is low and declining. The consequences of an accident or terrorist attack are minimal compared with other commonly accepted risks. Maintaining at least one of the radionuclide barriers during all imaginable accidents is, however, one of the most important tasks of reactor safety engineering. Providing that maintenance of this integrity is possible and available during all events is the main subject of reactor safety analysis.

Research on nuclear technology must be continued to ensure safe, efficient and reliable operation of nuclear reactors in South Africa. Safety analysis for nuclear reactor systems must be carried out to assure the public that nuclear energy is safe and reliable.

The safe operation of a reactor is highly dependent on the ability to predict the neutron flux precisely, which is needed to derive criticality, power distribution shapes, temperature distributions and feedback coefficients of reactivity. The evaluation of the neutron population in energy, space and time is performed throughout the reactor core and its surroundings to obtain the safety reactor parameters.

The South African government has plans to add about 9.6 GW of nuclear energy to the electricity grid, as stated in the IRP for electricity, IRP2010 (DOE, 2013). The IRP2010 states that the addition should be accomplished by 2030. The government has recently informed the country that procurement would start before the end of the country's financial year. In 2014 the South African government signed memoranda of understanding with several countries that are experienced in nuclear energy, Russia being one of the countries that will be assisting the country in implementation of the new nuclear project. The nuclear energy research team at the NWU School of Mechanical and Nuclear Engineering is performing studies on various types of reactors, one being the VVER-1000 type reactor.

This study is based on the VVER-1000, a pressurised water reactor (PWR) of Russian design. The abbreviation VVER stands for Voda Voda Energo Reaktor, which means water-cooled, water-moderated energy reactor. There are about 52 operational Russian-designed VVER-typed PWR power plants among the 437 nuclear power plants currently in operation globally (Katona, 2011). Safety analysis models for the VVER-1000 have been developed by several organisations throughout the world. In this study the aim is to develop a neutronics model of a VVER-1000 and to investigate some neutronics parameters that are important for safety analysis of a reactor. The reactor core is modelled and calculations for fission power and neutron fluxes reactivity feedbacks are done using an internationally recognised code, Monte Carlo N-Particle, version 6 (MCNP6).

The neutronics of a nuclear reactor involve the steady state and the transient behaviour of the reactor core, which includes the reactivity effects of fuel, moderator and control rods, as well as nuclear reaction cross-sections. In this study a steady state neutronics simulation model for the VVER-1000 is established.

1.1.1. Motivation for Research

This study was motivated by the government's announcement on the new nuclear project. South Africa is looking to build more nuclear power stations, with their reactor type choice most probably being the PWR. The government has signed intergovernmental agreements with several countries, including Russia. The agreements between these countries have been concluded so that knowledge of nuclear energy can be shared with South Africa. Therefore, it is important that the Russian reactor be added in studies done at the NWU School of Mechanical and Nuclear Engineering. It is in the best interest of the North-West University to continue developing more expertise in South Africa in the nuclear field. The research focuses on different types of reactors and this study will be focused on a PWR Russian design reactor, the VVER-1000.

1.1.2. VVER-1000 type Reactor

The VVER-1000 reactor type is a four-loop Russian version of the PWR. The VVER-1000 is a generation III reactor producing 1000 MW electric power output and it incorporates international safety standards. A generation III reactor is a generation II reactor with evolutionary design improvement in the areas of fuel technology, modularized construction, safety systems, and standardized designs (Goldberg & Rosner, 2011). Some of the countries that have a VVER-1000 operating are Russia, China and India (Gidropress, 2008). It is a design that is based on long-term experience feedback from 1000 reactor years of VVER nuclear power plant operation.

The latest VVER-1000 reactor plant is a result of an evolutionary development of well-proven VVERs, which guarantees an entirely mastered technology. The VVER-1000 has many common features with western PWR's, including passive safety systems and double containment. These are very important features since they improve the reliability of the reactor plant equipment. They also prevent and mitigate design basis accidents and beyond design accidents more effectively (Prof. Dr. Saygin, 2011).

The country's decision to choose the VVER for nuclear power would be based on experience in design, construction and operation of the nuclear plants with Russian VVER-type reactors. The reactor has hexagonal fuel assemblies (FAs). This makes it different from other PWRs, which have square arrays. The hexagonal assemblies are not the only feature that distinguishes the VVER from other PWRs. It also has horizontal steam generators, no bottom penetrations in the pressure vessel and high-capacity pressurisers providing a large coolant inventory. A more detailed description of the VVER reactor is given in more detail in Section 2.5.

1.2. Background

A nuclear reactor is defined as a collection of components of different geometries made up of fuel assemblies (FAs). Each FA can be different from each other. Constituting the reactor core, they must contain the right amount of mass of fissile material in order to sustain the controlled nuclear fission chain reactions. One of the main components of a nuclear reactor is the fuel assembly (FA), which usually contains fuel pins that are sintered into a cylindrical shape for solid fuels. Fuel pins are made of heavy fissile nuclei, which undergo fission chain reactions when they interact with neutrons. Since neutrons are electrically neutral, they can penetrate deeper into matter than other particles. The existence of neutrons in a fission reactor is the most important part in the production of nuclear energy (Alexander, 2010).

The nuclear fission reaction is the principal source of nuclear energy. It is the reaction between a neutron and a heavy nucleus (e.g. uranium, plutonium) and it results in the production of a highly unstable compound nucleus, which splits into fragments accompanied by the emission of a few neutrons and a large amount of energy. However, the fission reaction is not the only reaction that takes place in a reactor; radioactive capture is one of many other reactions (Alexander, 2010). The theory of neutronics also involves determination of nuclear reaction cross-sections. The neutron interactions (reactions) with matter can be categorised as seen in Figure 1-1:

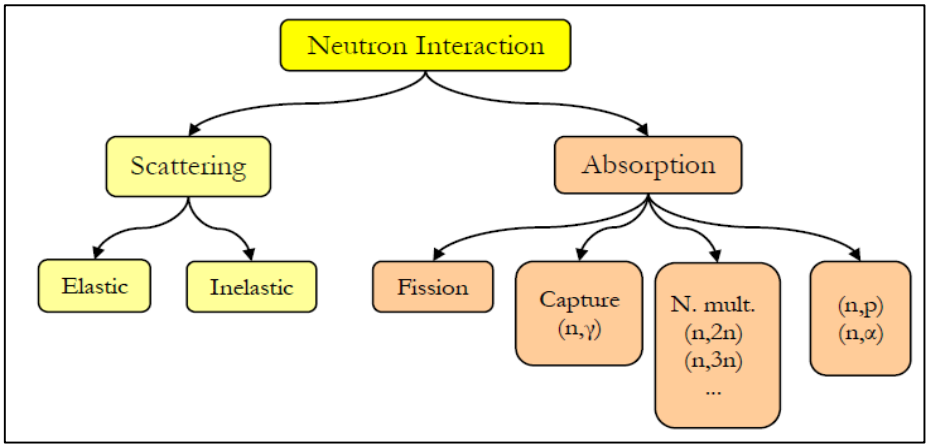

Figure 1-1: Types of neutron interaction with matter (Arzhanov, 2010)

The probability that a neutron will react with matter in a nuclear reactor is defined by the cross-section. Each probable reaction that a neutron can undergo with a nucleus is associated with its specific cross-section. These cross-sections that define each interaction can be summed up to give the total cross-section in the system.

The total cross-section is the sum of all the possible reactions that can occur in a reactor system, as seen in Equation (1-1) below:

$$\sigma_T = \sigma_{se} + \sigma_{si} + \sigma_a \tag{1-1}$$

where:

σ_{se}: Elastic cross-section
σ_{si}: Inelastic cross-section
σ_a: absorption capture cross-section.

Neutrons in a reactor can either be absorbed or scattered. The probability that a neutron will undergo absorption and/or scattering in a reactor is given by Equations (1-2) and (1-3) respectively:

$$\sigma_a = \sigma_\gamma + \sigma_f + \sigma_{n+\ldots} \tag{1-2}$$

and

$$\sigma_s = \sigma_{se} + \sigma_{si}. \tag{1-3}$$

It is important to understand the cross-sections explained above, since they contribute to the regulation of a neutron population in a reactor system.

In a nuclear reactor system, a nuclear chain reaction is required and it must be controlled and sustained at a steady rate. A nuclear chain reaction is a series of nuclear fissions, each initiated by a neutron released in a preceding fission. Sustainability of the chain reaction can

be achieved by keeping the ratio between the numbers of neutrons of one generation to the number of neutrons in the next generation constant. This ratio is called the multiplication factor and it is an indication of the nature of the chain reaction, as defined in Equation (1-4):

$$k = \frac{number\ of\ neutrons\ in\ the\ current\ generation}{number\ of\ neutrons\ in\ the\ preceding\ generation}. \quad (1\text{-}4)$$

The reactor is said to be critical when the ratio is unity, and the chain reaction will proceed with a constant neutron population (Stacey, 2007). This is one of the objectives of this study, to determine the criticality parameters of this kind of reactor.

1.3. Problem Statement

Research on the PWR systems has commenced at the NWU. This arises from the need to develop locally based expertise in reactor analysis as applied to PWR systems. In view of the government's intention to build a new fleet of nuclear reactors and the VVER-type being a possible choice, it is important that this type of reactor be included in studies.

This study is aimed at building a neutronics model of a VVER type reactor, using the fresh core as a base.

1.4. Aims

The aims of this study are to:

- Obtain current literature on the VVER and develop a specification sheet as required for a neutronics calculation in this work.
- Build an MCNP6 input model for a VVER-type fresh core at 300 K using the North-West University Reactor Code Suite (NWURCS).
- Verify the in-house code, NWURCS, used to generate the MCNP6 input (INP) files
- Calculate neutron fluxes and fission power and perform criticality analysis of the model using MCNP6.
- Calculate the reactivity effects of the fuel, moderator and control rods.
- Verify the above calculations for a full core (FC), 1/6th core and a fuel assembly (FA) models.

1.5. Outline of the Dissertation

The outline of the chapters is briefly explained below. The dissertation contains five chapters, with the first chapter giving the overview of the scope of the study.

In Chapter 2, theory and literature review relevant to this study are given. The theory presented in the chapter is based on Monte Carlo methods, together with an overview of the VVER-1000 reactor.

Chapter 3 describes the method of employing MCNP to perform the calculations in the study. This chapter provides the details of all the models that are used in this study, i.e. the FC, $1/6^{th}$ core and the FA models. The chapter also deals with the methodology used to carry out verification of the NWURCS code.

In Chapter 4 the results and subsequent analysis are supplied. Verification and comparison of these results are also provided in the chapter.

Chapter 5 draws the conclusion and makes recommendations on further studies.

2. Theory and Literature Review

2.1. Reactor Physics Calculations

Reactor physics is the study of the interaction that occurs between neutrons and matter, as well as the transport of neutrons in space. A neutron collides with a nucleus of a specifically chosen nuclide. The nuclear reactor is a three-dimensional (3D) assembly of components of different geometries made of a selection of materials whose interaction characteristics with neutrons vary strongly with the energy of the neutron and the temperature of the medium.

The neutron transport equation is solved by using various computational techniques. In this study, the focus is on Monte Carlo techniques, since they are applied in the MCNP6 code. The major advantages of the Monte Carlo method are the continuous energy treatment and the precise modelling that can be carried out on the 3D geometry. However, the Monte Carlo method involves considerable computational time. This chapter outlines in detail the procedures used in MCNP6 to perform reactor physics calculations.

2.2. Monte Carlo Techniques

Advances in nuclear reactor design lead to more and more complex geometries and a need to model an increasing amount of detail of the geometries. Monte Carlo statistical sampling methods are able to capture details in complex 3D geometries. The Monte Carlo-based code, MCNP6, is used to compute the fission and the subsequent heating energy deposition in the defined models of the study and the surrounding media. It is also used to analyse the neutron flux in the reactor core and to determine how the power is distributed in the core. The theory on how the Monte Carlo method obtains these parameters is explained in the sections that follow.

2.2.1. Description of Monte Carlo Methods

The general form of the neutron transport equation is written as (Stacey, 2007):

$$\begin{aligned}\frac{\partial N}{\partial t}(r,\Omega,t)drd\Omega = v\big(N(r,\Omega,t)\big) - \big(N(r+\Omega dl,\Omega,t)\big)dAd\Omega \\ + \int_0^{4\pi} d'\Omega\Sigma_s(r,'\Omega\rightarrow\Omega)vN(r,'\Omega,t)drd'\Omega \\ + \frac{1}{4\pi}\int_0^{4\pi} d'\Omega v\Sigma_f(r)vN(r,'\Omega,t)drd\Omega + S_{ex}(r,\Omega)drd\Omega \\ - (\Sigma_a(r)+\Sigma_s(r))vN(r,\Omega,t)drd\Omega\end{aligned} \quad (2\text{-}1)$$

where:

r: Position vector.
v: Neutron velocity.
Ω: Characterises the direction of motion.
t: Time
N: Number of neutron in the volume element dr.

When the above equation is applied in a reactor system, each term of the equation represents a different event occurring in the reactor system. The events are defined below:

$\frac{\partial N}{\partial t}(r,\Omega,t)drd\Omega$:	Rate of change of the number of neutrons in the volume element
$N(r,\Omega,t)$:	Number of neutrons in volume element dr at position r moving in cone direction $d\Omega$ about direction Ω
$N(r,\Omega,t)dAd\Omega$:	Rate at which neutrons are flowing into the volume element
$\big(N(r+\Omega dl,\Omega,t)\big)dAd\Omega$:	Rate at which the neutrons are flowing out of the volume element
$\int_0^{4\pi} d'\Omega \sum_s(r,'\Omega\rightarrow\Omega)vN\,(r,'\Omega,t)drd'\Omega$:	Rate at which the neutrons travelling in direction Ω are being introduced into the volume element by scattering of neutrons within the volume element from a different direction $'\Omega$
$\frac{1}{4\pi}\int_0^{4\pi} d'\Omega v\sum_f r\,vN(r,'\Omega,t)drd\Omega$:	Rate at which the neutrons are being introduced into the system volume by fission
$S_{ex}(r,\Omega)drd\Omega$:	Rate at which the neutrons are produced into the system by an external source
$(\sum_a(r)+\sum_s(r))vN(r,\Omega,t)drd\Omega$:	Rate at which the neutrons are being absorbed or scattered in the volume

The neutron transport equation can be analysed by using either deterministic methods or Monte Carlo methods. Deterministic methods are used to solve the transport equation for the averaged behaviour, while Monte Carlo methods are used to solve the transport equation by simulating individual particles and tracking these individual particles. The basic idea of the Monte Carlo method is to create a series of life histories of the particles by sampling random variables.

The statistical sampling technique uses probability laws to describe the neutron's behaviour and to trace out each step of the particle's random walk through the system until the end of its life. The history of the particle is followed from the beginning of its life to the point where it can no longer supply any information on the problem of interest. The solution to the neutron

transport equation is obtained by the simulation of the individual particle histories run a large number of times and by tracking the specific aspects, which are described as tallies, of the behaviour of particles.

Because Monte Carlo methods are of statistical nature, the core calculations will usually involve considerable computer time to attain reliable converged results for both integrated and local distributions.

2.2.2. Probability Density Function

Assume a continuous random variable, defined by x over the interval a≤x≤b and that a probability density function (PDF) f(x) exists, such that f(x)dx is the probability that a variable takes on a value within dx about x. The normalisation is chosen such that

$$\int_a^b f(x)dx = 1, f(x) \geq 0. \tag{2-2}$$

In general, f(x) will be a non-monotonically increasing function of x, which indicates that a given value for f(x) might not correspond to a unique value of x (Stacey, 2007).

2.2.3. Criticality Calculations

In a nuclear reactor, the most important purpose of the reactor operation is to achieve a controlled sustainable chain reaction. As stated above in Section 1.2 a sustainable chain reaction means that the ratio between the number of neutrons that are produced and the number of neutrons that are absorbed or leave the system through the outer boundary must remain constant in the next generation. One of the methods of controlling the chain reaction is the movement of the control rods.

The criticality of the nuclear reactors is characterised by k_{eff} (multiplication factor), which is the eigenvalue to the transport equation. One of the ways of representing the multiplication factor is by Equation (2-3) below:

$$k_{eff} = \frac{fission\ neutrons\ in\ generation_{i+1}}{fission\ neutrons\ in\ generation_i}. \tag{2-3}$$

This definition of k_{eff} is applied in MCNP6 where the neutron generations are referred to as cycles.

When $k_{eff} = 1$, the system is considered critical; with $k_{eff} > 1$, the system is supercritical and the number of fissions in the chain increases with time. With $k_{eff} < 1$, the system is subcritical and the chain reaction will not be sustained, since the generation of neutrons will be terminated.

A symmetric system that uses reflective boundary conditions would have no leakage; therefore the multiplication factor of such a system is the infinity multiplication factor k_∞ (Giust, 2012). The k_∞ would differ from the criticality $k_{eff} = 1$ because the leakage causes the criticality flux to differ from an infinite medium flux. A Monte Carlo-based code has its unique way of calculating the criticality of the reactor core, which involves using statistical sampling techniques to simulate the interaction of nuclear particles with matter.

When performing a criticality calculation, an estimate of the mean number of fission neutrons produced in one generation per fission neutron is required. The actual process includes the follow-up of each neutron from its emission from a neutron source throughout its life until the end of life. The life of a neutron can be ended by the neutron escaping the system, by radiative capture, or absorption leading to fission. In MCNP6 the next value of k_{eff} and the next generation of the fission source distribution are obtained by a single generation of neutron random walk that is carried out for a cycle. Because of its statistical nature, Monte Carlo calculations must be done for a number of generations, resulting in a statistical spread in k_{eff}, taking into account the standard deviation.

2.2.4. Tally Definition

Tally specification in MCNP6 is important. It is the process of scoring the quantities of interest that will provide the user with the required answers, such as answers on the track length estimator of the flux of a cell, or fission energy deposition. The quantities of interest are tallied during the simulation of neutrons. A tally in an MCNP6 INP file is defined by using an Fn:a number, where “n” is a unique number and must not be repeated in the same tally job (the number must not exceed <999), and “a” is the particle type that can be neutrons, protons or electrons. A tally can be altered by adding a multiple of 10, which means F4, F14, F24 are all type F4 tallies, specified for different reasons (Shultis, 2008).

In the study the tally of interest is the track length estimate of cell flux (F4) and the fission energy deposition (F7). The tallies are investigated to study the behaviour of the neutrons in the models.

2.2.4.1. Track length estimate of the cell flux (F4)

The track length estimator calculates the flux from the number of particle-track lengths per unit volume.

Consider a neutron passing through a volume with energy *E* in MeV (Mega-electronvolt), travelling at velocity v (cm/sec) at time t (sec). Let the distance the neutron travels through the volume be defined by s (cm). The average particle flux in a cell is defined as (Espel, 2010):

$$\overline{\phi_V} = \frac{1}{V}\int dE \int dV \int dt v N(\vec{r}, E, t) \tag{2-4}$$

where

$N(\vec{r}, E, t)$is the density of particles at a specific point given in neutrons/cm^3,

$\psi(\vec{r}, E, t) = vN(\vec{r}, E, t)$ is the scalar flux

and

$\overline{\phi_V}$ is the defined average flux over a cell and the units are neutrons/sec-cm^2.

Taking vdt=ds, Equation (2-4) is represented as follows:

$$\overline{\phi_V} = \frac{1}{V}\int dE \int dV \int ds N(\vec{r}, E, t). \tag{2-5}$$

In the above equation $\int \mathrm{dsN}(\vec{\mathrm{r}}, \mathrm{E}, \mathrm{t})$ is the distance traversed by the neutrons in the volume under consideration. This, however, can be written in terms of the track length TL as:

$$\int dsN(\vec{r}, E, t) = \sum_{i=1}^{N} TL^i \tag{2-6}$$

where N is the number of particles tracked.

In addition, the tally process can assign a weight for each neutron. The equation then becomes:

$$\int dsN(\vec{r}, E, t) = \sum_{i=1}^{N} W * TL^i. \tag{2-7}$$

The flux is therefore written as:

$$\overline{\phi_V} = \frac{\int dE \int dV \sum_{i=1}^{N} W * TL_V^i(E)}{V}. \tag{2-8}$$

This can then be written in terms of the sum of all particles tracked for the chosen energy range and volume as:

$$\overline{\phi_V} = \frac{\sum_{i=1}^{N} W * TL}{V}. \tag{2-9}$$

2.2.4.2. Energy Deposition Estimator (F6, 7)

The energy deposition tally is given as (Pelowitz, 2013):

$$F_{6,7} = \frac{\rho_\alpha}{m} \iiint_{V\,t\,E} H(E)\Phi(\vec{r}, E, t) dE dt dV. \tag{2-10}$$

The $\rho_\alpha$and m are respectively the atomic density and mass (grams) and H(E) is the heating response (MeV/g or jerks/g, for $F_{6,7}$ 1MeV=1.60219E-22 jerks). H(E) has different meanings depending on the particle type. For example, H(E) for neutrons is given by (Pelowitz, 2013):

$$H(E) = E - \sum p_i(E)\left[\bar{E}_{i,out}(E) - Q_i + \bar{E}_{i,\gamma}(E)\right] \quad (2\text{-}11)$$

where:

$p_i(E) = \frac{\sigma_i(E)}{\sigma_T(E)}$: is the probability of reaction i at neutron incident energy E

$\bar{E}_{i,out}(E)$: average exiting neutron energy for reaction i at neutron incident energy E

Q_i: Q-value of reaction i (MeV)

$\bar{E}_{i,\gamma}(E)$: average exiting gamma energy for reaction i at neutron incident energy E.

These tallies are track-length estimators of the flux with an energy-dependent multiplier, H(E). The F4 tallies with the proper energy dependent multiplier, given by the FM card, can be made equivalent to the F6 or F7 tallies. The F6 tally includes all reactions and the F7 scores the fission energy deposition. The F7 score is therefore available only for neutrons (X-5 Monte Carlo, Team, 2013).

2.3. Convergence Study of MCNP6 Problem

A steady state calculation of the nuclear reactor core produces the reactor effective multiplication factor k_{eff} and also the neutron flux distribution. In this study Monte Carlo methods are used for the calculations of the criticality of the reactor and also the neutron flux distribution. The convergence of MCNP6 calculations, for both k_{eff} and the fission source distribution H_{src}, are obtained by considering guiding parameters of the convergence. Convergence in MCNP6 is when the fission source has settled across the geometry.

To examine convergence of the MCNP6 calculation, one can check the convergence of both the fission source and k_{eff} by the computed values of k_{eff} and a quantity called the Shannon entropy of each cycle against the number of cycles. With the two plots one can identify if the source or the k_{eff} has converged, by visually inspecting the behaviour of the plots. As the source distribution approaches convergence, the Shannon entropy convergences to a steady state value, which will indicate convergence. The results from calculations are called biased when either of the two tests has not converged. Convergence can be reached by increasing the number of skipped cycles and by increasing the number of fission source neutrons. The core symmetry is taken into account, when the core is symmetrical, either axially or radially. In this case, a symmetrical power/flux distribution should be obtained when the calculations have converged.

MCNP6 has a built-in capability that is used to compute the Shannon entropy for the fission source distribution.

This parameter is used to characterise the convergence of the fission source. The importance of the source convergence is that it can also indicate the convergence of k_{eff}. MCNP6 computes the Shannon entropy at the end of each cycle by the use of the spatial mesh that is constituted specifically for the Shannon entropy tallies. The source convergence is not determined by the computed value for the Shannon entropy, but by a statistical spread in the Shannon entropy. Attention should be paid when the fission source converges more slowly than k_{eff} instead of converging at the same rate as k_{eff} (Forrest, 2006).

2.3.1. Shannon Entropy of the Fission Source Spatial Distribution

The Shannon entropy is a parameter that is calculated by MCNP6 in order to analyse the convergence of the fission source spatial distribution. The Shannon entropy of a fission source distribution is expressed by (Forrest, 2006):

$$H_{src} = -\sum_{j=1}^{N_s} P_j * ln_2(P_j) \tag{2-12}$$

where N_s represents the number of grid boxes, and P_j is the ratio of the number of source sites in j-th grid boxes to the total number of source sites. The Shannon entropy provides a single number for each cycle to assist with characterising the convergence of the fission source distribution. MCNP6 produces the value of H_{src} for each cycle of a criticality calculation. For MCNP6 to compute H_{src}, it is important to superimpose a 3D grid on a problem encompassing all of the fission regions, then to tally the number of fission sites in a cycle that fall into each of the grid boxes. The tallies may be used to form a discretised estimate of the source distribution. The grid used to determine H_{src} can either be specified by the user or automatically determined by MCNP6.

2.3.1.1. Referral work on convergence study

Farkas performed a convergence study called *WWER-440 criticality calculations using MCNP5 code.* The purpose of the convergence study was to determine detailed and accurate modelling of the WWER-440 reactor type. This would be achieved by establishing a precise criticality calculation where the fission source and k_{eff} have converged. The assessment of the Shannon entropy of the fission source together with k_{eff} was done in order to ensure the accuracy of the MCNP5 results.

It was said that a sufficient number of neutrons in each cycle must run in order to meet a well-converged neutron source point.

Figure 2-1 gives an indication of what happens when the neutron source points are changed to reach convergence (Farkas, et al., 2005):

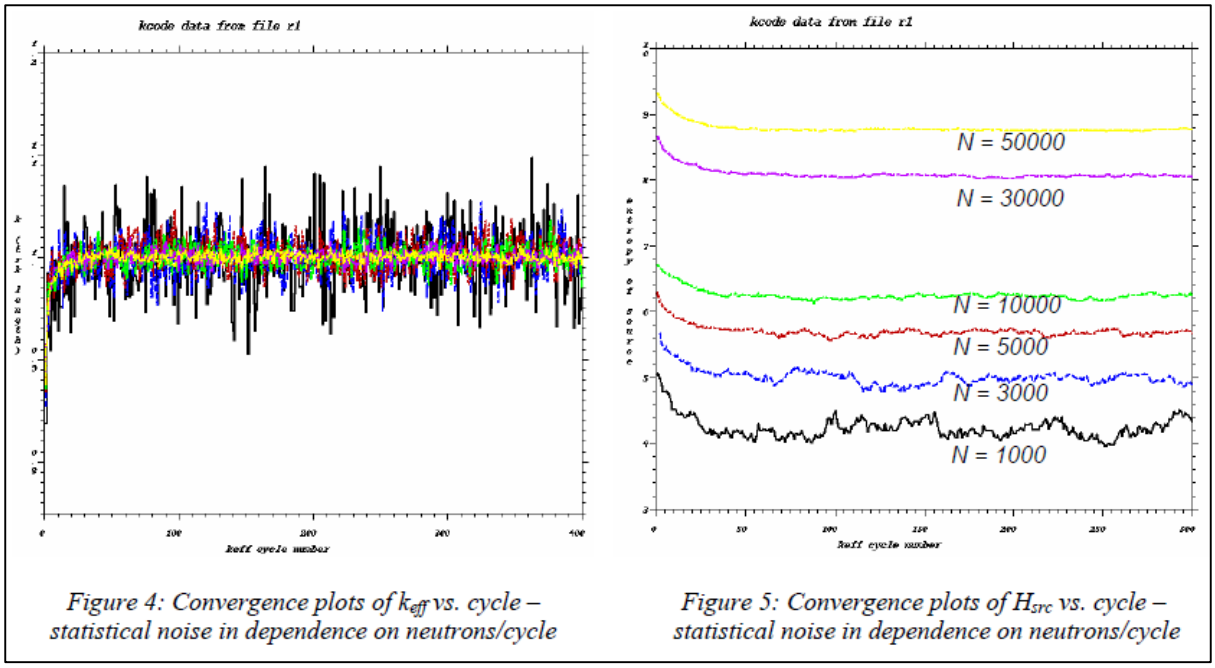

Figure 4: Convergence plots of k_{eff} vs. cycle – statistical noise in dependence on neutrons/cycle

Figure 5: Convergence plots of H_{src} vs. cycle – statistical noise in dependence on neutrons/cycle

Figure 2-1: Source convergence

The cases demonstrated above show that the varying statistical noise inherent in the random walks of the neutrons in each generation is dependent on the value of the N parameter. It is also observed that the neutron source becomes well converged when about 50 000 cycles are chosen. It should be stated that the choice of initial neutron sources is influenced by the geometry of the model. The more complicated the model, the higher the number of neutrons necessary for each cycle.

2.3.2. Tally Convergence of the Monte Carlo Problem

In MCNP6, tally checks are used to analyse the convergence of the tally of interest in the Monte Carlo calculation. Monte Carlo calculations are normalised to per starting particle history and it is important to analyse the statistical tally checks as well in order to obtain true statistical estimates for the tally results. The tally has a fractional standard deviation, which is relative error for each answer obtained. The tally checks performed in MCNP6 are defined as follows:

- Estimated mean value

In MCNP6, the results are obtained by simulating particle histories and giving a score x_i to each particle history run. The particle histories typically generate a range of scores depending on the choice of tally. By taking f(x) as a PDF for selecting a particle history that scores x to the estimated tally, the true answer/true mean is the expected value of x where

$$\langle x \rangle = \int xf(x)dx = true\ mean. \tag{2-13}$$

The sample mean $\bar{x}$ is then used to estimate the true mean:

$$\bar{x} = \frac{1}{N}\sum_{i=1}^{N} x(i). \tag{2-14}$$

Equation (2-14) supports the law of large numbers on which the Monte Carlo method is based. The law of large numbers states that the mean value of a sample of N trials chosen from a distribution f(x) where x(i) is the result of the ith trial, approaches the true mean <x> as N gets larger.

Because of the law of large numbers, <x>and $\bar{x}$ are related. If <x>is finite, $\bar{x}$ converges to <x> as N approaches infinity (Dunn & Shultis, 2009):

$$\lim_{N\to\infty} \bar{x} = \langle x \rangle \tag{2-15}$$

as long as the x(i) used to compute $\bar{x}$ is taken from the guiding PDF f(x).

- Relative error/fractional standard deviation

The Monte Carlo method represents an average of the contributions from many histories sampled during a simulation. An important quantity estimated by MCNP is the statistical uncertainty associated with the result, which is defined as one estimated standard deviation. This uncertainty can be used to form a statement about what the true result is. The relative error of the estimated mean is defined as (Booth, et al., 1994):

$$R = \frac{\sigma_{\bar{x}}}{\bar{x}} = \sqrt{\frac{\sum x_i^2}{(\sum x_i)^2} - \frac{1}{N}} \tag{2-16}$$

where $\sigma_{\bar{x}}$ is the standard deviation of the estimated mean. The equation that defines the standard deviation is as follows (Booth, et al., 1994):

$$\sigma_{\bar{x}} = \frac{1}{N}\sqrt{\frac{1}{N}\cdot\sum_{i=1}^{N}(x(i)-\bar{x})^2}. \tag{2-17}$$

The R is important because the estimated statistical uncertainty in the result is given as a fraction of the result. N is the number of histories.

- Variance of the Variance

The variance can provide an estimate of how much the individual sample is spread around the mean value. It is the measure of how accurate the estimate of relative error R is. The variance of the population is given by Equation (2-18) (Saidi, et al., 2013):

$$\sigma^2 = \int (x - \langle x \rangle)^2 f(x) dx = \langle x^2 \rangle - \langle x \rangle^2 \tag{2-18}$$

where <x> is the true mean and f(x) is the PDF. Since σ is not known, MCNP can estimate it as S, the sample standard deviation. If one calls $\bar{x}$ the sample mean, the sample variance of $\bar{x}$ can be defined as:

$$s^2 = \frac{1}{N-1}\sum_{i=1}^{N}(x(i)-\bar{x})^2 \approx \bar{x}^2 - x^2(i). \tag{2-19}$$

Therefore $\bar{x}^2$ becomes:

$$\bar{x}^2 = \frac{1}{N}\sum_{i=1}^{N}x^2(i). \tag{2-20}$$

The estimated variance of the mean $\bar{x}$ then becomes:

$$S_{\bar{x}}^2 = \frac{S^2}{N}. \tag{2-21}$$

After the above definition, the relative variance of the variance (VOV) can be defined as (Booth, et al., 1994):

$$VOV = \frac{S^2(S_{\bar{x}}^2)}{S_{\bar{x}}^4} = \frac{\sum_{i=1}^{N}(x_i-\bar{x})^4}{[\sum_{i=1}^{N}(x_i-\bar{x})^2)]^2} - \frac{1}{N} \tag{2-22}$$

where $S_{\bar{x}}^2$ is the estimated variance of $\bar{x}$ and $S^2(S_{\bar{x}}^2)$ is the estimated variance in $S_{\bar{x}}^2$.

The VOV is important, since the S must be a good approximation of σ in order to be used in forming confidence intervals (Briesmeister, 2000).

- Figure of Merit

The metric of efficiency for a given tally is estimated by the quantity called the figure of merit (FOM). The equation that defines the FOM is:

$$FOM = \frac{1}{R^2T} \tag{2-23}$$

R represents the relative error for a sample mean, and T is the amount of time taken by the computer to simulate N histories. The amount of time each history will take on average should be proportional to the number of histories N (T~N), so that R^2T approximately constant indicates a well-behaved and reliable tally. If not constant, it means that the results are not statistically stable.

The above equation expresses a direct relationship between the computer time and the value of FOM. If the FOM for a given tally is increased, the amount of time required to reach a desired level of precision will be reduced.

The FOM is also used to estimate the required computer time needed to reach a desired level of precision.

$$T = \frac{1}{R^2 \times FOM} \tag{2-24}$$

- Central limit theorem

Because the law of large numbers does not specify how large N must be in order to obtain good estimates, the central limit theorem (CLT) is taken into account. The CLT states that the sampling distribution of $\bar{x}$ can be approximated by a normal distribution when a sample size N is sufficiently large, irrespective of the shape of the population distribution (Devore & Farnum, 2005). The CLT assists with estimating how rapidly $\bar{x}$ converges to <x> as N increases. In MCNP the CLT yields the following relation (Dunn & Shultis, 2009):

$$\lim_{n\to\infty} Prob[\langle x\rangle + \alpha\frac{\sigma}{\sqrt{n}} < \bar{x} < \langle x\rangle + \beta\frac{\sigma}{\sqrt{n}}] = \frac{1}{\sqrt{2\pi}}\int_{\alpha}^{\beta} e^{\frac{-t^2}{2}dt} \quad (2\text{-}25)$$

where α and β are arbitrary values and n denotes the number of histories simulated. The uncertainty in a Monte Carlo estimate can be calculated by using the calculated sample standard deviation s to approximate the usually unknown standard deviation σ. The above equation can then be written as (Dunn & Shultis, 2009):

$$Prob\left[\frac{\bar{x}-\lambda_{s_{\bar{x}}}}{\sqrt{n}} \le \langle x\rangle \le \frac{\bar{x}+\lambda_{s_{\bar{x}}}}{\sqrt{n}}\right] \approx \frac{1}{\sqrt{2\pi}}\int_{-\lambda}^{\lambda} e^{\frac{-t^2}{2}dt} \quad (2\text{-}26)$$

where

$$Prob = \alpha < \frac{\bar{x}-\langle x\rangle}{\alpha\sqrt{n}} < \beta \approx \frac{1}{\sqrt{2\pi}}\int_{\alpha}^{\beta} e^{\frac{-t^2}{2}dt}. \quad (2\text{-}27)$$

λ represents the number of standard deviations, from the mean over which the unit normal is integrated to obtain the confidence coefficient.

The CLT indicates the probability that the estimated mean value differs from the true expected value by an amount less than $\lambda\sigma/\sqrt{N}$, for large N.

The estimated mean value of x is generally stated as:

$$\bar{x} \pm \frac{\lambda_{s_{\bar{x}}}}{\sqrt{n}}. \quad (2\text{-}28)$$

2.3.2.1. Ten MCNP6 statistical tests

In MCNP6, the tally checks that were discussed earlier in Section 2.3.2 are divided into 10 statistical tests, as given in Table 2-1. Table 2-1 below explains how the tally checks are implemented in MCNP6. When any of the 10 tests fails, MCNP6 will automatically produce additional output to assist the user in interpreting the failed tests. If the error that is obtained from any of the tallies is too large, MCNP indicates this in the output. The error that is quoted is the estimated relative error as defined in Section 2.3.2.

The 10 statistical tests as defined in the MCNP manual must provide the following information about the problem (X-5 Monte Carlo, Team, 2013):

Table 2-1: Statistical tests

Statistical tests	Meaning
Estimated mean	1. The true mean must show, for the last half of the problem, only random fluctuations as N increases. No up or down trends must be shown.
Relative Error R	2. R<0.1 to be taken as an acceptable value. 3. For point/ring detectors, R<0.05. 4. R must decrease monotonically with N for the last half of the problem.
Variance of the Variance	5. VOV is expected to be less than 0.1 for all types of tallies. 6. VOV is expected to decrease monotonically with N for the last half of the problem. 7. The first four moments must be finite.
Figure of Merit	8 FOM must remain statistically constant for the last half of the problem 9 FOM must exhibit non-monotonic behaviour in the last half of the problem
Tally PDF	10 The slope determined from the 201 largest scoring events must be greater than 3.

Figure 2-2 below is an example of how the 10 statistical tests will appear on the MCNP6 output:

results of 10 statistical checks for the estimated answer for the tally fluctuation chart (tfc) bin of tally 8

tfc bin	--mean--	---------relative error---------			----variance of the variance----			--figure of merit--		-pdf-
behavior	behavior	value	decrease	decrease rate	value	decrease	decrease rate	value	behavior	slope
desired	random	<0.10	yes	1/sqrt(nps)	<0.10	yes	1/nps	constant	random	>3.00
observed	random	0.02	yes	yes	0.00	yes	yes	constant	random	10.00
passed?	yes	yes	yes	yes	yes	yes	yes	yes	yes	yes

Figure 2-2: Ten statistical tests as they appear in MCNP6 output

2.4. Neutronics Code

The neutronics code used in the study is the Monte Carlo-based code, MCNP6. MCNP is a general-purpose continuous, generalised-geometry, time-independent computer code designed to track many particle types over broad ranges of energies. MCNP6 is the latest version of MCNP, which combines the capabilities of MCNP5 and MCNPX, together with new building capabilities (Pelowitz, 2013).

To perform the neutronics analysis of the study, MCNP6 requires an INP file (MCNP input file) that contains the information that describes the specific geometry and materials of the medium, a selection of cross-section evaluations, the type of particles to be transported, the geometry of the source and the type of tallies required to perform the calculations. Other information can also be input. The input lines (cards) are required to have a maximum of 72 columns, of which the command mnemonics are located in the first five columns. MCNP6 applies units as follows: length in centimetre, energy and temperature in MeV, mass density in grams per cubic centimetre, atomic density in atoms/barn-cm, and time (shakes, where 1 shake = 10^{-8} s).

An MCNP INP file may be a very long file that accommodates all the descriptions of the geometries, tallies, source and optimisation parameters that define the model at hand. Because it is a long file, it is possible to generate errors in the input, therefore it is important that once the INP file is created, the user spends some time on plotting and testing the geometry of the model in order to check for errors. This type of test can be done using a code called MCNPX Visual Editor (VISED) that is employed by MCNP to perform the job. MCNPX VISED is a code that works with MCNP to assists users with displaying the geometry and to determine the model information or errors generated in the geometry of the model (Schwarz, et al., 2011). In this study MCNPX VISED was used to verify the geometries of the models.

As discussed in Section 1.2, in nuclear reactors the existence of neutrons is the most important part in the production of nuclear energy by fission. The neutron interaction with matter depends greatly on the cross-section. The nuclear cross-section data are used in MCNP to explain the frequency and outcome of interactions between particles (such as neutrons) and materials through which they are traversing. The type of nuclear data that are used in MCNP is point-wise cross-section data. The nuclear data in this form are saved at a significantly large number of energy points such that the point-wise data keep the particle energy as a continuous variable.

The cross-section data for neutrons' interaction are obtained from the evaluated MCNP libraries evaluated nuclear data files ENDF/B-VII at set temperatures. For temperatures that are not set in the ENDF/B-VII libraries, NWURCS will generate pseudo-materials as follows: Assume that the temperature T is such that $T_{S1} < T < T_{s2}$, where T_{S1} and T_{S2} are two adjacent cross-section data sets in the ENDF/B-VII library. The material is then represented by the mixture of the cross-sections at temperature T_{S1} and T_{S2} with the fractions $f_1$and f_2 defined by (Ponomarev, et al., 2015):

$$f_1 = \frac{\sqrt{T} - \sqrt{T_{s2}}}{\sqrt{T_{s1}} - \sqrt{T_{s2}}}, f_2 = 1 - f_1 \tag{2-29}$$

A simpler weighting can also be used,

$$f_2 = \frac{T - T_{s1}}{T_{s2} - T_{s1}}, f_1 = 1 - f_2. \tag{2-30}$$

Both options are available in NWURCS.

2.5. VVER-1000 model definition

2.5.1. VVER-1000 Reactor Core Configuration

2.5.1.1. Reactor core design

The reactor core of the VVER-1000 consists of 163 FAs placed in a lattice of hexagonal symmetry. The core layout at the beginning of cycle (BOC) is shown in Figure 2-3:

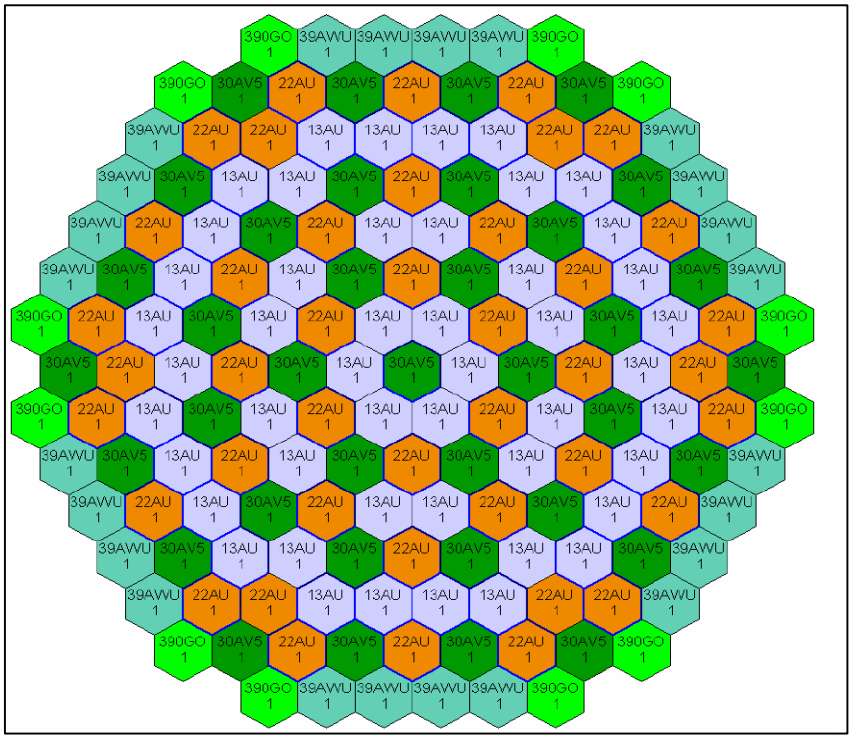

Figure 2-3: Core layout at BOC (Lotsch, et al., 2010)

The fresh core consists of FAs, which differ from one another by the enrichment of the fuel. There are seven different enrichments of the fuel pins in the core. Some of the fuel pins have 5 % of the Gd_2O_3 integral burnable poison in their compositions. A burnable absorber is normally used in the fuel rods to compensate for the excess reactivity at the BOC. The use of the Gd absorber allows for a reduction in the quantity of the initial boric acid concentration in the water. Low boric acid concentration helps to ensure a negative moderator temperature coefficient (MTC) of reactivity (Allen, 2003). The ^{235}U of the UO_2 has an enrichment of up to 4 %. The following table contains brief details of the FAs. The information in the table is extracted from Lotsch et al. (2010).

Table 2-2: FA types loaded in the core

FA type	No of UO_2 pins/enrichment (w/o %)	No. of Gd-pins(w/o Gd_2O_3/^{235}U)	No of FA in the core
13AU	312/1.30%	-	48
22AU	312/2.20%	-	42
30AV5	303/3.00%	9(5.0/2.4)	37
39AWU	243/4.00%	9(5.0/3.3)	24
	60/3.60%		
390GO	240/4.00%	6(5.0/33)	12
	66/3.60%		
			Total =163

The core is constructed by arranging the FAs into the pattern of a hexagonal lattice, as shown in Figure 2-3. The active core is surrounded by different layers of reflectors of different material radially and axially, in order to reduce fast neutron leakage and flatten the core power distribution. A reactor pressure vessel of the reactor is included in the reactor and it covers the reflectors of the core. Information about the reflectors is given in Annexure A. The reactor core characteristics are shown in Table 2-3 below:

Table 2-3: Reactor core characteristics (Lotsch, et al., 2010)

Reactor core characteristics	
Equivalent core diameter (cm)	415
Active fuel height (cm)	353
Number of fuel assemblies	163
Fuel assembly pitch (cm)	23.6
Number of fuel assemblies with control rods	61
Thermal power (MW)	3000
Boron concentration (ppm)	525
Coolant/moderator	$H_2O+H_3BO_3$
Rods per assembly	331
Rod pitch (cm)	1.278
Coolant pressure at core outlet (MPa)	15.7
Average coolant temperature (K)	578
Coolant temperature at core inlet (K)	563.15
Coolant temperature at core outlet (K)	592.75
Reactor pressure vessel (RPV) material	steel
RPV thickness (cm)	19.2

2.5.1.2. Fuel assembly layout

An FA contains 312 fuel rods, 18 guide tubes and one instrumentation tube. The FAs in the core have a different pin layout, as will be seen in Figure 2-4 to Figure 2-4. The fuel pin of the VVER-1000 reactor has a different structure from that of the western type PWR. It contains a central hole in its fuel pellet, which is filled with helium. The central hole provides lower centre temperatures and a free volume to allow any released fission gas to expand and thus reduce internal pressure (IAEA, 2006). The spacer grids mentioned in Table 2-4 are used to support the fuel rods laterally and vertically. The dimensions of the spacer grids were obtained from an article by Pazirandeh et al. (2010).

The layouts of the fuel assemblies are represented below in Figure 2-4 and Figure 2-5 (Lotsch, et al., 2009):

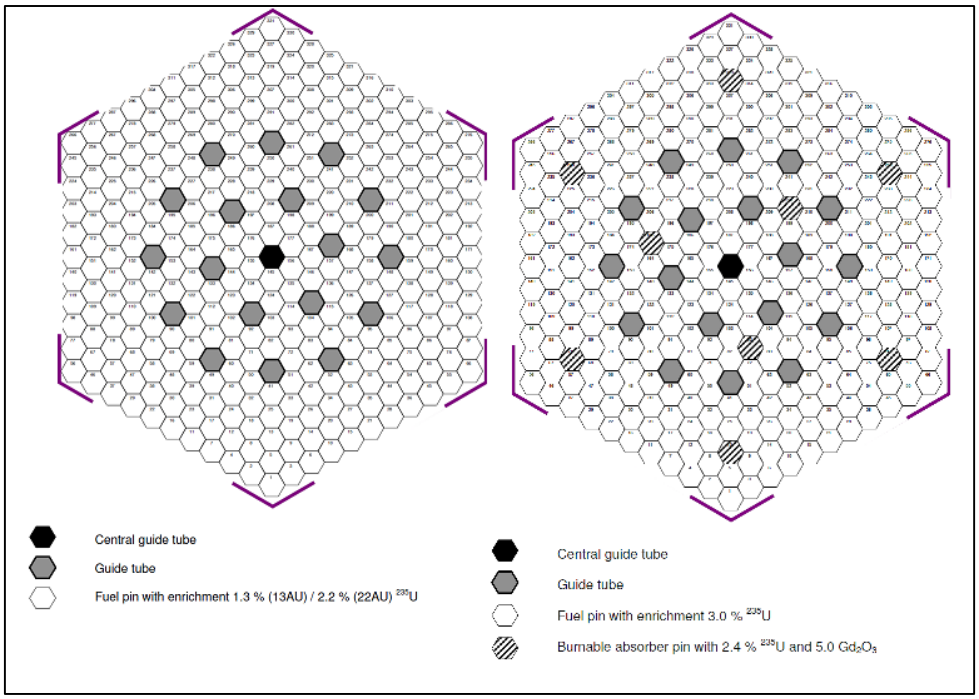

Figure 2-4: The pin layout for FA 13AU/22AU and 30AV5 respectively (Lotsch, et al., 2010)

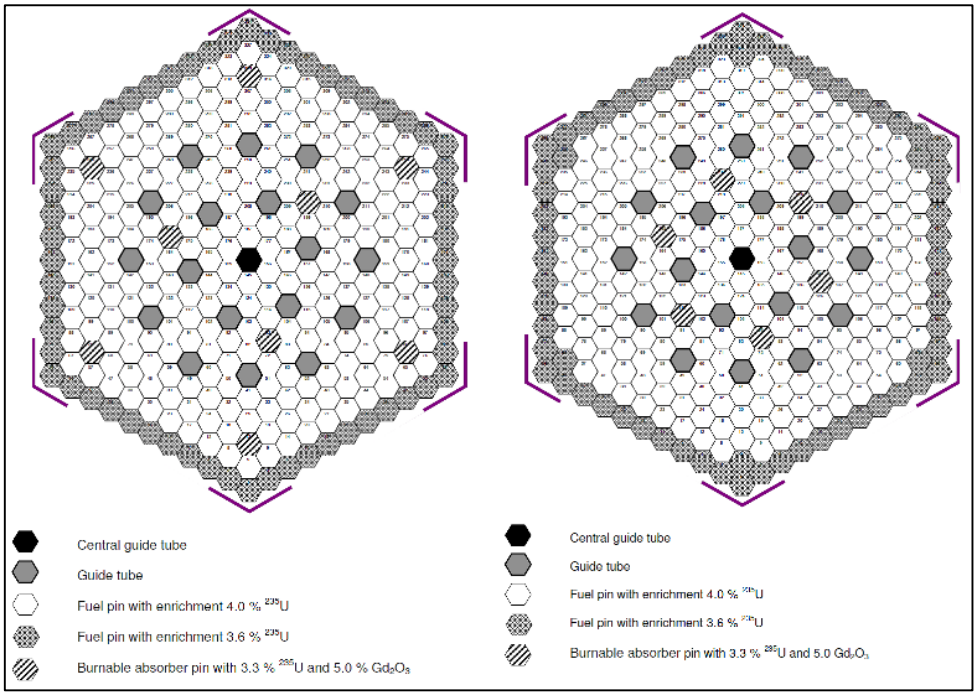

Figure 2-5: The pin layout for FA 39AWU and 390GO respectively (Lotsch, et al., 2010)

The key parameters for the fuel assemblies are presented in Table 2-4 (Lotsch, et al., 2010).

Table 2-4: Fuel assembly design data

FA Design Data	Value
Average maximum fuel temperature (K)	1005
Average moderator temperature (K)	578
Lattice type	Hexagonal
Assembly pitch (cm)	23.6
Number of pins in the FA	331
Fuel pin pitch (cm)	1.275
Length of fuel pin (cm)	353
Diameter of fuel pellet central hole (cm)	0.15
Outer/inner diameter of fuel pin (cm)	0.757/0.15
Outer/inner diameter of cladding (cm)	0.91/0.773
Outer/inner diameter of guide tube (cm)	0.126/0.106
Outer/inner diameter of central tube (cm)	0.13/0.11
Fuel pin material	UO_2
Density of fuel pin material (g/cm^3)	10.4
Material of clad	Alloy E110
Density of clad material (g/cm^3)	6.4516
Guide/central tube material	Alloy E110
Composition of clad material (%)	98.97 Zr, 1 Nb, 0.03 Hf
Density of guide tube material (g/cm^3)	6.4516

FA Design Data	Value
Absorber material	Gd_2O_3
Mass fraction of absorber material in fuel (w/o %)	5
Density of absorber material (g/cm^3)	7.41
Number of spacer grids in active core	13
Material of spacer grid	Alloy E635
Composition of material (%)	98.97 Zr, 1 Nb, 1.3 Sn, 0.3 Fe
Density of material (g/cm^3)	6.55

2.5.1.3. Control rod design specification

The reactor core contains 61 control rod cluster assemblies, which are divided into 10 groups in a VVER-1000. The arrangement of the control rod groups in the core is demonstrated in Figure 2-6. The reactor control system provides a way of starting the reactor by bringing the power output up to a desired level and maintaining it at that level by compensating for the changes in the properties of the system that take place over its lifetime. Control rods have materials with large cross-sections for neutron absorption. The insertion or withdrawal of control rods will thus have an effect on the k_{eff} of the system. The control rod type used in a VVER reactor type is composed of two different materials, which are B_4C (boron carbide) and Dy_2O_3•TiO_2 (dysprosium titanate), with the B_4C located in the upper part and Dy_2O_3•TiO_2 located in the lower part of the rod.

Boron carbide accumulates large radiation-induced damage caused by (n, α)-reactions on ^{10}B isotopes, helium formation and swelling (Risovany, et al., 2000). Because of the large radiation damage, research suggests that the control rod B_4C can be combined with Dy_2O_3•TiO_2, since Dy_2O_3•TiO_2 has high dimensional and structural stability. The suggestion is that the Dy_2O_3•TiO_2 will occupy the part of the rod where the highest radiation dose is experienced, while B_4C will occupy the other part of the rod.

Table 2-5 below gives the details of the control rods that are used.

Table 2-5: Key control rod parameters

Characteristics	
CR diameter (cm)	0.7
CR materials	B_4C Dy_2O_3•TiO_2
Densities of the materials	1.8 5.1
Length of the CR column (cm) ▪General ▪Upper part ▪Lower part	 350 320 30
Outer/inner diameter of clad (cm)	0.82/0.70
Clad material Clad density (g/cm^3)	Steel 06x18H10T 7.75
Composition (%)	0.08 C, 18.5 Cr, 1.5 Ni, 1 Ti, 69.92 Fe

The following Figure 2-6 represents the control rod assembly layout in the core.

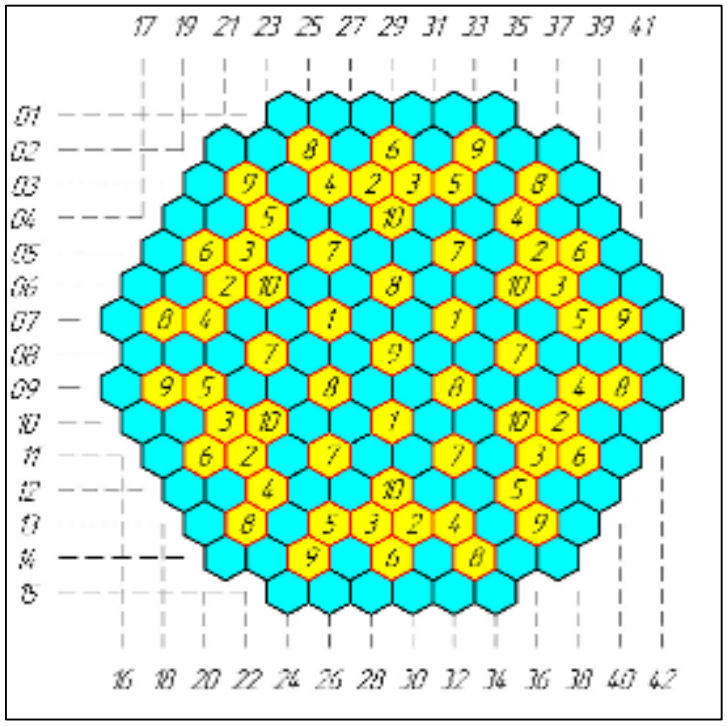

Figure 2-6: Position of the control rods in the reactor core

During normal operation, all groups of control rods may be in the top position above the core, except for group 10, which is a work group that serves to compensate for small changes in reactivity due to oscillations in temperature and boron concentration (Lyon, 2005)

2.5.2. VVER-1000 Core Symmetry

A VVER-1000 reactor core can be divided into 60^0 symmetry, with each containing about 28 fuel assemblies (Pirouzmand, 2014). This means that the VVER-1000 can have two symmetry options, which include a $1/6^{th}$ and $1/12^{th}$ symmetry. In many studies it is shown that for an investigation of the behaviour of a FC, $1/6^{th}$ (displayed in Annexure A) or $1/12^{th}$ core symmetry can be used (Pirouzmand, 2014; Jahanbin & Malmir, 2011). The results from a symmetry core can be used to investigate the FC behaviour of interest. The reactor power distribution for the $1/6^{th}$ model may be investigated and compared with the FC model. If the neutron flux of a $1/6^{th}$ model can be determined, the distribution of the FC axial and radial power may be calculated. For such models, a reflective boundary condition would be required on the lateral sides of the segment to model the symmetry.

2.6. Reactivity Coefficients

Reactivity coefficients are very important parameters to be calculated for a reactor core system, since the changes in reactivity coefficients would suggest the consequences (such as transient, prompt criticality or accidents), of sudden changes in the reactor's operating parameters. Therefore, it is important to have reliable methods to measure the reactivity coefficients in a reactor system. At the BOC, large excess reactivity can be experienced. Excess reactivity is defined as the value of reactivity when all control poisons and rods are not loaded in the reactor system. Large excess reactivity must be avoided at BOC.

The general criterion for a reactor system is that the total of all the reactivity coefficients must be negative when the reactor is in a critical state. A specific reactivity coefficient may, however, be positive, but the effect of that positive feedback must be negligible. However, in particular for VVERs, the Russian requirement is that each one of the reactivity coefficients must be negative under all power conditions (IAEA, 2003).

The reactivity coefficients that are considered most important for PWRs are the MTC and the Doppler coefficient (DC) (Oka, 2010). Other temperature coefficients (e.g. the expansion coefficient) were not considered in this study.

The limits on reactivity feedback coefficient in all reactor states for PWRs are as follows (IAEA, 2003):

Table 2-6: Reactivity feedback coefficient limits for a typical PWR

Parameter	Limitation
Boric acid coefficient pcm/ppm	$-10.86<C_B<-5.71$
Moderator temperature coefficient pcm/K	$-70.0<\alpha_{T,m}<0.00$
Doppler coefficient pcm/K	$-4.90<\alpha_{T,f}<-2.90$

For any analysis of reactivity coefficients, the reactivity of the system must be established. The reactivity of a reactor system defines the state of the reactor core. The equation that represents reactivity is as follows:

$$\rho = \frac{k-1}{k} \tag{2-31}$$

where k is the multiplication factor defined in Section 1.2.

Reactivity is measured in per cent mill (pcm, 10^{-5}) (Anglart, 2005). When a reactivity is obtained such that ρ < 0, it means that the reactor system is subcritical, if ρ > 0 the reactor system is supercritical and lastly at ρ = 0 the system is critical. A change in reactivity can be measured when applying new changes in the reactor. The measure of the change in reactivity is used in determining the reactivity coefficients of the several temperature changes introduced in the system. The temperature coefficient of reactivity can be defined as (Stacey, 2007):

$$\alpha_T \equiv \frac{\partial \rho}{\partial T} \cong \frac{1}{k}\frac{\partial k}{\partial T}. \tag{2-32}$$

This can be further divided into individual components characterising specific aspects (geometry, materials) of the reactor, as will be discussed below.

2.6.1. Doppler Coefficient

The behaviour of the reactor core and the multiplication factor are greatly affected by the core temperatures associated with the fuel, hence the temperature effect and the temperature feedbacks (DC) must be accounted for in the core calculations. The neutrons and nucleus interaction vary rapidly with the incident energy. When the neutron absorption in ^{238}U changes in response to a change in temperature, Doppler effect is introduced. As the fuel temperature increases, a resonance broadening of ^{238}U occurs, as shown in Figure 2-7. As a result, neutron absorption by ^{238}U increases, which leads to fewer neutrons being available for the fission reaction (Lewis, 2008). This reduces the reactivity, therefore generating a negative reactivity (Bernard, 2012).

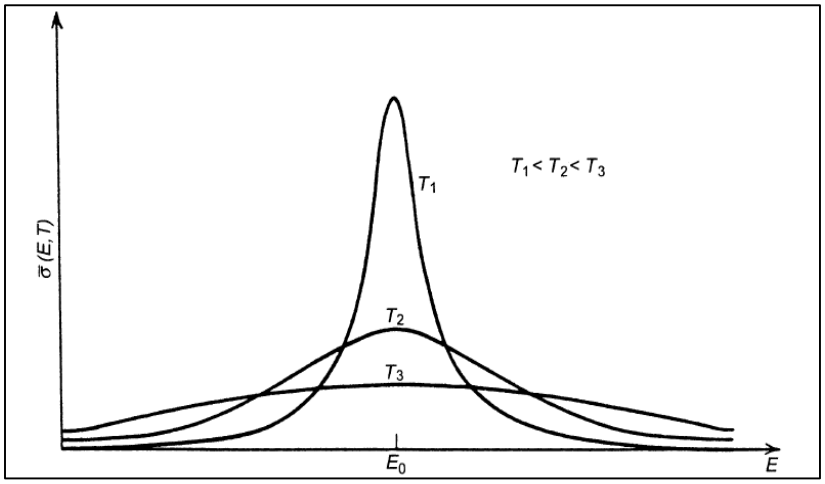

Figure 2-7: Doppler broadening

The DC then indicates the reactivity change with respect to change in fuel temperature, keeping other parameters, such as the moderator temperature, constant. The approximate DC can be calculated using the equations (Anglart, 2005):

$$D_C \equiv \frac{\partial \rho}{\partial T_f} \cong \frac{1}{k}\frac{\partial k}{\partial T_f} \tag{2-33}$$

where, ∂T_f is the change in fuel temperature.

A study was done on the DC, in which an analysis of the DC on UO_2 was performed using MCNP5 with ENDF/B-VI and ENDF/B-V for the cross-sections (Thilagan, et al., 2007). The calculations were performed at hot zero power (HZP) (at 600 K) and hot full power (HFP) (900 K). The DC was analysed for a fuel pin cell configuration with several different kinds of uranium enrichments in a typical PWR. To model this particular pin cell, reflective boundary conditions were assumed on all four sides of the pin cell. The thermal scattering treatment option was used to take care of the binding effect of the hydrogen in water. For UO_2 with 2.4% and 3.1% ^{235}U enrichment, the results for k_{eff} ± σ and DC were obtained as 1.17185 ± 0.00017 and -2.14168 pcm/K, and 1.09377 ± 0.00017 with -2.38849 pcm/K respectively. In the current study, the DC is investigated for an FA model at cold 300 K. In the above-mentioned study, the fuel enrichments match the fuel enrichments of the pins that are used in the FA model. The study can be used to compare the calculations with the calculations of the current study.

2.6.2. Moderator Temperature and Density Coefficient

The MTC is defined as the measure of the change in reactivity due to a change in specific coolant parameters such as temperature and density, pressure or void of the coolant. In water-moderated, water-cooled reactor cores, the effect of the moderator temperature on reactivity is mainly due to the temperature changes in the moderator and the effect these have on the moderator density. As mentioned earlier, a reactor core must be designed such that the MTC has a negative value, to ensure that negative reactivity feedback will be provided in the event of a power excursion (Mourtzanos, et al., 2000). However, the value of the MTC must not be too negative because certain off-normal sequences may exist, in particular cool-down accidents in PWRs, which are made worse by a large negative MTC (USNRC, HRTD, n.d.).

An increase in moderator temperature would result in a decrease in moderator density, which means fewer neutrons will be produced. These effects will add negative reactivity into the core. The negative reactivity will cause the reactor power to decrease and it will limit any condition that could cause an increase in the power. Operating with a negative MTC is desired in PWRs. As stated at the beginning of the section, a reactor would have excess reactivity at BOC. Because various operating limits require the control rods to be fully withdrawn from the core, the moderator will have boric acid to compensate for the excess reactivity (USNRC, HRTD, n.d.).

The soluble boron used in the coolant for reactivity control will have an impact on the moderator coefficient, since the soluble boron density and the water density decrease together with the rise in water temperature. As the soluble boron decreases in the core, a positive reactivity effect may result. This added positive reactivity would disrupt the negative reactivity added owing to the decrease in the moderator temperature.
For MTC calculations the following relationship is applied (Anglart, 2005):

$$MTC = \frac{\partial \rho}{\partial T_m} \cong \frac{1}{k}\frac{\partial k}{\partial T_m} \tag{2-34}$$

The recommended range for the temperature change in the MTC reactivity analysis goes from 3 ºC to 5 ºC (Mourtzanos, et al., 2000). A large temperature change will produce an MTC that might not reflect the value of the MTC of interest, whereas a small temperature change might produce a reactivity change that is determined more by interpolation accuracy and round-off. In a particular study where the MTC was analysed, the MTC value was determined to be -48 pcm/K using a temperature change of 4 ºC.

It is stated that the study was done to determine the effects of the core reflectors and the effect of the magnitude of the moderator temperature change. In this study, the reactivity coefficient of the moderator temperature is investigated at 300 K.

2.7. Critical Boron Concentration

In order to avoid large excess reactivity, a material with a high neutron absorption cross-section such as soluble boron (boric acid) may be loaded to compensate for the reactivity at BOC. Soluble boron is added in a way that the concentration is decreased from the BOC to the end of cycle (EOC), so that their negative contribution to the reactivity becomes negligible in the later stage of the cycle (Caprioli, 2004). Thus, boric acid is added into the system in order to control reactivity variations due to the fission product concentration variation and fuel burn-up.

This is a slow process used only to control slowly varying reactivity effects and the control is accomplished by varying the concentration of the absorber in the coolant (Manassah, 1981). The limit on the boron concentration in the Russian Federation is 16 g/kg boric acid concentration, which is equivalent to about 2700 ppm boron concentration (IAEA, 2003). The limit on the boron concentration is required because a coolant density decrease due to a temperature rise will lead to a decrease in boric acid concentration; this could introduce a positive reactivity effect on the MTC. The requirement for a negative MTC will limit the amount of boric acid concentration allowed.

The boron in the water can be used to achieve criticality when all rods are withdrawn. In the coolant, the boron decreases as the reactor is operational until it reaches 0 at EOC. To convert the boric acid units from ppm to g/kg and vice versa, the equivalency in Equation (2-35) is used (IAEA, 2003):

$$2100 \text{ ppm} = 12 \text{ g/kg}. \qquad (2\text{-}35)$$

For the criticality solution, a study based on *Determination of reactor parameters during start up tests at the Tianwan NPP, unit 1* was reviewed (Astakhov, et al., 2006). An experiment was performed to measure the reactor neutron physics parameters during physical start-up. One of the purposes of the study was to reach criticality parameters without the use of an external neutron source. The experiment was performed at HZP. The criticality of the system at HZP was reached with the boric acid concentration at 7.54 g/kg (1319.5 ppm). The critical boron that was applied to reach criticality was 2% larger than the design value of the system, which is 7.38 g/kg (1291.5 ppm).

Another study was performed in which the effects of spacer grids were investigated using different types of models (Pazirandeh, et al., 2011). For the current study, spacer grids where included and it is therefore relevant to look at the parameters that were obtained from Parizandeh. The model of interest was the heterogeneous model of the spacer grid. The core calculations were performed for the core with control rods fully withdrawn. The critical boron concentration at CZP for the heterogeneous model was found to be 1429 ppm. The results obtained from the current study will be compared to those of the studies mentioned above.

The efficiency of the boric acid in the water can be determined by investigating the boron worth. Boron worth is described as the fraction change in the k_{eff} per unit concentration of boron in parts per million (Manassah, 1981):

$$W_B = \frac{1}{k_{eff}} \cdot \frac{dk_{eff}}{dC_B} \tag{2-36}$$

In the literature study that is mentioned in this section, the boric acid worth was analysed to be −2 ± 0,2 %/g/kg H_3BO_3, (-11.429 ± 1.143 pcm/ppm) with the design value being −2,06 %/g/kg H_3BO_3 (-11.771 pcm/ppm)

2.8. Control Rod Worth

In a reactor system, control rods are employed to maintain the desired state of fission reactions within a nuclear reactor. The control rods can either be inserted in or removed from the reactor to achieve criticality of the reactor. When moving a reference control rod a few steps into the reactor core, an amount of negative reactivity is inserted and the neutron flux signal begins its exponential decline. The change in reactivity due to the control rod movement is referred to as the control rod worth. To calculate the control rod worth, a control rod can be inserted or withdrawn in small increments, and the change in reactivity determined by following each increment (Anglart, 2005). The control rod worth analysis is divided into two types, namely the differential and integral worth.

The differential worth (pcm/cm) is the reactivity change that is brought about by the movement of a rod and the integral rod worth (pcm) at a given position is the summation of the entire differential rod worth up to the point of withdrawal (Burn, 1988).

In addition to controlling criticality, control rods are also used for emergency shutdown/SCRAM of the reactor. This can be an example of an accident situation. In this case the control rods are inserted to their maximum depth and the reactor core is then shut down. In this case, the integral worth of the control rods becomes an important parameter.

The Figure 2-8 represents shapes that can be expected from the control rod worth (Burn, 1988).

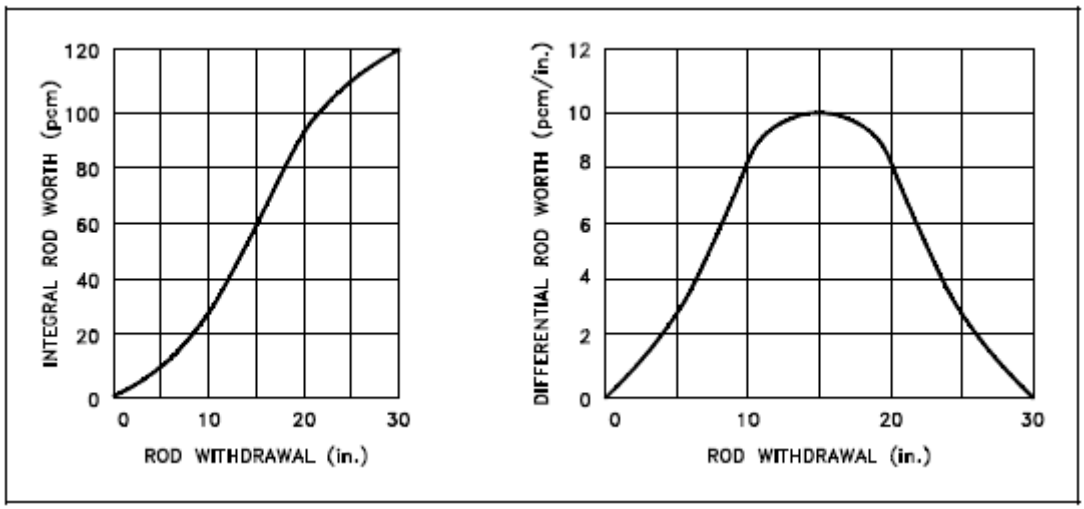

Figure 2-8: Control rod worth

The differential rod worth has a bell shape. It has very low values at the top and bottom of the core and a maximum value at the centre of the core. The curve has this shape because rod worth is related to neutron flux, and flux is highest in the centre of the core.

The integral rod worth is expected to have an “S” shape, which has a relatively flat slope at the top and bottom of the core and a maximum slope at the centre of the core. However, in the European pressurised reactor’s (EPR) final safety analysis report (FSAR) it has been seen that the integral rod worth does not necessarily show a flat slope at the top of the core. During the first few steps of insertion the slope is seen to be too flat, as is evident in Figure 2-9 below.

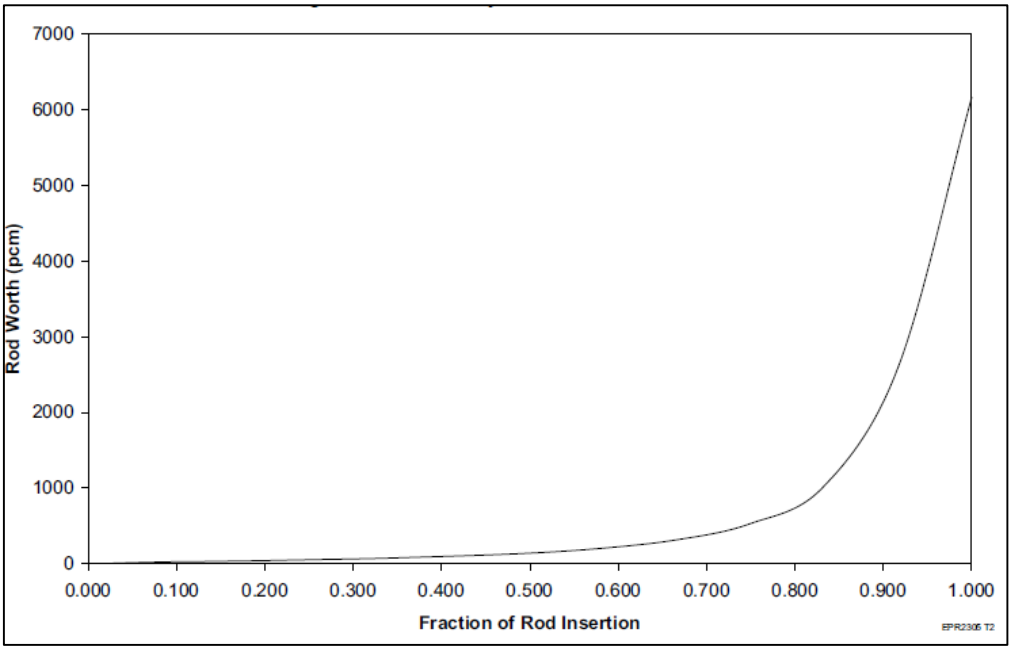

Figure 2-9: EPR's control rod worth (AREVA, 2012)

A study was also performed on the rod worth of the EPR at 300 K (Montwedi, 2014), using MCNP5. The results were seen to be in good agreement with the results from the FSAR of the EPR (AREVA, 2012). Therefore it means that although the integral is expected to take the shape of an “S” curve as in Figure 2-8, it can also look as it does in Figure 2-10.

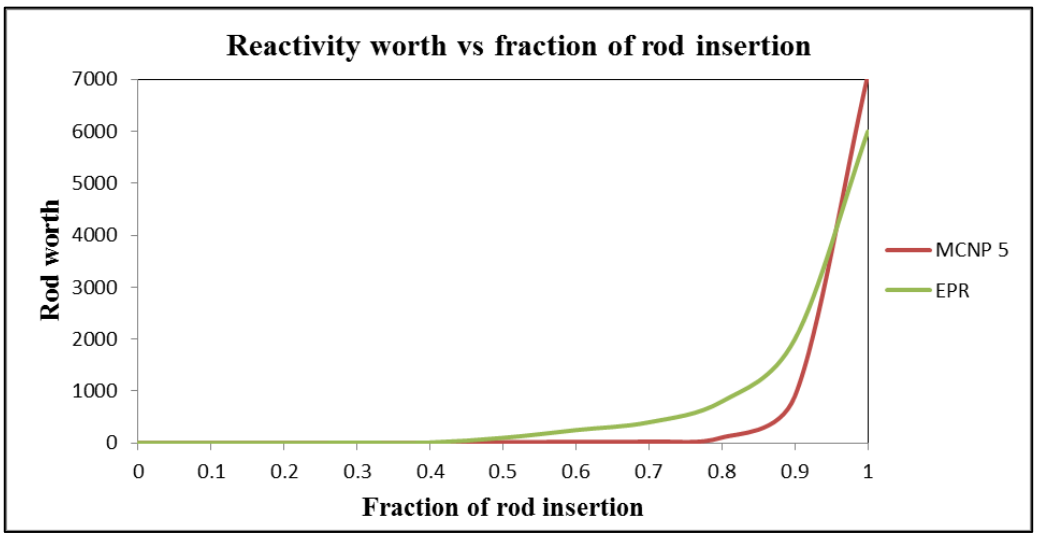

Figure 2-10: Integral rod worth of EPR (Montwedi, 2014)

2.9. Delayed Neutrons

Typically 0.65% of the neutrons emitted in the fission process are delayed by up to several tens of seconds in the light water reactor (Bernard, 2012). The remaining 99.35% are emitted immediately upon fission and they are called prompt neutrons. The delayed neutrons result from the decay of the fission products and each fissionable isotope has its own distribution of fission products. Because the effective neutron fraction plays an important role in the reactivity transient analysis (safety and control of nuclear reactors), the determination of this phenomenon is of great importance in the reactor physics calculations.

Power changes in the initially critical reactor may depend on the effective delayed neutron fraction. If the reactivity exceeds beta effective, the power would increase dramatically within a very short period of time (Rineiski, 2011).

The following study was reviewed for this type of analysis: *Kinetic parameters evaluation of PWRs using static cell and core calculation codes* (Jahanbin & Malmir, 2011)

In the above-mentioned article, effective delayed neutron fraction and prompt neutron lifetime were evaluated for a typical VVER-1000 using static cell and core calculation codes. The results were compared with results from an FSAR of the reactor (BNPP-1, 2007).

The calculations were done at BOC and also at EOC of the VVER-1000 core. The interest in this case is in the calculated results at BOC. The result that was obtained for β_{eff} at BOC was β_{eff} = 0.00761, and the result from the FSAR is β_{eff} = 0.0074, with the relative error being 2.29 %. The results were observed to be in good agreement.

Equation (2-37) was used to calculate the relative error:

$$RPE = \left|\frac{actual\ value - calculated\ value}{actual\ value}\right| \times 100\%. \qquad (2\text{-}37)$$

2.10. Verification

One of the aims of the research is to verify the NWURCS suite of codes. The NWURCS code is used in the study to generate the INP file of MCNP6 (discussed further in Section 3.3) VVER-1000 model. Verification of the NWURCS code means the code must accurately produce the input file that can be built manually. Verifying the NWURCS code means checking the input file that is generated by the code to ensure that it represents the actual definition of what it should look like, that is initially given by the user.

Verification is one of the primary means to assess accuracy and reliability in code model simulations. Verification gives evidence that the model is solved accurately by the mathematics embodied in the code.

In the current study, the verification process is applied in order to ensure that the NWURCS code produces the exact geometry with all the needed information of the model as defined in literature.

3. Methodology

The current section, will give the methodology that was followed to conduct the study. A neutronic calculation was performed for the three models of the study, namely an FA model, FC model, and a 1/6th core model. The method that was used to perform the neutronic calculations such as the critical boron concentration, reactivity coefficients, control rod worth and beta coefficient is given. As mentioned in Section 2.2, MCNP uses Monte Carlo techniques in order to complete its simulation, below is the practical overview of the methodology of the MCNP. The verification method is also given below.

3.1. MCNP INP file

The NWURCS code was used in this study to generate the MCNP6 INP file. The MCNP6 INP file is a file that contains the reactor geometry, the surfaces that bound the reactor, the type of materials and the materials' nuclear data libraries used in the reactor, etc. Most importantly, the MCNP6 INP file defines the type of problem to be modelled. The structure that the INP file follows is given in Table 3-1 below.

Table 3-1: MCNP INP file format

Message block {optional} Blank line delimiter {optional} One-line problem title card Cell cards [Block 1] Blank line delimiter Surface cards [Block 2] Blank line delimiter Data cards [Block 3] Blank line delimiter {optional}

The NWURCS code was used in this study is to generate the MCNP6 INP file. The NWURCS code verification was done by verifying that the generated INP files retain the structure that is envisioned by the model developer. In this regard, one should note that when modelling any real system, the model in most cases cannot be an exact representation of the real system. It is then the task of the model developer to decide on how close one can come to modelling the real system.

The definitions of the cards shown in Table 3-1 are provided in this section.

3.1.1. Title Card

The title card is used to write the title that defines the model. Users can determine which names they want to give their models. The title is in free format.

3.1.2. Cell Card

The geometry of the model is defined using two cards, namely the cell card and surface card. The cells of a reactor in MCNP are defined by intersections, unions and complements of regions bounded by surfaces. The general form of a cell card is as follows:

j m d geo (params)

where:

- j: Describes the cell number. This number must be a positive integer.
- m: Gives the material number, which will correspond to the material number that is specified in the material card (m = 0, the cell is used as a void)
- d: Defines the density of the material, which can be positive or negative. A positive number indicates that the density is in units of 10^{24} atoms/cm^3, and a negative number gives the units in g/cm^3.
- geom: Specifies the geometry of the cell, and consists of a list of surfaces that bound the area in question. It uses Boolean operators together with allocated surface numbers to describe how surfaces bind regions of space to form a cell.
- params: Specifies the cell parameters by entries in a keyword.

An example of a cell card follows:

```
14      4   0.073556 -44 -11 12                imp: n=1 u=    1
        tmp= 4.912E-08     $   570.0000 K    296.8500 deg C
```

The number 14 denotes the cell number, and 4 is the material number of the material in cell 14, with a density of 0.073556 given in units of atoms/barn-cm. The surfaces that bind the cell are -44 -11 12. If the surface is a cylinder, then a negative value means that the volume inside the cylinder must be considered, and a positive value would be the opposite. If the surface is a plane, then a negative value means that the volume to be considered is in the negative direction of the plane, normally starting from the plane, and vice versa if positive. Other types of surfaces can also be defined in a similar fashion. The cell requires neutron reactions only, which is indicated by imp: n=1. Because MCNP6 can define cells in universes, u=1 implies that cell 14 is contained in universe 1. The temperature of the material in the cell is given as tmp = 4.912E-8 in units of MeV. The values after the dollar sign ($) are commented out, which means they will not be simulated in the model. These values show the temperature in K and ℃.

Universes in this case are used to define repeated structures of the models. The following points define what universes are in MCNP:

- A universe is either a lattice or an arbitrary collection of cells that, once defined, can be used to fill other cells within their geometry.
- The universe card is entered in the “params” section of the cell card. Universe numbers are arbitrary integers chosen by the user.

A full description of how universes are implemented in MCNP6 can be obtained in the MCNP6 manual (Pelowitz, 2013).

The strategy that is used in NWURCS to generate universes is discussed in Annexure B together with the structure that the universes would retain in an INP file. The universes are important in the study because they assist with accurate definition of the geometry of the model, since they have repeated structures.

3.1.3. Surface Card

The surface card contains information on the surfaces that make up the geometry of the problem of interest. Surfaces can be defined by equations, points or macro-bodies (as described in the manual (Pelowitz, 2013)). The format that the surface definition has is as follows:

j (n) a (list)

where j denotes the surface number, which uniquely identifies each surface, and n is used for the coordinate transformation. The ‘a’ denotes the equation mnemonic. The list parameter contains the card entries, which are the dimensions of the equation mnemonic. Two examples of a surface definition are given below.

Example 1: 101 rhp 0.00000 0.00000 - 89.00000
0.00000 0.00000 0.75000
0.63850 0.00000 0.00000

Example 2: 1 pz -176.50000

In example 1, the surface is defined by a macro-body right hexagonal prism (RHP). The number 101 is a surface number for a RHP about the z-axis whose base is at z= -89.00 cm with a height of 0.75 cm and whose first facet is normal to the x-axis at x= 0.6385 cm. In example 2, the number 1 is a surface number for the plane that is normal to the z-axis at z= -176.5 cm.

3.1.4. Data Card

Data cards are used to define how the problem of interest should be simulated. The information defined in the data card, is the material definition (M card), source definition, tally type specification, energy, reaction types and other data required, depending on the calculation.

3.1.4.1. Material specification

The material specification involves the following definition:

- Material number
- Material isotopic composition
- Cross-section evaluations to use
- MT thermal neutron scattering card.

The material (Mm) cards are used to specify the material for all cells. The “m” on the material cards denotes the material number being referenced in the cell card. The choice of libraries in MCNP6 is made through a unique identifier for each library called the ZAID. The ZAID identifier comprises the atomic number (Z), mass number (A) and the library identifier (ID) (Pelowitz, 2013). An example of an M card is given below.

```
m19 8016.80c 6.67E-01
      8017.80c 2.54E-04
     92235.80c 4.39E-03
     92238.80c 3.29E-01
mt19      o2/u.20t u/o2.20t
```

Material 19 defines the fuel material UO_2 with enrichment of 1.30%, with ZAID numbers of 92235, 92238, 8017, and 8016. The 80c entry represents a particular cross-section evaluation. The atomic fraction is the last entry after the cross-section evaluation. A positive number on the atomic fraction represents atomic fraction instead of mass fraction (also known as weight fraction).

The mt card is used to specify thermal scattering cross-section data treatments for isotopes of the materials in the thermal regime. The reason for using an mt card is that the isotopes are bound in materials, where the binding has effects in the energy loss in collisions experienced by slow neutrons. To take the binding effects into account, the mt card is given in the calculations.

3.1.4.2. Criticality calculations

A criticality code (KCODE) card is used in MCNP to accomplish the criticality calculations. The KCODE card specifies the criticality source that is to be used to determine k_{eff}. The KCODE is represented in the following manner:

KCODE NRSCK RKK IKZ KCT

where:

NRCK: is the number of source histories/ neutrons per cycle,

RKK: is the initial guess of k_{eff},

IKZ: is the number of cycles to be skipped (to ensure convergence before averaging calculations)

KCT: is the number of cycles to be done.

An example of a KCODE would look like this:

KCODE 100000 1.0 300 500

The above example tells MCNP to sample and track 100 000 starting neutrons for each cycle or each generation of neutrons, and the initial guess for k_{eff} is 1.00. The first 300 cycles are to be skipped so that the fission sites can reach equilibrium. From 301 cycle, MCNP will build an average of the calculated k_{eff} after each cycle. When it has completed all 500 cycles, a final result of k_{eff} is obtained. The spatial distribution of fission points requires either a criticality source or source definition card in the KCODE card to be defined. The format of the SDEF or KSRC card can be seen in Annexure B.

3.2. Preparation of the MCNP6 INP File

The MCNP6 INP file for the VVER-1000 model was prepared based on the literature discussed in Section 2.5. In NWURCS code, the INP file is generated by running executive files in the MCNP command window (Naicker, et al., 2015). A brief description of each of the executable files is given in Section 3.3.

The assemblies for this model are denoted as follows:

Table 3-2: Model definition of FA

FA type	NWURCS Model Definition of FA type
13AU	200
22AU	300
30AV5	400
39AWU	500
390GO	600

As defined in (Naicker, et al., 2015), the FA in NWURCS must be specified as numbers 100, 200, 300, etc. The FA numbers in this study start from 200, because the integer 100 for FA was used to define the core baffle of the reactor core.

3.2.1. Model assumption

The calculations of the VVER-1000 model are performed at 300 K. This is done so that thermal-hydraulic coupling is not required. It is envisioned the thermal-hydraulic studies will be performed in a follow-up study, and thereafter, neutronic-thermal-hydraulic coupling will be performed.

The assumptions are as follows:

- The study is based on a fresh fuel model at 300 K; therefore burn-up calculations are not included in the study.
- The central guide tube is assumed to be filled with water. The central tubes are not investigated in the study, although literature states that the central tube is filled with water (Pazirandeh, et al., 2011). However, most studies that have been done do not state clearly what the central tube must be filled with.
- A homogeneous material is assumed for the reflectors. Accounting for the heterogeneity of the reflectors is reserved for later studies.
- No change in boron and xenon is assumed during the neutronics analysis.

3.3. North-West University Reactor Core Suite

The NWURCS is a suite of codes that can be used to generate the INP files for MCNP6 and RELAP5. The in-house code is used to generate the MCNP6 INP files for this study. Furthermore, the suite of codes is also used for coupling calculations between flux and temperature calculations (coupling of MCNP6 with RELAP5). The suite of codes can also be used to extract data from the output; making the data analysis easier for the user.

The NWURCS suite of codes is developed using the computer language FORTRAN, by the NWU School of Mechanical and Nuclear Engineering team (Naicker, et al., 2015). The motivation for developing this FORTRAN code was that the MCNP INP file has about 300 000 lines and writing these lines manually would require a large amount of time and also introduce human error. The NWURCS code allows the user to describe each section of the MCNP INP file separately. In this way, it is easy for the user to navigate through each section

to confirm whether any errors have been made before even running the calculations. A sequence of commands is performed in the windows command window to generate the file.

The sequence that is followed when generating the MCNP INP file is as follows (Naicker, et al., 2015):

I Apr0415: creates a batch file “createfolders.bat”

II Createfolders: The iter00 and iter01 are iteration sub-folders. When running this step, the contents from subfolder iter00 is transferred to iter01.

III Apr0615: sets up control rods from control banks. The user specifies the layout of the control banks and also the depth of insertion of the rod into the reactor in a file called controlbank.

IV Apr0315: prepares the material library

V Mar2915: prepares the starting temperature field

VI Apr0215: prepares the FA files

VII Mar2715: prepares the core loading pattern

VIII Mar3115: prepares the MCNP6 INP file

IX Run MCNP6 for the calculation.

If any errors are detected in one of the sequence, the error is indicated in the command line before one can continue running the next executable, thus immediately indicating where the problem is. Whether the INP file is generated manually or by an automated code, it must still retain the same format of an MCNP INP file as described in 3.1. To verify that the INP file contain the information of the model as described in Section 2.5, the geometry, material, tally and control rod movement must be tested.

3.4. NWU High Performance Computing

NWU High Performance Computing (HPC) was used in the study for the calculations that were performed in MCNP to help reduce the time that MCNP would normally take when running on a standard windows PC. The HPC is a dedicated computer cluster that provides the means for extensive parallelised mathematical computations. The HPC has processors that can perform a calculation with a maximum of 32 nodes; the 32 nodes are equivalent to a Dual Quad-Core Intel Xeon E5450. The installed memory of HPC is 320 GB RAM and the storage memory is about 20 TB. The HPC system operates in the Linux system environment (van der Merwe, 2013). An MCNP calculation has the tendency to take a very long time to complete. To reduce the calculation time of MCNP6, the neutronics calculations were therefore done using HPC.

The HPC operates as a remote controlled system. Two systems are used to access the HPC system. The first is called FILEZILLA and was used to transfer files from the laptop computer to the HPC system. The second is called PUTTY, an open-source terminal emulator, which was used to initiate the MCNP6 calculations by automatically reading the data provided by FILEZILLA.

3.5. Model Verification Method

3.5.1. Verification

The method used to verify the NWURCS code was divided into three steps. The NWURCS code was verified by inspecting the INP file, and by visually inspecting the VVER-1000 models developed in this study.

3.5.1.1. Verification by visual inspection

The VISED code was used for visual inspection of the models. When viewing an INP file, the user will first open the VISED code window and then open the file by going to the directory where the desired file has been placed. The VISED will require the user to specify how the code should display the geometry of interest. Figure 3-1 below gives a brief on what type of options are available in VISED for the display of the geometry.

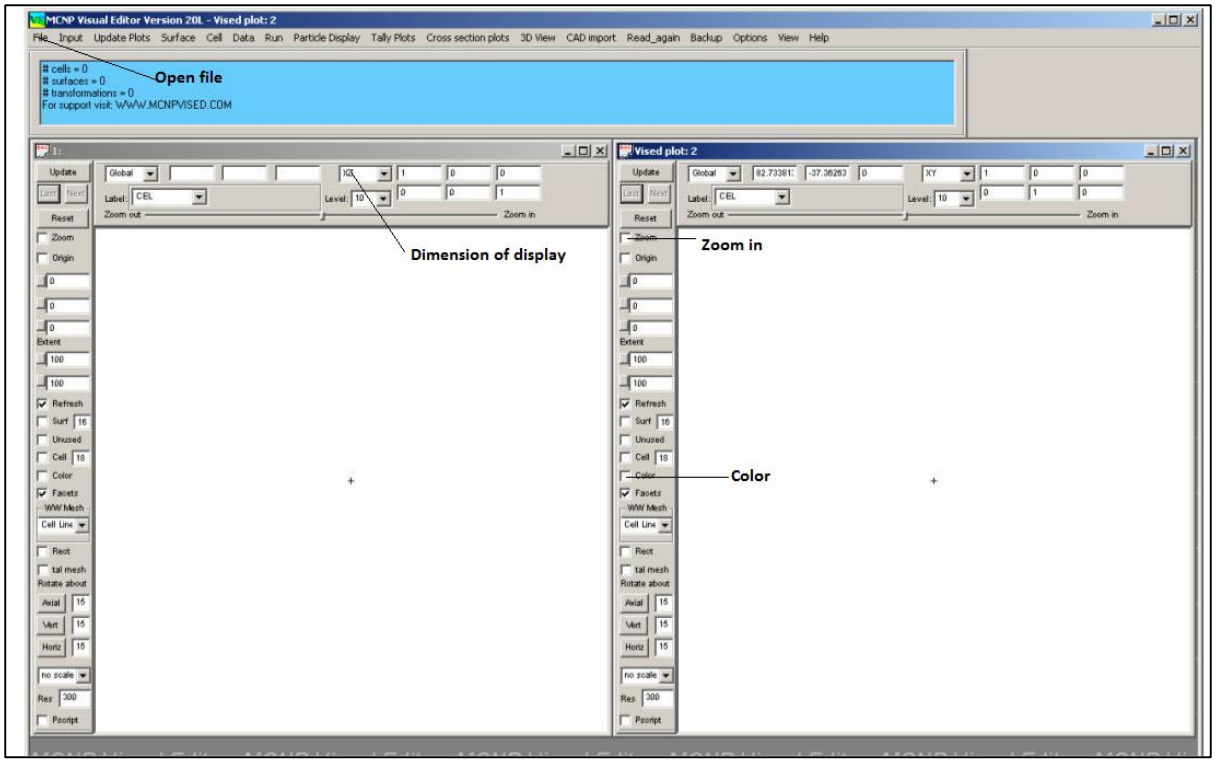

Figure 3-1: VISED display screen

As can be seen in Figure 3-1, when the file has been opened, an option to show colour, or in which plane the geometry be must shown in the display screen of VISED, etc. must be chosen. Once everything has been defined by the user, the geometry will be displayed in VISED. A detailed method according to which VISED works is provided in the VISED manual (Schwarz, et al., 2011).

3.5.1.2. Verification by inspection of the INP file

By thoroughly going through each cell, confirming each material and the surfaces that bind the materials, verification of the NWURCS code can be performed. An INP file can sometimes be very huge, and it would be hard for one to go through each line for verification. To confirm that the verification was correctly done, one can create a spread sheet in which the surfaces of the cells are noted step by step to see if they retain the model definition. In the study, a spreadsheet was created through which the materials and surfaces of the fuel pin, guide tube, etc were verified. This was done by going through the cells and noting the surfaces and materials they contained.

3.5.1.3. Verification by performing calculations on Excel

When verifying the materials involved in the models one can either perform manual calculations or if provided in literature, compare the materials' atomic fractions and densities that were generated by NWURCS to see if they match. The calculations can be done in Excel by using the chosen available data on the materials provided in literature.

3.5.2. Boundary Conditions

Two types of boundary conditions were applied for the models, namely reflective and vacuum boundary conditions. The reflective boundary condition is applied to reflect the neutron back into the geometry, while the vacuum boundary condition causes MCNP6 to stop tracking the neutron once it moves out of the geometry, i.e. past the boundary (Leppanen, 2015). For FA and $1/6^{th}$ core, reflective boundary conditions are used and FC calculations make use of vacuum boundary conditions

3.5.3. Cross-section Libraries

The cross-section data for neutrons are obtained from ENDF/B-VII libraries available in MCNP6. For the treatment of thermal neutrons, MCNP6 is capable of using S(α,β) to account for the effect of chemical bonding and crystal structure of incident neutron energies of less than 4eV. Due to the use of the free gas model, MCNP assumes that the hydrogen is a free gas. One can also use the free gas model in MCNP6 (X-5 Monte Carlo, Team., 2003).

3.6. Convergence Method

MCNP6 uses an initial distribution of source points, with the number of particles decided by the user, and randomly samples from distributions to determine the outcomes of the particles. The particle histories are then tracked and recorded for each cycle. The MCNP6 code uses the power series method, which involves using the results of previous cycles of particles as inputs to the next cycle. This will cause the initial guesses of the positions of the source particles and k_{eff} to converge to their true values gradually. The power series method is used as part of solving a criticality calculation (Macdonald, 2012). This should not be confused with power iterations on the fission source that can be used in solving neutron transport using deterministic methods (Stacey, 2007).

Table 3-3 and Table 3-4 contain the cases that were investigated for convergence of the Shannon entropy H_{src} and also the k_{eff}/k_{∞} for FC and FA models. For the first five cases of the FC model the number of in-active and active cycles is kept constant and the neutron source points are varied. Cases 4b, 6, and 7 of the FC model keep the source points and inactive cycles constant, while changing the active cycles. In the FA model, the first three cases keep

the in-active and active cycles constant, while varying the neutron source points. Cases 4 and 3b of the FA model keep the source points and in-active cycles constant, while changing the active cycles.

Table 3-3: Investigated cases for FC model

Neutron source convergence			
Case	**N-neutrons/cycle**	**In-active cycles**	**Active cycles**
1	400 000	200	600
2	600 000	200	600
3	700 000	200	600
4	800 000	200	600
5	1 000 000	200	600
Active cycles convergence			
4b	800 000	200	400
6	800 000	200	600
7	800 000	200	800

Table 3-4: Investigate cases for FA model

Neutron source convergence			
Case	**N(neutrons/cycle)**	**In-active cycles**	**Active cycles**
1	100 000	200	600
2	200 000	200	600
3	300 000	200	600
Active cycle convergence			
4	300 000	200	400
3b	300 000	200	600

3.6.1. Source Convergence

MCNP looks at Shannon entropy convergence by checking for the first cycle after which all Shannon entropy results should be within one standard deviation of the Shannon entropy value for the second half of the cycles, which can include inactive cycles. A sufficient number of neutrons per cycle must be used in order to ensure timely convergence, accurate results and meaningful statistics. It is also important to determine the number of cycles required to run to converge the fission source distribution. Sufficient initial cycles must be discarded before the tallying begins, so that contamination of the results by the initial source guess becomes negligible.

The methods described below were used to determine the number of neutrons per cycle needed to converge the fission source. Initially a trial run was performed, during which an initial guess of the number of neutrons per cycle and the number of cycles to run was provided by the user. The next step was to analyse the results and observe whether the Shannon entropy had converged well or not. The analysis was done by creating of a plot of the Shannon entropy versus the number of cycles. The third step was to make another trial run, either by increasing the neutron numbers or by decreasing the numbers, depending on what was observed. This method could be repeated until the desired number of neutrons per cycle was reached. One would consider decreasing the numbers in terms of calculating time economy.

As discussed in Section 2.3.1, MCNP requires the definition of a mesh for the source entropy assessment for the models. The mesh described above is automatically generated in MCNP6 in this model, based on the average number of particles per bin. For the FC model, the mesh is 32 x 32 x 32 = 32 768 mesh cells with the following limits

Xmin= -1.3444E+02 Xmax= 1.2088E+02
Ymin= -1.0928E+02 Ymax= 1.1612E+02
Zmin= -2.4710E+02 Zmax= 2.4710E+02

For the FA model, the mesh is 27 x 27 x 27 = 19 683 mesh cells with the following limits:

Xmin= -2.8612E+01 Xmax= 2.8613E+01
Ymin= -1.6520E+01 Ymax= 1.6519E+01
Zmin= -2.4709E+02 Zmax= 2.4709E+02

The coordinates are in *cm*.

For source convergence, the cycle numbers were fixed as can be seen in Table 3-3 and Table 3-4 for both models.

3.6.2. K_{eff}/K_{∞} Convergence

The convergence of k (k_{eff} / k_{∞}) is done in parallel with the source convergence because k convergence can also be an indication of convergence of the fission source. The k convergence was established by post-process examination of the resulting trends in estimator.

3.6.3. Convergence of the MCNP Statistical Tally Tests

Tally checks were performed to determine the paths for convergence of the tallies and also to determine their effects on the precision of the results, as discussed in Section 2.3.2. The convergence of the tally of interest is as important as the convergence of k_{eff} and the convergence of fission source distribution in an MCNP calculation. The total number of active

cycles may be determined from tally checks analysis, because a well-converged tally must run through a certain number of active cycles.

There are 10 statistical tally tests available in MCNP, as discussed in Section 2.3.2.1. The table below gives the acronyms of the tally checks as analysed later.

Table 3-5: Acronyms used in statistical tests

Acronyms	Definition
Mean B	Mean Behaviour
RE V	Relative Error Value
RE D	Relative Error Decrease
RE DR	Relative Error Decrease Rate
VOV V	Variance of Variance Value
VOV D	Variance of Variance Decrease
VOV DR	Variance of Variance Decrease Rate
FM V	Figure of Merit Value
FM B	Figure of Merit Behaviour
PDF slope	Probability Density Function slope
F	Fail
P	Pass

3.6.4. Fission Energy Deposition

A fission energy deposition (F7) function (discussed in Section 2.2.4) is used in this study. By analysing the power profiles produced in the MCNP output, convergence of the tally is done. MCNP uses iteration methods for particle generation for the total number of cycles specified and when the total numbers of cycles is reached the generation of particles is terminated. The final value of k_{eff}/ k_{∞} and fission energy deposition from F7 tallies are recorded and produced as output. Therefore the right number of active cycles needed for convergence must be used. The tally convergence is observed by performing a series of criticality calculations where the cycles are varied, keeping the neutron source fixed, as seen in Table 3-3 and Table 3-4.

It is important to calculate the fission energy deposition, so that a well-converged power distribution profile can be obtained throughout the reactor core. The well-converged power distribution profile is used to confirm the number of neutron sources per cycle and number of cycles to run. The solution satisfying the symmetry condition with respect to the position at x=0 is $\varphi(x)=A\cos Bx$ (Coster, 2013). This equation is in most cases only applicable in the co-ordinate direction in which the material can be considered uniform (homogeneous)

3.7. Critical Boron Concentration

At the beginning of cycle the reactor is supercritical, and the reactivity could be expected to be significantly higher than a core in equilibrium. Addition of boric acid into the moderator is necessary at the beginning of life, to compensate for the excess reactivity.

In the MCNP6 calculation, the critical boron is obtained by initially performing a calculation with an initially guessed boron concentration value. The k_{eff} is analysed, and by observing that it is either subcritical or supercritical, a second guess at the boron concentration is made and the calculation is performed. Thereafter, the boron concentration is estimated using the linear interpolation method, until $k_{eff} = 1$. It is important to calculate the critical boric concentration before continuing any further calculations because a critical system would be the best state for the calculations to follow.

3.8. Boron Worth

The change in reactivity brought upon by the boric acid added to the water is called the boron worth. The boron worth of the added boron can be calculated using Equation (3-1).

$$W_B = \frac{1}{k_{eff}} \cdot \frac{dk_{eff}}{dC_B} \cong \frac{1}{k_{eff}} \cdot \frac{\Delta k_{eff}}{\Delta C_B}. \tag{3-1}$$

It is important to obtain the boron worth in order to see how much reactivity was added when a certain level of boron concentration is added in the reactor system.

3.9. Reactivity Coefficients

The analysis of the MTC was done by performing a sequence of static criticality calculations for different moderator temperatures T_m and then determining the MTC value from a table of k_∞ as a function of T_m. The value is determined by calculating the reactivity change due to a change in the moderator temperature approximating Equation (2-32) as:

$$MTC \cong \frac{\Delta\rho}{\Delta T_m}, \qquad (pcm/T). \tag{3-2}$$

The temperature step for the MTC analysis was 5 K. The recommended range for the temperature step is from 3 to 5 K (Mourtzanos, et al., 2000). Because the analysis was based on the moderator of the system, the rest of the materials in the FA were fixed at 300 K.

For the DC, a series number of static criticality calculations were performed at different temperatures of the fuel T_f and then the DC value was determined from a table of k as a function of T_f. The value is determined by obtaining the reactivity change due to a change in the fuel temperature, using the following approximation:

$$DC \cong \frac{\Delta\rho}{\Delta T_f}, \qquad (pcm/K). \tag{3-3}$$

The temperature step used for this analysis was 10 K, since a suitable value from the open literature could not be found. The cladding, helium gap, spacer grid and water were fixed at 300 K.

The reactivity coefficients as a function of temperature were calculated at CZP and without the control rods in the reactor system.

An FC model for this analysis was also performed. However, it was later discovered that even though the temperatures for the particular analysed materials were varied, the cross-sections for these temperatures were not interpolated. In the NWURSC code, a switch is defined on pseudo-materials to interpolate the cross-sections and correctly define the temperatures at the correct cross-section libraries; NWURCS did not seem to perform this for an FC model. This was discovered to be a problem (code bug) that was produced by the program, therefore the results that were obtained for the FC were not regarded as be reliable.

3.10. Control Rod Worth

As explained in Section 2.8 the control rod worth is the measure of the reactivity changes brought about by insertion or removal of the control rods in the core. Equation (3-4) was used to determine the worth of the control rod group 10 for this study. The reason for using group 10 for this study was that it is a regulating group used for fine adjustment and to maintain desired power/temperature shape. It should be noted that for an emergency shutdown/SCRAM study, the shutdown banks should be studied. The position of this group is shown in Figure 2-6. Both the integral and differential control rod worths were used to determine the reactivity change due to control rod movement between two points.

Rod worth:

$$Rod\ worth = \frac{\Delta\rho}{\Delta x}. \tag{3-4}$$

Equation (3-4) is used to calculate the differential worth in units (pcm/cm).

The integral rod worth at a given withdrawal is the summation of the entire differential rod worth up to the point of withdrawal (pcm) (Burn, 1988). The control worth was calculated by performing a series of calculations at various control rod positions.

The VVER-1000 reactor type makes use of two materials in a single control rod. Because of the fact that B_4C is normally used in PWR reactors, an analysis was done with B_4C only, and with both B_4C and Dy_2O_3•TiO_3. The analysis was done in order to see the different effects it might have on the reactivity of the system. The control rod model was performed for an FA model.

3.11. Effective delayed neutron fraction (β_{eff})

The beta coefficient as discussed in Section 2.9 gives the number of delayed neutrons that are obtained in the system. The following equation was used to calculate the delayed neutron fractions (Michalek, et al., 2003):

$$\beta_{eff} = 1 - \frac{k_p}{k_T} \tag{3-5}$$

where, k_p is the multiplication factor obtained by prompt neutrons and k_T is the multiplication factor using both prompt and delayed neutrons. In MCNP6 the beta delayed neutron fraction is computed by using a feature, TOTNU, provided in the code. It is mentioned in the manual (Pelowitz, 2013) that when the TOTNU card is not stated, by default, both prompt and delayed fission neutrons are used for all fissionable nuclides. The calculations without a specified TOTNU card would produce k_T. To compute the calculations where only prompt neutrons are available, a TOTNU NO card is provided. The resulting value will be k_p. Using Equation (3-5), β_{eff} can then be calculated.

4. Results and Discussion

The following chapter contains the results and discussions of all the model analyses that were performed for this study. The results discussed were performed for an FC, FA and a 1/6th core of the VVER-1000. The verification of the in-house code is presented. The FC was divided into 13 axial nodes and the FA was divided into eight axial nodes. The statistical uncertainty for the computed k_{eff}/k_{∞} for each calculation is presented next to each k_{eff} /k_{∞} result as the standard deviation σ.

4.1. Verification of NWURCS for the VVER-1000 Models

One of the purposes of the study is to verify as far as possible the NWURSC in-house code developed at the School of Mechanical and Nuclear Engineering. The code is used to generate input files for several codes, such as MCNP. In MCNP the INP file is a file defining the reactor geometry, the surfaces that bind the reactor, the isotopes of which the material in the reactor consists and the nuclear data libraries that the material uses. Most importantly, the MCNP INP file, defines the type of problem that is to be modelled. The INP file follows a certain structure, discussed in Section 3.1.

The in-house code is useful in this study because it reduces the amount of time it would take for an INP file to be written. Because the NWURCS code is still a developing code for several reactors, verification of the model is crucial to ensure that what the user has defined is exactly what is generated and to note if there are any computer bugs to be detected from the code. To verify this code for this model, the verifications below were made done.

4.1.1. Verification of the Geometry

4.1.1.1. Reactor core

The reactor core of the model consists of 163 FAs, with six side reflectors, three bottom reflectors and three top reflectors. Figure 4-1 is the core layout of the VVER-1000 generated by the NWURCS code. According to literature, the reflectors are heterogeneous; however, in the model the reflectors that have different materials were taken as homogenous materials. This was done in order to make it easy for the reflectors to be modelled. The full heterogeneity of reflectors will be investigated in later studies. The core layout given in Figure 2-3 gives the core loading at BOC, which was applied to this model.

Figure 4-1 shows that the core layout of a VVER-1000 reactor type, as can be seen in Annexure A, has been developed successfully. The only difference was the reflectors of the model, since they were assumed to be homogeneous. VISED was used for the visual verification.

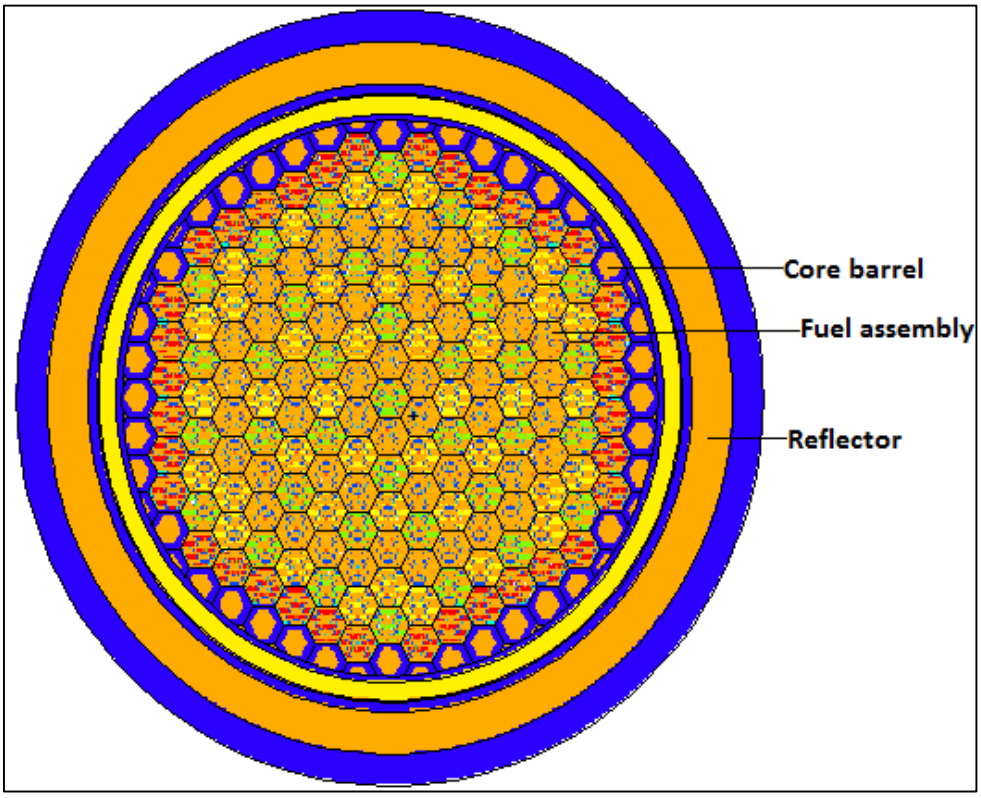

Figure 4-1: VVER-1000 core layout

The RPV was included in the NWURSC code, and it was generated as defined in the literature. The radial and axial reflectors are visible in Figure 4-1.

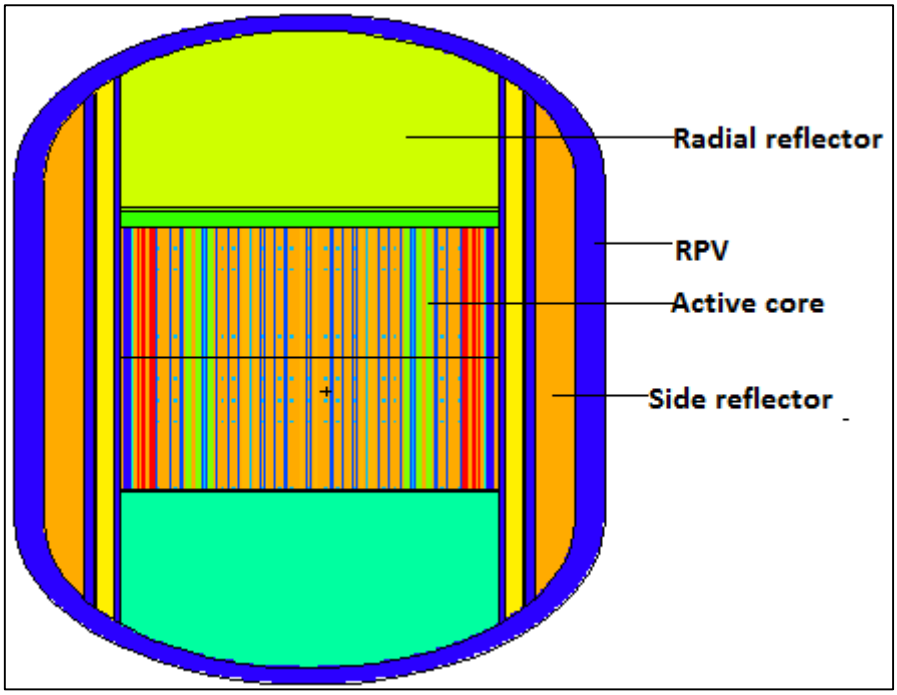

Figure 4-2: Reactor pressure vessel

Figure 4-2 does not clearly show all the bottom reflectors, because the dimensions are too small.

4.1.1.2. One-sixth core

The VVER-1000 core display specific symmetry; therefore the VVER-1000 core was cut into a 1/6th core to utilize the symmetry of the core. The NUWRSC code has generated the 1/6th core, and the visual verification was done using the VISED code. Figure 4-3 demonstrates that the 1/6th core was defined correctly in the input.

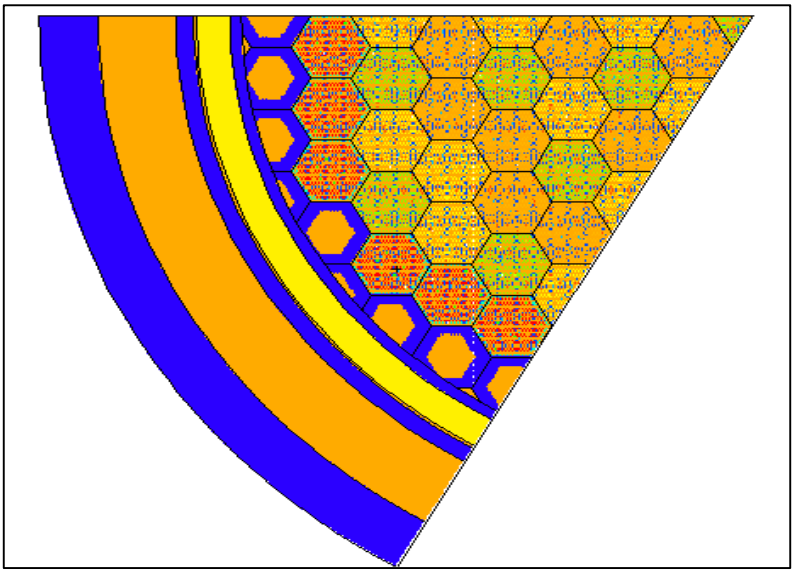

Figure 4-3: One-sixth core from NWURSC code

The reflectors seen in Figure 4-3, were modelled in homogeneous geometry to avoid complications when performing calculations.

4.1.1.3. Fuel assembly

The FA pin layout used for the FA model has been verified to match the one from the literature study using VISED. The dimensions of the FAs were properly defined when examined in the INP file. Figure 4-4 gives the FA layout of the model generated by the NWURSC code.

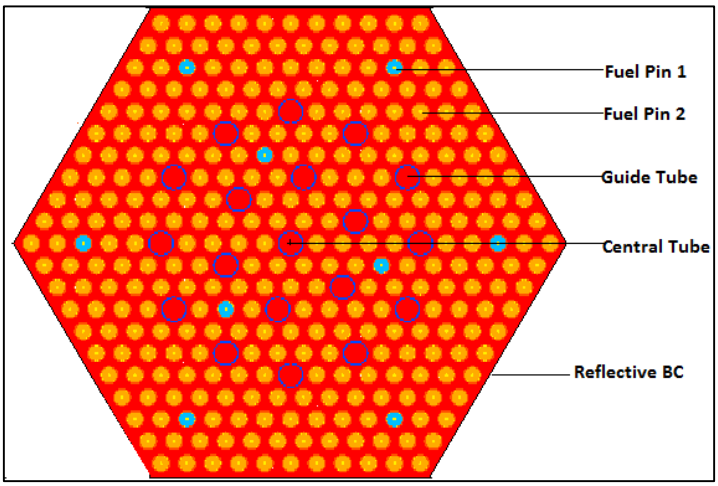

Figure 4-4: FA verification

From Figure 4-4 it has been confirmed that in terms of geometry generation, the NWURCS code does exactly what has been defined by the user.

4.1.1.4. Rod type

To verify the rod types that are found in the FA, a visual inspection was done to view the radial part of the rods. For the axial part, an inspection of the INP file was done, and an Excel spreadsheet was made available to note the surfaces and materials of the rods. The top view (radial) is given in Figure 4-5 and the side view (axial) in Figure 4-6.

In Figure 4-6, the control rod verification performed by an Excel spreadsheet is demonstrated.

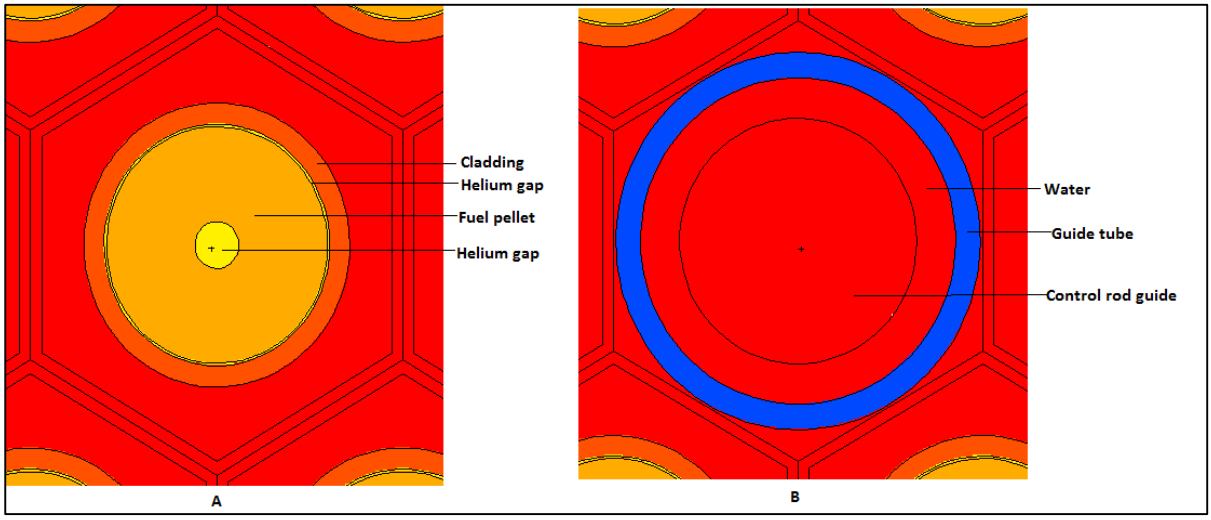

Figure 4-5: Rods' top view

It should be noted that the red section in the figure above represents the moderator in the system. In VISED, the colours were automatically chosen to represent each of the materials. The image labelled B (on the right-hand side) is the guide tube, which guides the movement of the control rods in the core. In the absence of a control rod in the core, water is assumed to be flowing in the guide tube. As stated in literature, the fuel rod of a VVER includes an annular ring in the fuel pellet and in the image labelled A (on the left-hand side) it is observed that the annular ring was also modelled.

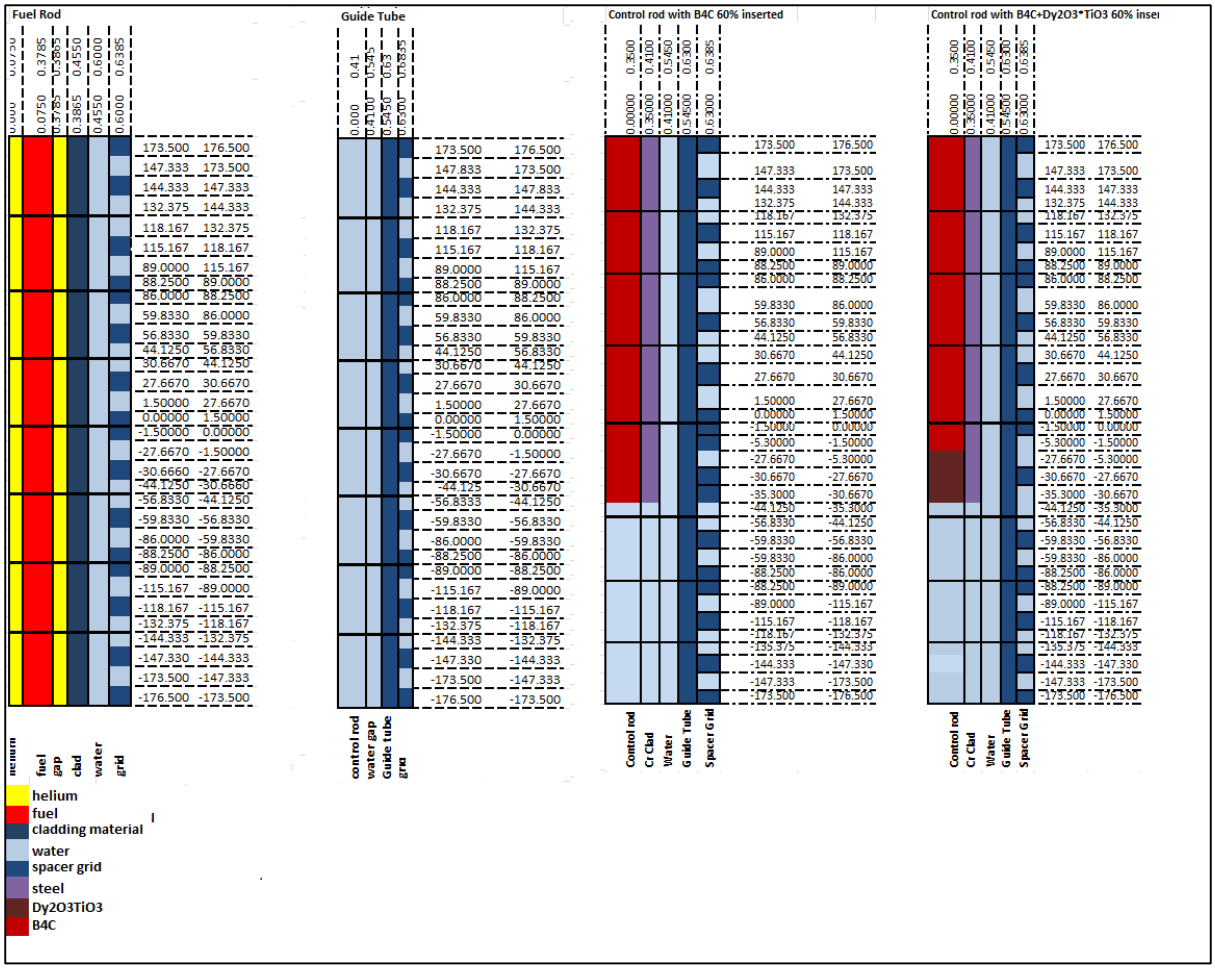

Figure 4-6: Rods' side view

It was observed that in the INP, the definition that was made by the user for the dimensions were correctly generated. Figure 4-6 above shows that the FA model was built properly in terms of axial geometry. An FA mode had eight axial nodes, as can be seen in Figure 4-6. To formulate the Excel spreadsheet for the rod type verification, the material number of the materials of interest was observed from the INP file. After obtaining the material number, the cell containing that material was inspected. From the cell, the surfaces that bind the material were obtained. Because the model was divided into eight axial nodes, to make up the whole geometry of the material, more than one cell was inspected in the INP file. The numbers that are seen in Figure 4-6 are the radial and axial positions defined for each surface in the cells that make up all the surfaces of the geometry of the material.

4.1.2. Verification of Material

To verify the material definition in the INP file, an inspection of the INP file was done, followed by manual calculations of the atomic fractions to see if they corresponded. Figure 4-7 shows a part of the INP file required by NWURCS and Figure 4-8 gives a sample of the output generated by NWURCS, which is a part of the input for MCNP6.

```
Input material
water___
 1  1  1 1          material number/number of densities/number of s(alpha,beta)
 1                  index number for s(alpha,beta), MCNP
 1                  index number for s(alpha,beta), Serpent
 1.000  100  2      density/%/number of elements
 1 2.0 0 8 1.0 0    /Z/stochiometry/enrichment
fuel22__
 20  1  2  0        UO2  3.0% enriched
 2  3                index number for s(alpha,beta), MCNP
10.376  100  2      density/%/number of elements
 92 1.0 2 8 2.0 0   /Z/stochiometry/enrichment
 3.0 97.0
```

Figure 4-7: Input defined by user

In Figure 4-7, the definition of the materials is given in the format demonstrated in the figure above. The figure gives two examples of the materials, one of which is water (moderator/coolant) and the other a fuel. The example was extracted from an FA model.

```
Generated input
c water___
m11
     1001.80c 6.6657E-01
     1002.80c 1.0000E-04
     8016.80c 3.3321E-01
     8017.80c 1.2700E-04
c fuel22__
m9
     8016.80c 6.6641E-01
     8017.80c 2.5400E-04
    92235.80c 1.0124E-02
    92238.80c 3.2321E-01
```

Figure 4-8: Material input generated by NWURSC

An Excel spreadsheet was created to calculate the numbers shown in Figure 4-8, and these numbers were confirmed. Table 4-1 gives the results for one of the materials demonstrated above.

The method of calculating the atomic fractions and atomic densities is as follows:

- Firstly, the atomic densities for each of the element in the compound were obtained using the formula below:

$$N_i = \frac{\rho_T W_i N_A}{A_{W,T}} \tag{4-1}$$

where:

ρ_T: The density of the compound

W_i: The weight fraction of each element

N_A: Avogadros's number (0.6022 atoms•cm^2/mol•barn)

$A_{W,T}$: Atomic weight of compound.

- Sum all the values of the atom densities of each element to obtain the atom density of the compound:

$$N_T = \sum_{i=1} N_i. \tag{4-2}$$

- To obtain the atomic fraction for each element, divide the number density of each element with the total number density:

$$f = \frac{N_i}{\sum_{i=1} N} \tag{4-3}$$

Table 4-1 gives an example of the calculation of the atomic fraction of a material.

Table 4-1: Verification of material number densities

Compound	**H_2O**			
ρ (g/cm^3)	1			
Elements	H(H_1,H_2)		O(O_{16},O_{17})	
Abundances	99.985	0.0150	99.962	0.03808
$A_{w,I}$ (g/mol)	1.008		16	
$A_{w,T}$ (g/mol)	18.016			
N_i (atoms/b-cm)	0.06685		0.03343	
N_T (atoms/b-cm)	0.100278			
f (atoms)	0.6666	0.0001	0.3332	0.000127

The comparison between the atomic fractions results in Figure 4-8 and Table 4-1 shows good agreement. In Figure 4-8, the atomic fractions of the isotopes of the materials are also

accounted for. The number density of the water calculated manually was confirmed in the INP file, on the cell that has the water.

4.1.3. Control Rod Movement Verification

The movement of the control rod into the core is determined, by defining the control group to move, and also the amount of movement. Figure 4-9 gives a demonstration of an FA with control rod material.

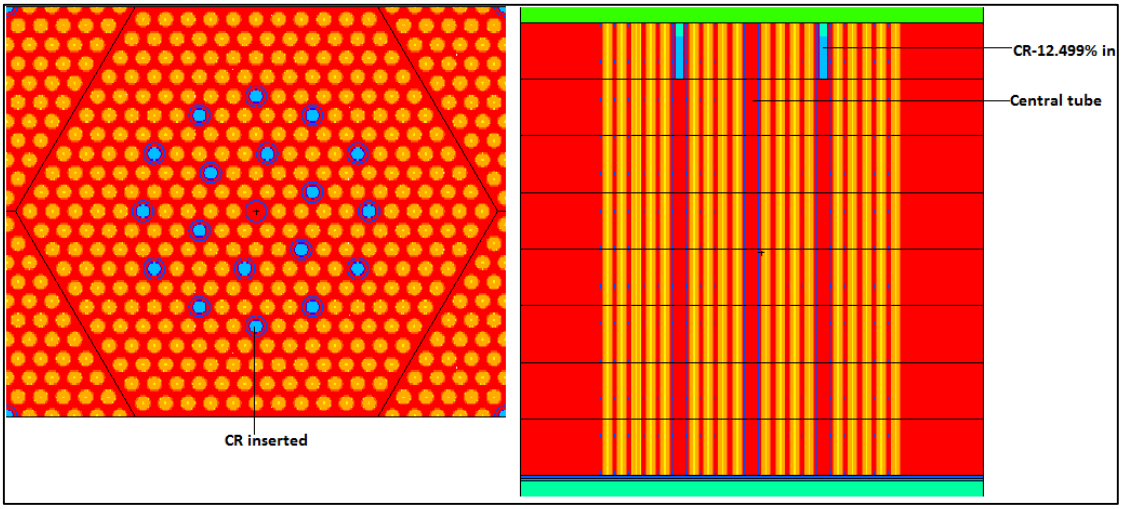

Figure 4-9: Control rod movement

From Figure 4-9 it has been verified that the rod movement as defined by the user was generated successfully by NWURCS. However, it was further observed that, at certain positions of the FA, the rod was inserted but created some kind of unexpected void in the system. The void that was created during the rod movement was not acceptable, because it created errors in the models. Figure 4-10 illustrates what a moved rod will look like with an unacceptable void.

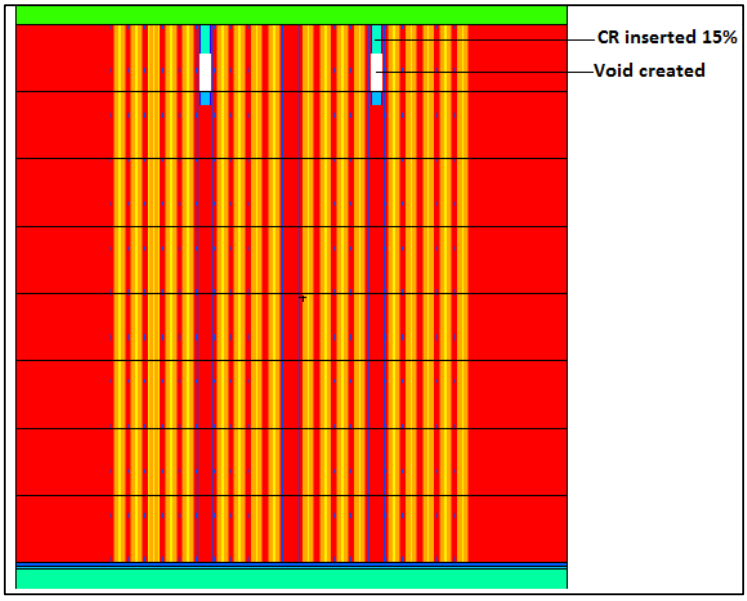

Figure 4-10: Control rod movement with voids created

Because further analyses on control rod movement such as rod worth were done, it was ensured that the positions that showed an error were not selected. The rod movement was confirmed each time by visual inspection. However, until this code error is fixed by the code developer, results that involve control rod insertion must be used with caution.

4.2. Convergence Results

The following results show the convergence results for the FC and the FA. For the convergence study, the FC model was discretized into 13 axial nodes, while the FA model was discretised to eight axial nodes. The results were obtained using the methods discussed in Section 3.6 to assess the convergence behaviour of k_{eff}/k_{∞}, fission source distribution, the convergence of the tally and power profile.

It should be stated that an error on the NWURCS code was established during the convergence investigation, which involved the densities of the moderator. A density definition at specific temperatures for the moderator would be given by the user. These values are used as interpolation points to determine the densities at other temperatures. Even though the densities for the entire temperature range under investigation were not defined by the user, NWURCS automatically generated the densities at temperatures outside the given range, which was seen as an error, because it was not defined as such. The difference between the densities that were automatically generated by NWURCS and the densities that were later correctly defined by the user were 9 %.

In the investigation of the convergence of MCNP results, the results were not rejected since it was considered that the methodology developed to establish the convergence of the MCNP results would not be affected by the densities. The convergence analysis focuses mainly on the neutron source points and the number of cycles to run. The convergence of results looks at decreasing statistical errors of the problem.

Table 4-2 and Table 4-3 give the results that were obtained for each case that was investigated on each model:

Table 4-2: Calculated results for various cases in FC

Neutron source convergence								
Case	**Source point**	**In-active**	**Active**	**k_{eff}**	**σ**	**H_{src}**	**Time (hrs)**	**Recommended discard**
1	400 000	200	600	1.00404	0.00005	12.5	12	169
2	600 000	200	600	1.00389	0.00004	13.0	17	42
3	700 000	200	600	1.00394	0.00004	13.2	19	203
4	800 000	200	600	1.00394	0.00004	13.1	22	42
5	1000	200	600	1.00399	0.00003	13.5	32	42
Active cycles convergence								
4b	8000000	200	600	1.00394	0.00005	13.1	22	42
6	8000000	200	400	1.00394	0.00004	13.1	25	42
7	8000000	200	800	1.00394	0.00003	13.1	25	205

Table 4-3: Calculated results for various cases in FA

Neutron source convergence								
Case	**Source points**	**In-active**	**Active**	**k_{∞}**	**σ**	**H_{src}**	**Time (hrs)**	**Recommended discard**
1	100000	200	600	1.06882	0.00010	10.8	12	2
2	200000	200	600	1.06886	0.00008	11.5	17	131
3	300000	200	600	1.06891	0.00006	12.2	19	159
Active cycles convergence								
3b	300000	200	600	1.06882	0.00010	10.8	12	2
4	300000	200	400	1.06886	0.00008	11.5	17	131

It should be noted that these tables will be referred to when discussing the results. The standard deviations obtained per each k_{eff} /k_{∞} proved to be acceptable for all the cases.

The recommended number of cycles to discard given in the tables is the number of in-active cycles needed to run before the source converges. In MCNP data accumulation begins after the source has converged; the cycles after the source has converged are called active cycles.

4.2.1. Source Convergence

The convergence behaviour of the fission source distribution has been examined by a quantity called the Shannon entropy H_{src} (discussed in Section 2.3.1), which is automatically produced in the MCNP calculation. The Shannon entropy versus the number of cycle plots for the FC and FA models is presented below. The fission source distribution is examined for different values of N (neutrons per cycle) specified by the cases given in Table 3-3 and Table 3-4.

Figure 4-11 presents convergence of H_{src} for an FC calculation.

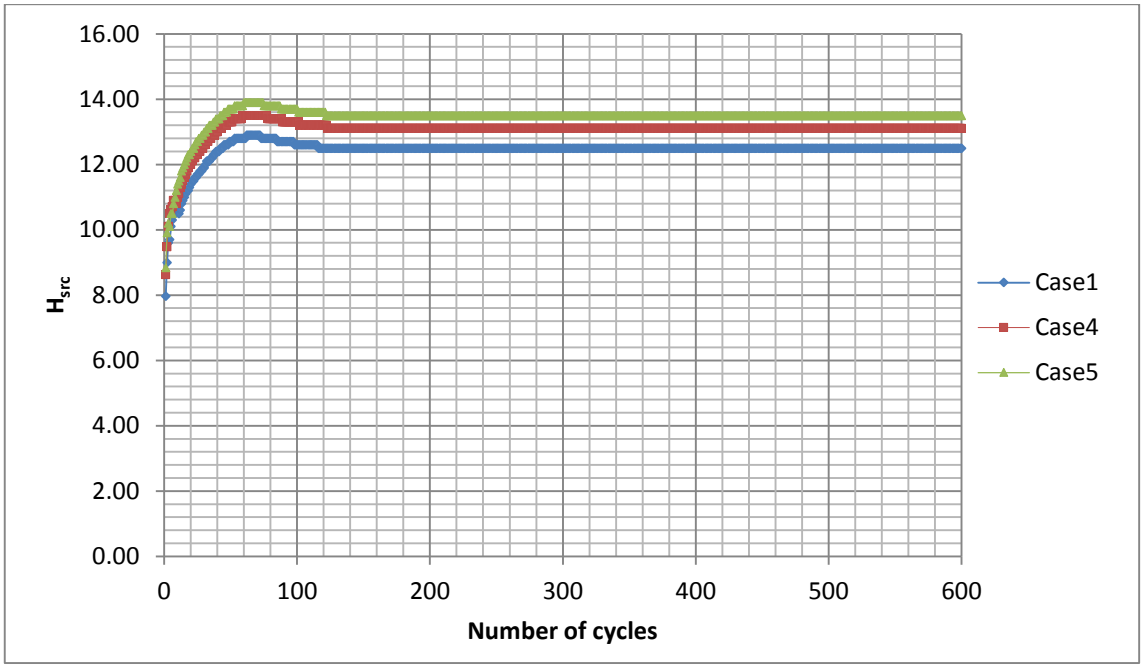

Figure 4-11: FC model fission source convergence

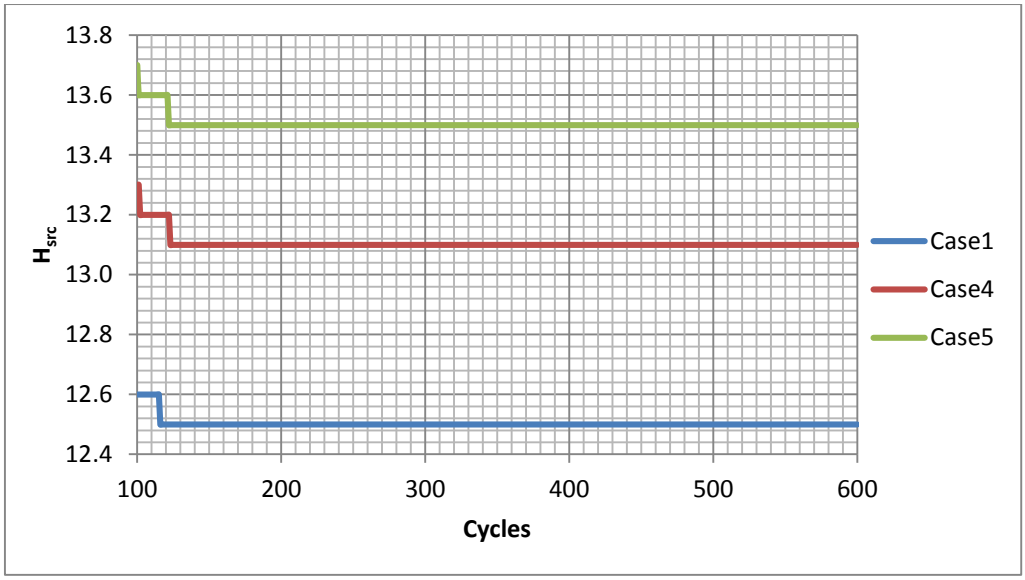

Figure 4-12: Shannon entropy from 100 cycles

For the H_{src}, it can be seen that the Shannon entropy of the fission source distribution increases during the first few initial cycles, as demonstrated in Figure 4-11. It was further observed that it then starts to decrease after a few cycles. From examining Figure 4-11, it can be assumed that after 100 cycles, the behaviour begins to stabilize. The plot in Figure 4-12 is shown so that the behaviour after 100 cycles can be seen clearly. It was observed that H_{src} drops to 13.6 and 13.2 for case 5 and case 4, at cycles 101 and 102 respectively. After these drops, the H_{src} then remains constant for a few cycles. At cycles 122, 123 and 116, the H_{src} drops again to 13.5, 13.1 and 12.5 for case 5, case 4 and case 1 respectively. The fission source then becomes constant for the rest of the cycles, as seen in Figure 4-12.

The constancy of the fission source results from the fact that MCNP expands the Shannon entropy mesh cells encompassing the geometry of the FC volume if need be, until the geometry volume has been covered with the mesh over which the Shannon entropy is determined. The increase in the Shannon entropy after the first cycle occurs because the initial source is replaced by sources at fission sites. The mesh cells are expanded after a few cycles, resulting in the decrease in entropy seen in Figure 4-11. The mesh cells expand further to encompass all fissile materials, which means a further increase in volume to result in a further decrease in the entropy, after which it remains constant.

From the plots it can be concluded that for case 5, case 4 and case 1, about 122, 123, and 116 cycles respectively are required to converge the fission source fully. Therefore, this means that at least that many cycles should be skipped before tallying any results.

For the FA the following results are obtained:

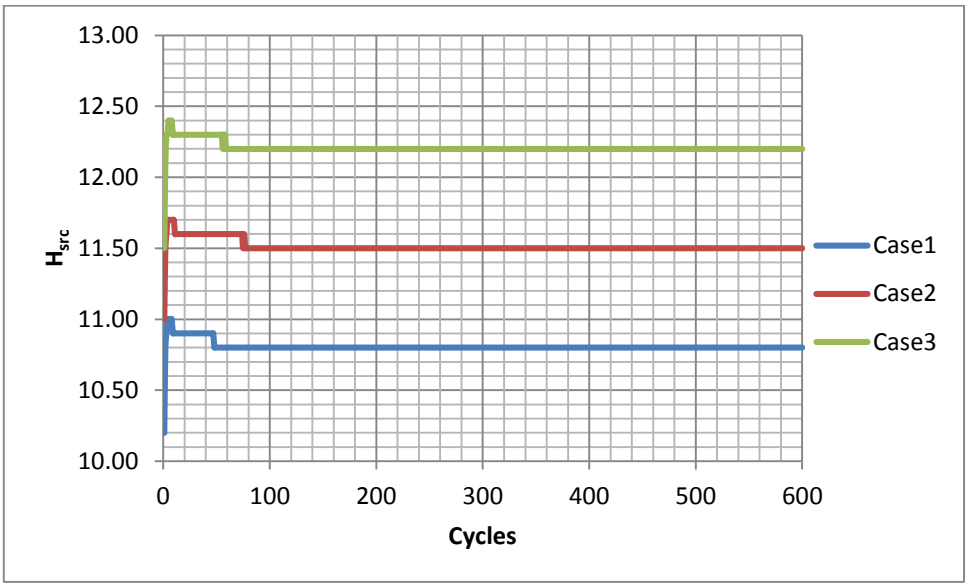

Figure 4-13: FA model fission source convergence

The same trend that is observed for the FC model is followed by the FA convergence. For the FA model, the source is seen to have converged at cycle 34, 60, 50 for cases 1, 2, and 3 respectively. Therefore, this means that at least that many cycles should be skipped before tallying any results for the FA model. However, after every calculation MCNP suggest its own cycles for a converged source, as can be seen in Table 4-4

4.2.2. K (K_{eff} /K_{∞}) Convergence

The convergence behaviour of the k has been examined from MCNP. MCNP computes a k value for each cycle. The k versus the number of cycle's plots for the FC and FA models is presented below. The k was examined for different values of N (neutrons per cycle) specified for each case in Table 3-3.

The results of the k_{eff} convergence for the FC model are presented below.

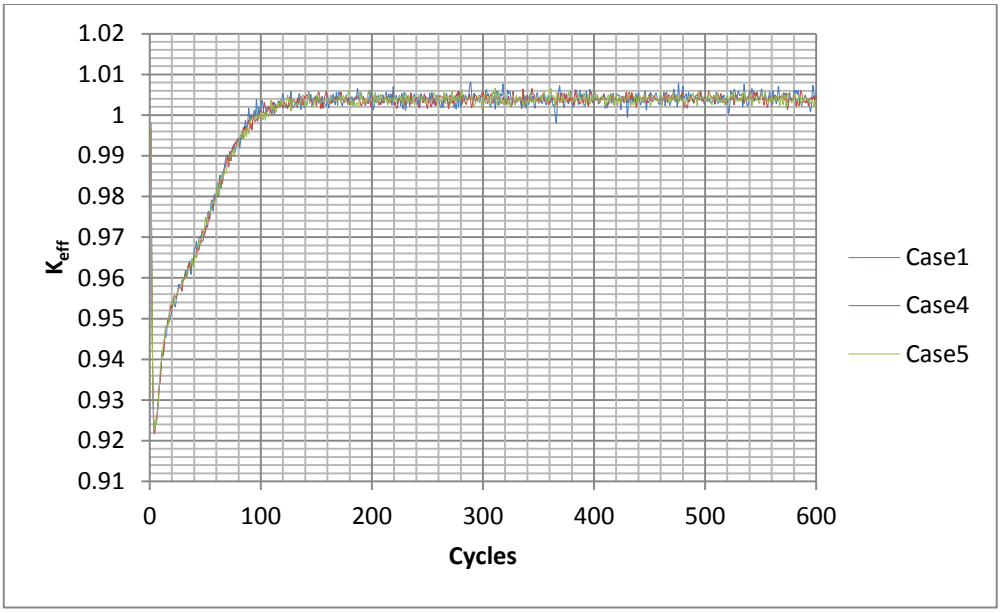

Figure 4-14: FC model k_{eff} convergence

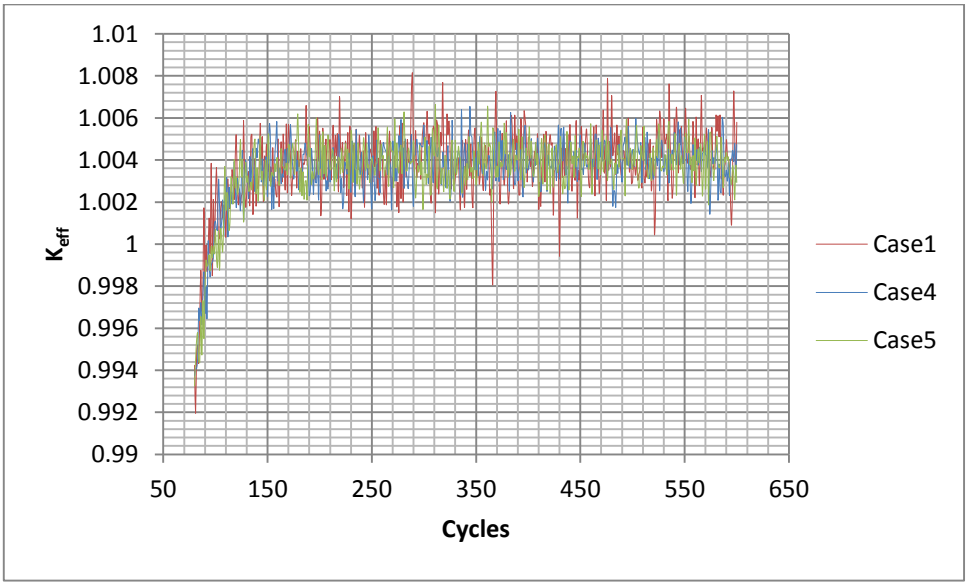

Figure 4-15: FC model k_{eff} convergence

From Figure 4-14, it is seen that during the first initial cycles, k_{eff} is observed to have decreased, and starts to increase immediately. However, it does not clearly indicate when it starts to converge; this is due to the statistical noise in the random walks of the neutrons in each cycle. One can make a conservative estimate that k_{eff} would be converged at about 100 cycles for all the cases, as can be concluded from Figure 4-15.

Figure 4-16 presents the results for the FA model.

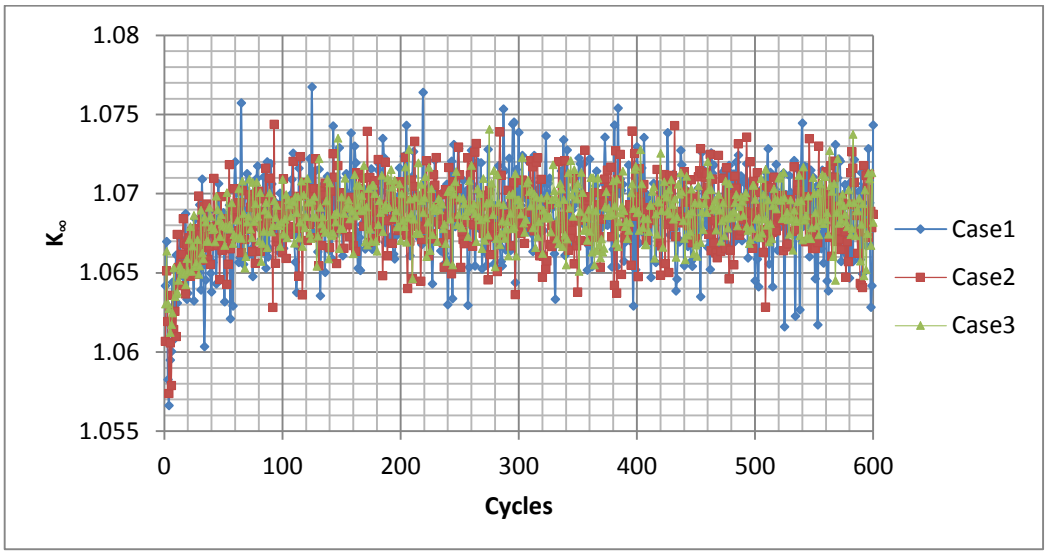

Figure 4-16: FA model k_∞ convergence

Because of the statistical noise in the random walks of the neutrons in each cycle, convergence of k_∞ is not clearly shown. Hence one can make a conservative estimate that for the FA model, k_∞ would be converged at about 50 cycles, for the FA model.

4.2.3. Further check on source convergence

For each cycle run in MCNP, both k_{eff} and H_{src} are computed. Hence the two parameters can be used to assess the source convergence. However, it should be noted that k_{eff} and H_{src} may not converge at the same time; this is observed in Figure 4-12 and Figure 4-15. The k_{eff} suggests that at about 100 cycles the k_{eff} would have at least converged, while H_{src} suggests that about 130 cycles will be needed to converge the fission source for all cases. This means that at least 130 initial cycles should be discarded (in-active) even though k_{eff} has already reached convergence, to avoid contaminating results with errors from an initial guess. However, according to Table 4-2, the suggested number of skips as calculated by MCNP is presented and they do not match the observations from the graphs. The suggested number to skip is smaller than the observed one, but for some cases it is seen to be larger. MCNP suggests the number of cycles to discard according to the cycles that have fission-source entropy within the standard deviation.

It is therefore best that the value chosen should be the larger of that recommended by MCNP6 and that estimated by the user. For this study, it was chosen as 200 for the FC cases and 200 for the FA cases.

Another way that was used to assess the convergence was to compare the power profile. The distribution of the neutrons in the core is proportional to the power distribution, so the neutron

distribution has an influence on the power distribution. This assessment assists in making an informed decision on the number of neutron sources that would be used for further calculations. The following diagram represents the power profiles for the cases.

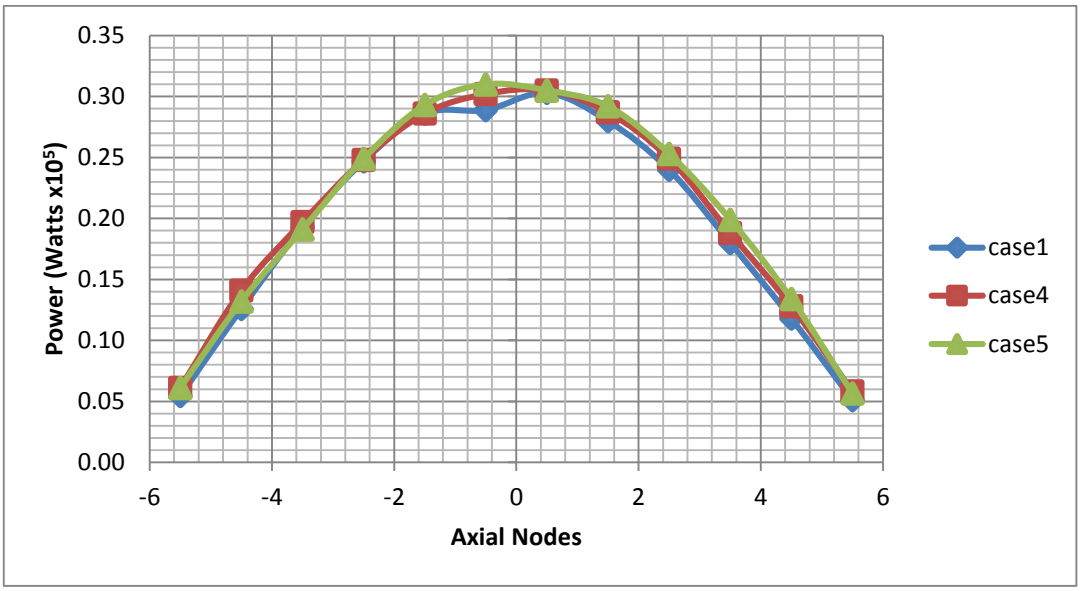

Figure 4-17: Power profile for neutron generation

As seen in Figure 4-17, case 1 does not present a good distribution of the power because the power is depressed at point -0.5. This would be because the convergence of the results was not met. Case 4 and case 5 seem to have a good power distribution; however, for further investigations of the study one case on the source convergence must be selected. Therefore the decision was to choose case 4, described in Table 3-3, to proceed with further calculations. This was because of the time advantage that would be gained in the calculations.

For the FA model, the power profiles are represented below.

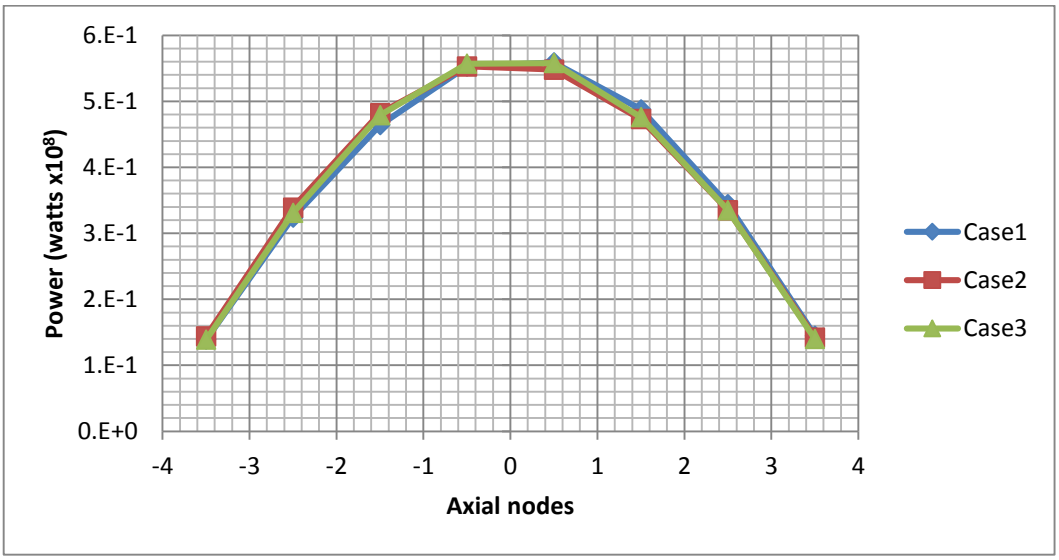

Figure 4-18: Power distribution profile (FA model)

From the above plot, it is observed that all the cases show good agreement in terms of cosine shape. This was to be expected since the FA is symmetric axially. However, one case had to be selected for further investigations in the study. Case 3 as described by Table 3-4 was chosen, since the time used for the FA calculations was at 100 000 source points, which compared to 300 000 source points was not significantly different.

4.2.4. Tally Convergence

After establishing the number of in-active cycles to run, tally accumulation convergence must be established. This is done so as to accumulate the tallies until the statistical uncertainties have become small enough. To reduce the statistical uncertainties, the number of active cycles must be determined. The tally convergence will then be established by the number of active cycles used to run the problem. An F7 tally card was the tally of interest in this current study. This tally is used to generate the fission energy deposition.

The tally convergence was done by assessing the 10 statistical tally tests. Table 4-4 and Table 4-5 give results for the 10 statistical tests where “P” means pass.

Table 4-4: Tally convergence for FC and FA models

FC Model										
Tally number	Mean B	RE V	RE D	RE DR	VOV V	VOV D	VOV DR	FOM V	FOM B	PDF
7	P	P	P	P	P	P	P	P	P	P
17	P	P	P	P	P	P	P	P	P	P
27	P	P	P	P	P	P	P	P	P	P
37	P	P	P	P	P	P	P	P	P	P
47	P	P	P	P	P	P	P	P	P	P
57	P	P	P	P	P	P	P	P	P	P
67	P	P	P	P	P	P	P	P	P	P
77	P	P	P	P	P	P	P	P	P	P
87	P	P	P	P	P	P	P	P	P	P
97	P	P	P	P	P	P	P	P	P	P
107	P	P	P	P	P	P	P	P	P	P
117	P	P	P	P	P	P	P	P	P	P
127	P	P	P	P	P	P	P	P	P	P
137	P	P	P	P	P	P	P	P	P	P
147	P	P	P	P	P	P	P	P	P	P
FA model										
7	P	P	P	P	P	P	P	P	P	P

The acronyms in the above table are defined in Table 3-5. For all the cases, all the statistical tests were passed. The results of the passed statistical tests were obtained from the output file of the MCNP6 results, and it was observed that all the cases had passed the tally checks.

For an FA model, it was observed that the MCNP6 tally problem passed all 10 statistical tally tests.

In Table 4-5, the results that are presented are for case 4 and case 7 of the FC model and case 1 and case 4 of the FA model. Not all the statistical indicators provided in the MCNP output are presented for these cases. The mean value, relative error and FOM are considered, since they are the statistical indicators that can assist with determining the most efficient case to choose from for further analysis in the study.

Table 4-5: Statistical indicators for FC and FA models

FC model						
	Case 4			Case 7		
Tally number	Mean	Relative E	FOM	Mean	Relative E	FOM
7	3.94E-07	0.0055	4.20E-01	3.71E-07	0.0045	3.20E-01
17	3.65E-07	0.0049	3.90E-01	3.64E-07	0.0045	3.20E-01
27	4.95E-07	0.0047	5.30E-01	5.16E-07	0.0038	4.50E-01
37	5.31E-07	0.0045	5.70E-01	5.50E-07	0.0037	4.80E-01
47	5.42E-07	0.0045	5.80E-01	5.46E-07	0.0037	4.80E-01
57	5.01E-07	0.0047	5.40E-01	5.12E-07	0.0038	4.50E-01
67	3.57E-07	0.0056	3.80E-01	3.63E-07	0.0045	3.10E-01
77	3.80E-07	0.0051	4.60E-01	3.96E-07	0.0041	3.80E-01
87	3.53E-07	0.0056	3.80E-01	3.79E-07	0.0044	3.30E-01
97	4.99E-07	0.0047	5.40E-01	5.31E-07	0.0037	4.70E-01
107	5.54E-07	0.0045	5.90E-01	5.84E-07	0.0035	5.10E-01
117	5.55E-07	0.0044	6.00E-01	5.87E-07	0.0035	5.10E-01
127	5.34E-07	0.0045	5.70E-01	5.43E-07	0.0037	4.70E-01
137	3.92E-07	0.0053	4.20E-01	3.90E-07	0.0043	3.40E-01
147	4.14E-07	0.0052	4.40E-01	3.91E-07	0.0043	3.40E-01
FA Model						
	Case 3			**Case 4**		
7	5.88E-05	0.0010	4.20E-01	5.88E-05	0.0010	44

The results in the table show that in case 7 there is a decrease in relative errors and FOM for each of the tallies when compared to case 4. The results in Table 4-5 show that the statistical quality of the tally results is good. The estimated error of the tallies is below the estimated error limit as stated in 2.3.2.1.This means that the results are reliable. The FOM value shows that a well-behaved estimator was used, which means that the tally results have converged to the correct solution, that is, the estimated mean gives a very reliable value of the actual value for the solution. Although the statistical checks have all been passed, they cannot solely influence the reliability of the whole model, hence the source convergence was also performed.

The value of the FOM will contribute to the amount of time a calculation would take to complete its simulations as well. It is said that a large value of FOM will result in a shorter time to complete simulations (Booth, et al., 1994). According to Table 4-2, the time it took for case 7

to complete calculating was longer than the time it took case 4. Consequently, case 7 has a smaller FOM value compared to case 4.

For an FA model, the statistical indicators prove to yield similar results for the different cases.

4.2.5. Power Profile Convergence

The power distribution profiles have been examined for active cycle convergences. Obtaining a well-fit symmetrical power profile indicates that the right number of source points and active cycles has been reached. As indicated in theory a symmetrical core, either radially or axially, would result in a symmetrical power profile distribution. The following graphs represent the axial distribution of the power. A homogeneous model was assumed axially and a cosine plot is obtained, as stated in nuclear reactor theory: a solution of the flux profile of a critical slab is $cos\left(\frac{\pi x}{ae_{ex}}\right)$ (Stacey, 2007).

The comparison of power profiles for convergence for each case was done for an FC model and also an FA model.

The following power profile results are for the FC model:

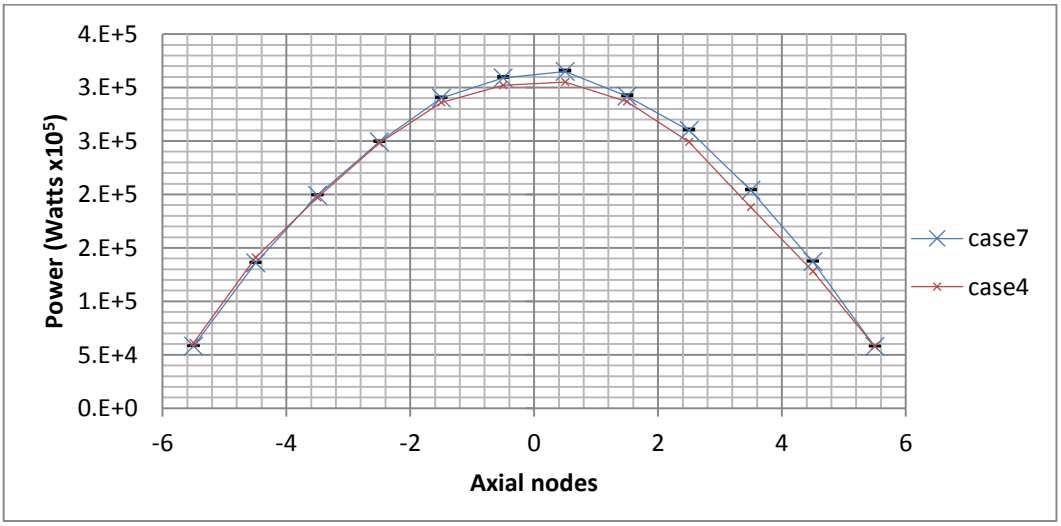

Figure 4-19: Power profile for cycle convergence in FC model

Figure 4-19 was plotted with error bars. The error bars are not very clear in the plot because the errors were very small in comparison to the value. The effects of the number of cycles on tally precision are evident from the plot and case 7 looks more symmetrical. It was proven that the power profile portrays the cosine graph and Figure 4-20 show an analytical plot of a cosine. In this graph, a cosine function was fitted against the numerically obtained power profile for case 7. Case 7 is in good agreement with the analytical cosine plot.

In conclusion, the decision on using an 800 000 neutron source points with 800 cycles was based on all the assessments that were done for convergence. From comparing the results for the tally and the statistic indicators given in Table 4-5 for both case 4 and case 7, it is evident that case 7 is more efficient.

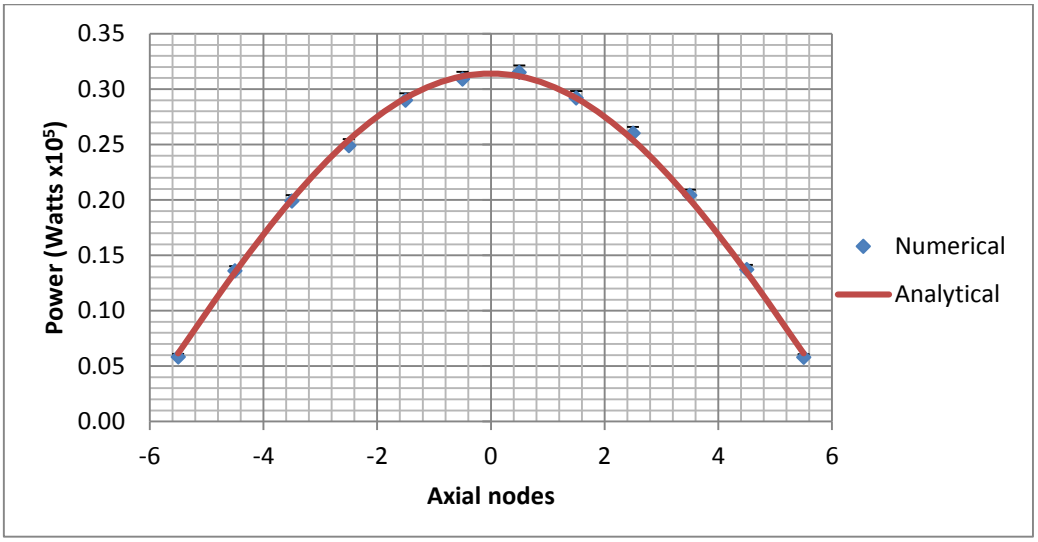

Figure 4-20: A cosine-fit of the Power profile

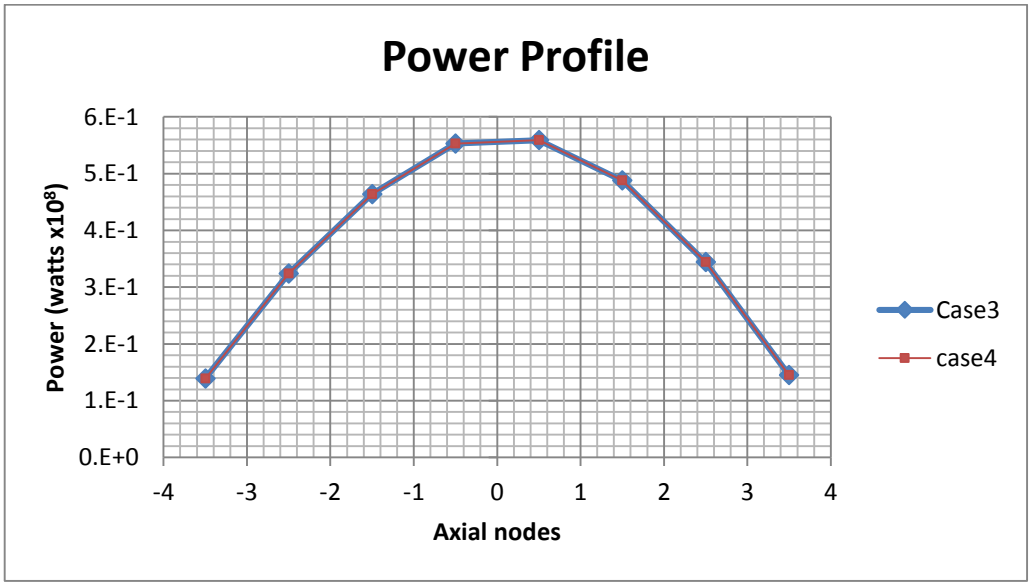

Figure 4-21: Power profile for cycle convergence in FA model

The FA model shows good agreement too because the power is seen in Figure 4-21 to be well distributed axially throughout the FA for both the cases presented.

For the FA, the number of cycles chosen was for case 3 with 600 cycles, having 600 000 neutron source points.

4.3. One-sixth core

Calculations for a 1/6th core were performed for the study. Because a VVER reactor is symmetrical in 60 degree as can be seen in Figure 4-3, it is important to observe the behaviour of a 1/6th symmetry core. The behaviour of a 1/6th symmetry core must match that of an FC analysis. In Table 4-6 below, the results of k_{eff} were obtained for a 1/6th core and a FC core.

The results for the multiplication factor k are as follows:

Table 4-6: Comparison of FC with 1/6th core

Parameter	Full core	One-sixth
k	1.00353	1.00366
σ	0.00003	0.00003
Time (hours)	77	52

The difference in the k_{eff} results is 13 pcm. The results obtained between an FC and 1/6th core are in good agreement, which means that for the model, a 1/6th core could be used to save the time the FC model would take to perform calculations. The power profiles are not shown since NWURCS cannot generate the power profile for the 1/6th core. Inclusion of this in the NWURCS code is a recommendation that will be given to the code developer.

4.4. Criticality Boron Concentration

The criticality of the system was reached without any control rods in the system, but by dilution of boric acid in the reactor core. The method that was used to reach a critical boron concentration is discussed in Section 3.7. The graph in Figure 4-22 is plotted to predict the critical boron by linear interpolation of results.

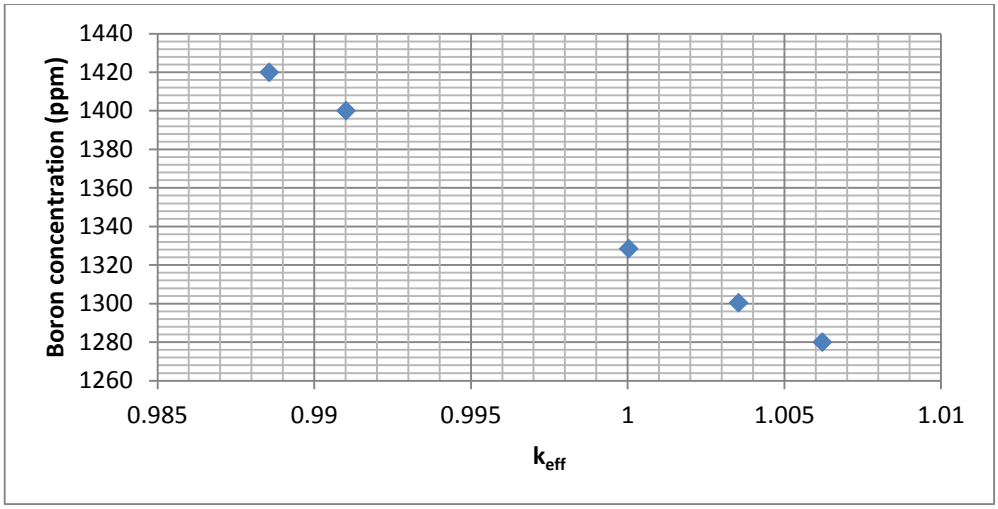

Figure 4-22: Reaching criticality

As observed in Figure 4-22, when the concentration of the boron was larger, the system went to a subcritical state where $k_{eff} < 1$, and when the boron concentration was small, the system went to super criticality where $k_{eff} > 1$. The critical state is reached at $k_{eff} = 1$.

The critical boric acid concentration was found to be equal to 1328.59 ppm for this model at 300 K with $k_{eff} = 1.00003$. The value of k_{eff} is larger from the theoretical value of 1 by 3 pcm, which is negligible. When comparing the results of the boron concentration with the literature value of Section 2.7, with the value of 1319.5 ppm, the difference between the boron concentrations is 9.09 ppm. The difference is small and this means that the model of the current study is in good agreement with the literature. It should also be stated that the state of the model in the literature was HZP, while the state of the current study is at CZP.

4.5. Boron Worth

To determine the worth of the boron on the reactivity of the system, the boron worth was calculated for this study is tabulated in Table 4-7 below.

Table 4-7: Boron Worth

k_{eff}	σ	ρ (pcm)	Δρ (pcm)	C_B (ppm)	ΔC_B (ppm)	Boron worth (pcm/ppm)
1.00353	0.00003	351.758	-1509.00	1300.42	119.58	-12.62
1.00003	0.00003	2.9999	-348.758	1328.59	28.170	-12.38
0.99101	0.00003	-907.155	-910.155	1400.00	71.410	-12.75
0.98856	0.00003	617.1674	-1524.32	1420.00	120.00	-12.70
1.00621	0.00003	-1157.24	-1774.41	1280.00	140.00	-12.67

When taking the averaged boron worth, the obtained value is -12.62 pcm/ppm. In the literature discussed in Section 2.7, the boron worth obtained was -11.771 pcm/ppm.

The difference between the obtained and the literature value is 0.85 pcm/ppm. The difference of the values is small. The results for the study seem to be in good agreement with the literature given in Section 2.7.

4.6. Reactivity Coefficients

The Doppler and moderator temperature reactivity coefficient (DC and MTC) were examined for the study. Other temperature coefficients (e.g. the expansion coefficient) were not considered in this study. An FA model was considered for this particular analysis. Table 4-8 and Table 4-9 give the DC and MTC results at different temperatures:

Table 4-8: DC results

T(K)	k_∞	σ	ρ (pcm)	Δρ (pcm)	ΔT (K)	DC (pcm/K)
300	1.06419	0.00007	6831.04	-	-	-
310	1.06374	0.00007	6780.28	-50.76	10	-5.08
320	1.06346	0.00007	6748.72	-31.56	10	-3.16
330	1.06316	0.00007	6714.92	-33.79	10	-3.38
340	1.06277	0.00007	6671.01	-43.91	10	-4.39
350	1.06243	0.00006	6632.75	-38.26	10	-3.83

When taking the averaged DC between temperatures at 300 K and 350 K, the value obtained is -3.52 pcm/K, as shown in the calculation below:

$$\frac{d\rho}{dT} = \frac{(1.06243 - 1.06419)}{(350 - 300)} 10^5 = -3.52\ pcm/K \tag{4-4}$$

The statistical error σ of k is calculated as follows (Larkin, 2011):

$$\sigma = \sqrt{\sigma_1^2 + \sigma_2^2} = \sqrt{(0.00007)^2 + (0.000006)^2} = 0.00009 \tag{4-5}$$

Assuming zero error in T, the error for Equation (4-4) becomes

$$\frac{d\sigma}{dT} = \frac{(0.00009)}{(50)} 10^5 = 0.18\ pcm/K \tag{4-6}$$

Therefore the averaged value of DC is -3.52 ± 0.18 pcm/K. The averaged value is in good agreement with the data mentioned in Section 2.6 which say that the DC should fall in the range of $-4.90 < \alpha_{T,f} < -2.90$ pcm/K. The individual DC shows some variability. The variations are most probably due to the stochastic uncertainty in the eigenvalues.

The MTC was calculated and presented in Table 4-9 below:

Table 4-9: MTC results

T(K)	k_∞	σ	ρ (pcm)	Δρ (pcm)	ΔT	MTC	Statistical σ (pcm)
300	1.0703	0.00007	6568.25	0.000	0	0	2.0
305	1.0705	0.00006	6585.71	17.46	5	3.49	2.0
310	1.0708	0.00007	6612.75	27.04	5	5.41	2.0
315	1.0709	0.00007	6620.59	7.848	5	1.57	2.0
320	1.0712	0.00007	6651.98	31.38	5	6.28	2.0
325	1.0715	0.00007	6680.73	28.74	5	5.75	2.0

The MTC in each temperature step was obtained to be positive, which is not desirable. A negative MTC is said to be desirable because of its self-regulating effect. However, it can be seen that the value is not much larger than zero in terms of the statistical error. Possible reasons for this could be the high boron concentration, thermal scattering evaluations, and the evaluations at 300 K. Further investigation is required.

4.7. Control Rod Worth

The analyses that were done on the control rod were divided into two. The first analysis was the rod worth of the control rod B_4C only and the second analysis was the rod worth of the control rod with B_4C+ Dy_2O_3•TiO_2. The control rod worth calculations were performed for an FA model. Because of the model error that was discovered and mentioned in Section 4.1.3, the FC calculations that were performed were not considered for this analysis. The error was discovered after the FC model calculations had been done, therefore because of the time scope of the study and the amount of time a FC calculation takes to run, it was decided that the control rod worth of the FC model would be excluded from the study.

The following diagram represents the integral rod worth for the group 10 rod.

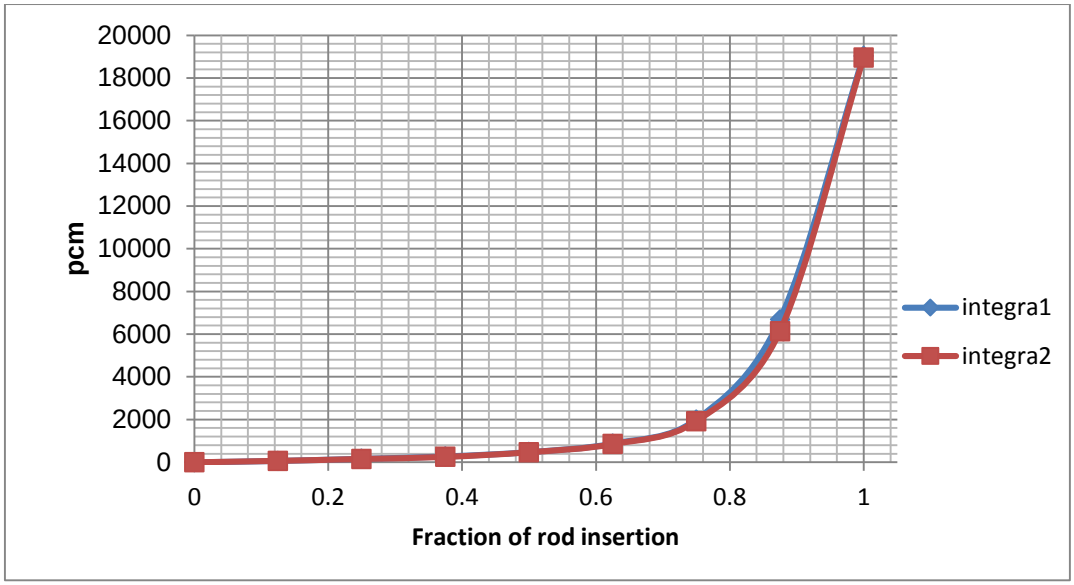

Figure 4-23: Integral Rod worth

From the plots obtained, the graph labelled “integra1” is the integral worth for the rod with B_4C only, and the graph labelled “integra2” represents the rod worth of the rod with B_4C +Dy_2O_3•TiO_2. It was observed that the trend obtained for the rod worth agrees with the trend shown in the literature discussed Section 2.8. In Figure 4-23, the rod worth for the control rod with B_4C is seen to be slightly larger than the rod worth of the rod with B_4C +Dy_2O_3•TiO_2. These observations indicate that the rod with B_4C is slightly more efficient than the rod with B_4C+ Dy_2O_3•TiO_2. However, Dy_2O_3•TiO_2 was included in the control rod because of its high dimensional and structural stability. The Dy_2O_3•TiO_2 occupies the part of the control rod with highest radiation dose (Risovany, et al., 2000).

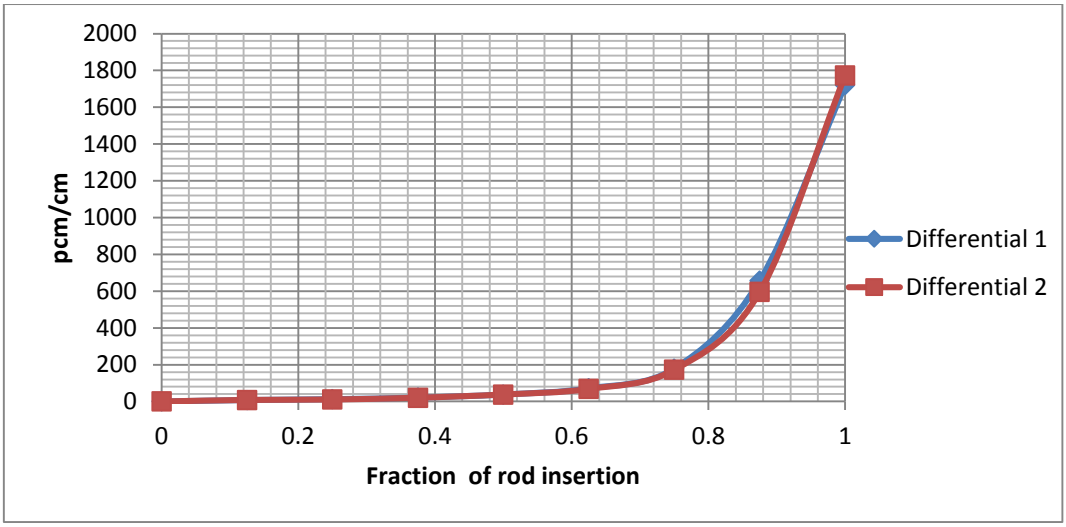

Figure 4-24: Differential worth

The differential worth reflects a behaviour that is similar to the integral rod worth. It is noted that with exponential functions the derivative displays the same behaviour as the function itself. More data should be obtained between rod fractional depths of 0.5 to 1.0.

However, due to the coding error in NWURCS regarding the movement of the control rods, only steps equal to that of the axial nodes increment could be studied, which are those as shown. Intermediate steps should be investigated when the computing error is fixed in NWURCS.

4.8. Effective delayed neutron fraction (β_{eff})

The first criticality calculation for this investigation was done without a TOTNU card, in which case MCNP uses the default value for TOTNU. The default is that both prompt and delayed neutrons are considered (the total number of neutrons). The result of k_{eff} for the total number of neutrons was:

$$k_t = 1.00353 \pm 0.00003$$

The second calculation results with TOTNU NO card gave the following value of k_{eff} for prompt neutrons only:

$$k_p = 0.99657 \pm 0.00003$$

The effective delayed neutrons fraction was calculated to be:

$$\beta_{eff} = 1 - \frac{k_p}{k_T} = 1 - \frac{0.99657}{1.00353} = 0.00694 \quad (4\text{-}7)$$

The standard error of the obtained value is calculated as follows (Larkin, 2011):

$$\sigma = \frac{k_p}{k_T}\sqrt{\left(\frac{\sigma_1}{k_p}\right)^2 + \left(\frac{\sigma_2}{k_T}\right)^2} = \frac{0.99657}{1.00353}\sqrt{\left(\frac{0.00003}{0.99657}\right)^2 + \left(\frac{0.00003}{1.00353}\right)^2} = 0.00004 \quad (4\text{-}8)$$

The final β_{eff} is 0.00694 ± 0.00004. The calculated β_{eff} together with the reference value is reported in Table 4-10.

Table 4-10: Delayed neutron fraction β_{eff}

Parameter	Value
Calculated value	0.0069
Literature Value	0.0074

The final value of the effective delayed neutron fraction is 0.006936. The value is 6.7% smaller than the literature value (0.0074), and the results are in good agreement.

5. Conclusions and Recommendations

The following chapter provides the conclusions that were reached in this study. It also gives recommendations on future studies and on the NWURCS code.

5.1. Conclusion

The study was divided into three models, namely: FA model, FC model and 1/6th model. The conclusions of the results of the models are given.

The first step was to develop a fresh FA and FC model and this was done as explained in Sections 3.2, 3.5 and 3.6. The verification of the NWURCS code formed part of the model development. The convergence of the MCNP6 results was done in order to obtain a good model with good statistical uncertainties. The model was successfully developed using the NWURCS code, and also with good statistical uncertainties. The NWU-HPC played a big role in the calculation time of the models since the code could be run using parallel processing which decreased the calculation time.

The verification of the NWURCS code was done successfully, although some errors were discovered in the model and are given in Section 5.2.2. It should be said that the errors did not affect most of the results that were obtained. For the sections where the errors affected the results, it was ensured that no further investigations were performed.

The convergence of the MCNP6 results was successfully reached with 800000 neutrons/generation with 200 inactive and 800 active cycles for the FC model. For the FA model, convergence was reached with 300000 neutrons/generation having 200 inactive and 600 active cycles. From the Shannon entropy and k_{eff} /k_{∞} convergence, it was concluded that at least 200 inactive cycles were needed to converge the fission source of the FC model and about 200 inactive cycles to converge the fission source of the FA model.

A 1/6th core calculation was performed and it was observed that the results showed good agreement when compared to the results of the FC. This proved that a 1/6th core could be used to study the behaviour of an FC in order to reduce the time of modelling. The results showed a 13 pcm difference which is negligible.

The criticality of the system was reached using soluble boron at concentration of 1328.59 ppm which had a worth of -12.38 pcm/ppm. The system was assumed to have had all the control rods withdrawn. This critical boron concentration was in good agreement with the values in the literature study which were 1319.0 ppm with a worth of -11.771 pcm/ppm.

The average value obtained for the DC was -3.53 pcm/K. The value showed good agreement with the value from literature and also fell within the limit for DC that was given.

The MTC was found to be positive and possible causes were given. This requires further investigation.

The control rod worth was investigated for rods with B_4C+ Dy_2O_3•TiO_2 and also the rods with B_4C only. The integral worth proved to have the same trend as the results from an EPR study mentioned in the literature studied. The rods with B_4C only proved to be more efficient than the rod with B_4C+ Dy_2O_3•TiO_2 and this was seen from the plot given in the results. However, the VVER-1000 reactor recommends the use of B_4C+ Dy_2O_3•TiO_2 because Dy_2O_3•TiO_2 has high stability. The differential worth reflected a behaviour that is similar to the integral rod worth.

The effective delayed neutron fraction was seen to be in good agreement with the results in the literature.

5.2. Recommendations

5.2.1. Recommendations for Future Study

- Further research on the study can be done, where other researchers will look at the reactor at HZP and HFP. This can then be continued to perform coupling of the neutronics and thermal hydraulics of the reactor system. Coupling of neutronics and thermal hydraulics is crucial in safety analysis. Since this methodology is still under development in the research group, it could not be done. Additionally, the scope would have become too much for the present study.
- The reactivity coefficients and control worth must be investigated for a FC model to see the effects of these parameters. In particular, the MTC must be further investigated.
- Further verification on the NWURCS code must be done by other researchers in parallel to the code developer. Note that this work has been done informally with the code developers and therefore not reported here.

5.2.2. Recommendations for the NWURCS

- Fuel assembly calculations were done for eight axial nodes using NWURCS; however, NWURCS does not allow any axial nodes above the number eight for FA models. It is recommended to the developer that the user should be free to choose the number of axial nodes, with the limit of nodes being limited by the memory capability of the machine. This should also be extended to the FC nodes.

- Because the temperature in a reactor system will not in most cases match those defined in the cross-section, an interpolation of the cross-section is necessary. Although this interpolation was available in the code, it was found to be implemented only for FA and not for FC models. This became apparent during the reactivity coefficient calculations. The cross-section interpolation key must be corrected to be included in full core model as well
- The control rod movement proved to be modeled successfully when the position of the control rod tip was exactly at one of the axial node positions. However, for control rod tip positions in-between the axial node positions, parts of the control rod were not modelled, resulting in voids in the geometry. Therefore the control rod movement must be looked at again in the code to correct this error.
- For a $1/6^{th}$ core, the boundary conditions were not defined precisely due to the numerical precision employed, and this resulted in the calculation terminating unpleasantly; the user had to fix them manually by changing the variable value. The boundary condition must be looked at in the code.
- In the beginning of the calculations, the user made an error and did not include the water density at 300 K in the interpolation data file. NWURCS should have detected this error and should have issued a warning to the user. However, even though the density at 300 K was not defined, the NWURCS continued to generate densities. This is taken as a computer bug. It is suggested that when densities are not defined at the limits of range accessed, NWURCS must create an error or warning in the command line to notify the user that the densities at the limits of the problem were not defined.
- The power profiles in the $1/6^{th}$ were not generated, and this should be a capability of NWURCS.

6. References

Alexander, A. 2010. Analytical models of critical reactors in simple geometries. Stockholm, Sweden.: Royal Institute of Technology (KTH). (Thesis).

Allen, K.S. 2003. Advanced Polymeric Burnable Poison Rod Assemblies for Pressurized Water Reactors. Florida: University of Florida. (MEng Thesis).

Anglart, H. 2005. Control Rods and Subcritical Systems. www.energy.kth.sa/courses/4A1627/Material2005/PhysicsPart/02%20Reactivity%20Rev%200.pdf Date of access: 13 November. 2015.

Anglart, H. 2005. Reactivity and Reactivity Coefficients. www.energy.kth.sa/courses/4A1627/Material2005/PhysicsPart/02%20Reactivity%20Rev%200.pdf Date of access: 13 November. 2015.

AREVA, NP. 2012. U.S. EPR Final Safety Analysis Report. Revision 5 ed. United States Nuclear Regulatory Commission.

Astakhov, S., Kravchenko, A., Kraynov, Y., Nasedkin, A. & Tsyganov, S. 2006. Determinition of Reactor Prameters During Start up Tests at the Tianwan NPP, Unit 1. http://www.vuje.sk/aer16/reports/2_1.pdf Date of access: 12 November. 2015.

Bernard, J.A. 2012. 22.921 Nuclear Power Plant Dynamics and Control. 22.921 Class Notes. Massachusetts: Massachusetts Institute of Technology.: John Bernard. (Class Notes).

BNPP-1 Fot. 2007. FSAR (Final Safety Analysis Report) of the BNPP-1. Bushir: Reactor (Chapter 4).

Forster, R.A., Pederson, S.P. & Booth, T.E. 1994. Ten New Checks to Assess the Statistical quality of Monte Carlo solutions in MCNP. (*In* 8th International Conference on Radiation Shielding. ArlingtonTX.)

Briesmeister, J.F. 2000. MCNP- A General Monte Carlo N- particle Transport Code Version 4C. LA–13709–M. Oak Ridge TN: Los Alamos National Laboratory. (Manual).

Burn, R.R. 1988. Introduction to Nuclear Reactor Operations Control Rods. ftp://ftp.ecn.purdue.edu/jere/BURN/Ch-04.pdf Date of access: 13 November. 2015.

Caprioli, S. 2004. In- Core Fuel Managements for PWRs: Investigation on solutions for optimal utilization of PWR fuel through the use of fuel assemblies with differently enriched ^{235}U fue

l pins. CTH RF 180. Goteborg, Sweden: Chalmers University of Technology. (Master of Scie nce Thesis).

Coster, S. 2013. Neutron Diffusion and Moderation. http://www.nuclear.lu.se/fileadmin/nucle ar/Undervisning/Reaktorfysik/Reactor_Physics_tutorials_2013.pdf Date of access: 13 Nove mber. 2015.

Devore, J. & Farnum, N. 2005. Applied Statistics for Engineers and Scientists. Second Editio n ed. USA,Belmont: Cengage learning.

DOE. 2013. Integrated Resource Plan for 2010- 2030. http://www.doe_irp.co.za/content/IRP 2010_updatea.pdf Date of access: 13 November. 2015.

Dunn, L.W. & Shultis, J.K. 2009. Monte Carlo methods for design and analysis of radiation detectors. *Radiat. Phys. Chem*, 78(2009):852-858.

Espel, F.P. 2010. High Accuracy Modelling For Advanced Nuclear Reactor Core Designs Usi ng Monte Carlo Based Coupled calculations. Pennsylvania: Pennsylvania State University. (Ph-D Dissertation).

Farkas, G., Petriska, M., Michalek S, Slegen, V. & Vankova, A. 2005. WWER- 440 Criticality Calculations using MCNP5 code. http://www.iaea.org/inis/collection/NCLCollectionStore/_Pu blic/40/059/40059704.pdf Date of access: 13 November. 2015.

Forrest, B.B. 2006. On the Use of Shannon Entropy of the Fision Distribution for Assessing Convergence of the Monte Carlo Calculations. (*In* PHYSOR- 2006, ANS Topical Meeting on Reactor Physics. Vancouver, BC, Canada.: Canadian Nuclear Society.)

Gidropress. 2008. Reactor plant for NPP WWER- 1000. http://www.gidropress.podolsk.ru/file s/booklets/en/wwer1000_en.pdf Date of access: 13 November. 2015.

Giust, F.D. 2012. Appraisal of Core Analysis Methods against Zer-Power Experiments on Full-Scale BWR Fuel Assemblies. Suisse: ÉCOLE POLYTECHNIQUE FÉDÉRALE DE LAUSAN NE. (PhD Thesis).

Goldberg, S.M, Rosner R. 2011. Nuclear Reactors: Generation to Generation. Cambridge, MA: American Academy of Arts and Sciences.

IAEA. 2003. Analysis of Difference in Fuel Safety Criteria for WWER and Western PWR Nucl ear Power Plants. IAEA- TECDOC- 1381. Vienna, Austria: International Atomic Energy Agency.

IAEA. 2003. Safety margins of operating reactors Analysis of uncertanties and implications f-or decision making. IAEA- TECDOC- 1332. Vienna,Austria:International Atomic Energy Age ncy.

IAEA. 2006. Current Trends in Nuclear Fuel for Power Reactors. https://www.iaea.org/About /Policy/GC/GC51/GC51InfDocuments/English/gc51inf-3-att5_en.pdf Date of access: 13 November. 2015.

Jahanbin, A. & Malmir, H. 2011. Kinetic parameters evaluation of PWRs using static cell and core calculation codes. *Annals of Nuclear energy*, 41(2012):2-6.

Katona, T.J. 2011. Long- term Operations of VVER Power Plants. http://cdn.intechopen.com/ pdfs-wm/19673.pdf Date of access: 13 November. 2015.

Larkin, J. 2011. larkinweb. larkinweb.co.uk/science/standard_deviations.html Date of access: 13 November. 2015.

Leppanen, J. 2015. Serpent-A Continuous-Energy Monte Carlo Reactor Physics Burn-up Calculation Code. Finland: VTT Technical Research Centre of Finland. (User's Manual).

Lewis, E.E. 2008. Fundamentals of Nuclear Reactor Physics. California, USA: Elsevier.

Lotsch, T., Khalimonchuk, V. & Kuchin, A. 2009. Proposal of a Benchmark for core burnup calculations for a VVER- 1000 reactor core. Munich: International Atomic Energy Agency. ht tp://www.iaea.org/inis/collection/NCLCollectionStore/_Public/41/035/41035568.pdf

Lotsch T, Khalimonchuk V, and Kuchin A. 2010. Correction and additions to the proposal of a benchmark for core burnup calculations for a VVER-1000 reactor. Munich: International Atomic Energy Agency. http://www.iaea.org/inis/collection/NCLCollectionStore/_Public/41/03 5/41035568.pdf

Lyon, R.B. 2005. WWER- 1000 Reactor Simulator (Material for Training courses and Worksh ops). Second ed. Vienna: IAEA.

Macdonald, R. 2012. Investigation of Improved Methods for Assessing Convergence of Mod els in MCNP using Shannon Entropy. Massachusetts: Massachusetts Institute of Technology . (Thesis).

Mahlers, Y.P. 2009. VVER- 100 Neutronics Calculation with ENDFB- VII data. *Annals of Nuc lear Energy*, 36(2009) 4 April.

Manassah, J.T. 1981. Alternative Energy Sources. London: Academic Press, Inc.

Michalek, S., Hascik, J. & Farkas G. 2003. Possibilities of Delayed Neutron Fraction Calculation and Measurement. Slovakia: International Atomic Energy Agency. http://www.iaea.org/inis/collection/NCLCollectionStore/_Public/40/059/40059715.pdf

Montwedi, E.O. 2014. Neutronic smulation of a European Pressurized Reactor. Potchefstroom: North-West University. (Master of Engineering dissertation).

Mourtzanos, K., Housiadas, C. & Antonoplous- Domis, M. 2000. Calculation of the moderator temperature coefficient of the reactivity for water moderated reactors. *Annals of Nuclear Energy*, 28(2001) 20 December.

Naicker, V.V., Du- Toit, M.H. & Nyalunga, G.P. 2015. NWURCS user guide. Potchefstroom: North-West University. (User Guide).

Oka, Y. 2010. Reactivity Characteristics. (*In*: Nuclear Reactor Design. Tokyo: Ohmsha,Ltd.).

Pazirandeh, A., Ghaseminejad, S. & Ghaseminejad, M. 2011. Effects of various spacer grid modelling on the neutronic parameters of the VVER- 1000 reactor. *Annals of Nuclear Energy*, 38(2011)

Pelowitz, D.B. 2013. MCNP6 USER'S MANUAL Version 1.0. LA- CP- 13- 00634, Rev. 0. (MCNP6 User's Manual).

Pirouzmand, A. 2014. VVER- 1000 Reactor Core Monitoring Using Ex- Core Neutron Detectors and Neural Networks. (*In* NuRER – 4. International Conference on Nuclear and Renewable Energy Resources. Antalya, TURKEY.)

Ponomarev, A., Travlee, A., Pfrang, W. & Sanchez, V. 2015. Coupled MCN- SAS- SFR Calculations for Sodium Fast Reactor core at Steady- State. (*In* Proceeding of ICAPP 2015. France: ICAPP.)

Prof. Dr. Saygin, H. 2011. Appendix II: Water Cooled Water Moderated Reactor and Its Evolutionary Designs. http://edam.org.tr/document/EDAMNukleer/NuclearReport2011_EN/appendix2.pdf Date of access: 13 April. 2016.

Rineiski, N. 12- 15 September. 2011. Fast neutron reactor: Principal features and experience. Varenna, Italy. www.kit.edu

Risovany, V.D, Varlashova, E.E. & Suslov, D.N. 2000. Dysprosium titanate as an absorber material for control rods. *Journal* of nuclear materials, 281(2000):84- 89. www.elsevier.nl/locate/jnucmat.

Saidi, P., Sadeghi, M. & Tenreiro, C. 2013. Variance Reduction of Monte Carlo Simulation in Nuclear Engineering field. InTech. http://www.intechopen.com/books/theory-and-applications-of-monte-carlo-simulations/variance-reduction-of-monte-carlo-simulation-in-nuclear-engineering-field

Schwarz, A.L., Schwarz, R.A. & Carter, L.L. 2011. MCNP/MCNPX Visual Editor Computer code manual. Vised Version 24E. (MCNP Visual Editor Manual).

Shultis, J.K. 2008. An MCNP primer. Manhattan: Kansas State University. (Manual).

Stacey, W.M. 2007. Nuclear Reactor Physics. 2nd ed. Atlanta USA: Wiley-VCH.

Thilagan, L., Sunil Sunny, C. & Subbaiah, K.V. 2007. Doppler Coefficient of Reactivity- Benchmark Calculations for Different enrichment of UO2. (*In* Joint International Topical Meeting on Mathematics & Computation and Supercomputing in Nuclear Applications. California.)

USNRC, HRTD. Westinghouse Technology Systems Manual. , Rev 1208

van der Merwe, W.J.S. 2013. NWU High Performance Computing (HPC). Potchefstroom: North-West University. (Power Point).

X- 5 Monte Carlo, Team. 2013. MCNP A General Monte Carlo N- Particle Transport Code, Version5 user guide. LA-UR-03-1987. (Manual).

X- 5 Monte Carlo, Team. 2003. MCNP A General Monte Carlo N- Particle Transport Code, Version5 Overview and theory. LA-UR-03-1987. (Manual).

7. Annexures

7.1. Annexure A

The dimensions of the reflectors that are found in the reactor core are given in Table 7-1

Table 7-1: Specification for Reflectors

Radial Reflector	
Material of layer 1	Steel
Inner radius of layer 1 (cm)	158.2
Outer radius of layer 1 (cm)	162.2
Material of layer 2	Moderator-Steel
Outer radius of layer 2 (cm)	173.5
Material of layer 3	Moderator
Outer radius of layer 3 (cm)	174.5
Material of layer 4	Steel
Outer radius of layer 4 (cm)	180.5
Material of layer 5	Moderator
Outer radius of layer 5 (cm)	206.95
Material of layer 6	Steel
Outer radius of layer 6 (cm)	226.75
Axial bottom reflector	
Material of layer 1	Moderator-Steel-Zircaloy
Inner radius of layer1 (cm)	177.5
Outer radius of layer1 (cm)	179.8
Material of layer 2	Moderator-Steel-Zircaloy
Outer radius of layer 2 (cm)	181.5
Material of layer 3	Moderator-Steel
Outer radius of layer 3 (cm)	206.5
Axial top reflector	
Material of layer 1	Moderator-Steel-Zircaloy
Inner radius of layer 1 (cm)	177.5
Outer radius of layer 1 (cm)	199.7
Material of layer 2	Moderator-Steel-Zircaloy
Outer radius of layer 2 (cm)	204.2
Material of layer 3	Moderator-Steel
Outer radius of layer 3 (cm)	209.7

The 1/6th core of a VVER-1000 is demonstrated in Figure 7-1.

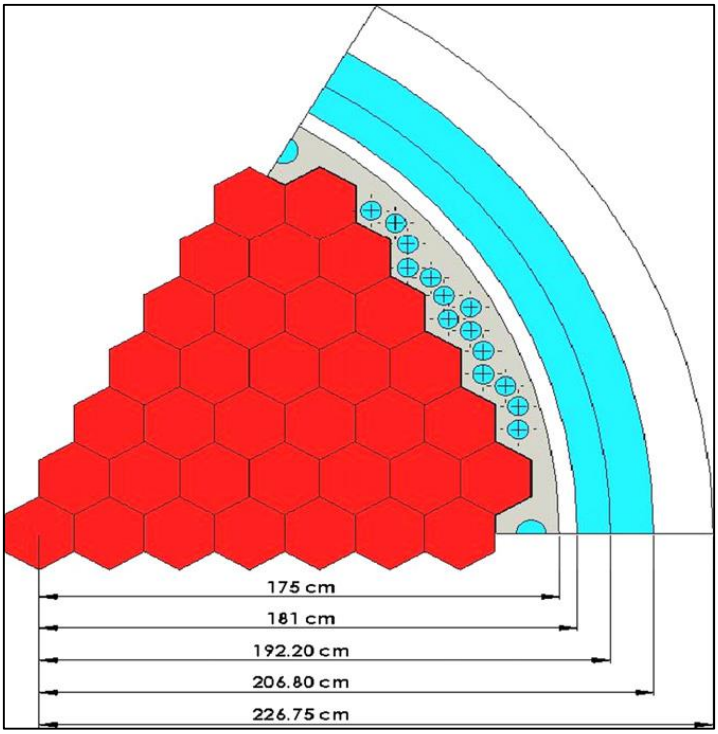

Figure 7-1: a 1/6th core with the display of the radial reflector (Pazirandeh, et al., 2011)

The reference core layout of the VVER-1000 is represented in Figure 7-2.

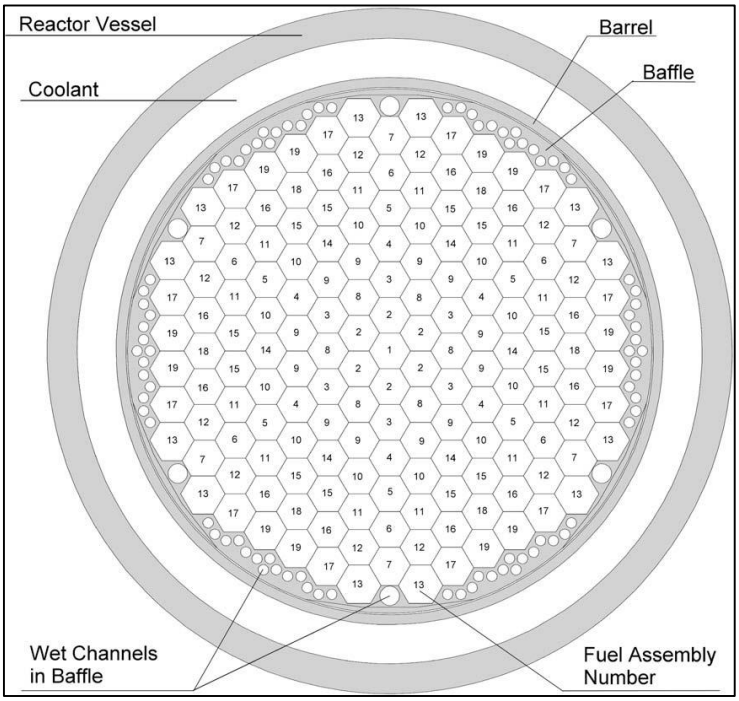

Figure 7-2: VVER reactor core configuration (Mahlers, 2009)

7.2. Annexure B

An overview of the geometry description for MCNP6 as provided by the NWURCS code is given below (Naicker, et al., 2015).

The reactor core together with the core barrel, core baffle, reflectors and RPV can be visualised as a system in which structures are placed inside other structures.

Taking the VVER-1000 as an example (with hexagonal geometry), this can be specifically stated as follows:

- The RPV encloses the core, reflectors, core baffle and core barrel.
- The core in turn is a lattice consisting of fuel assemblies.
- Each FA consists of a lattice arrangement of fuel pins, control rods and an instrumentation pin with their surrounding water hexagons
- Finally, the fuel pin consists of concentric cylindrical structures, namely, the annular ring, fuel pellet, the gap and the cladding. Similar structures also exist for the control rods and the instrument pins.

This description can be formulated in MCNP6 geometry as nested universes with appropriate lattice and cell definitions. In particular there are five nested universes, which are labeled as universes of level 1, 2, 3, 4, and 5 in NWURCS code (Naicker, et al., 2015).

The universe of level 0 contains a cell definition for the RPV as shown in Figure 7-4. Also in universe level 0 is the cell that contains the core, side reflectors, top reflectors, and bottom reflectors. This cell is filled using the “fill” command, with universes from universe level 1. The sample definition of the universe of level 0 in the MCNP input file is given in Figure 7-3.

```
c Universe RPV
100001     0              ((-64 -66  65):-62:-63)        imp:n=1 u=    0
         fill =    1
100002     1  0.084804 #100001 ((-69 -66  65):-67:-68)   imp:n=1 u=    0
         tmp= 2.585E-08     $   300.0000 K     26.8500 deg C
100003     0  #100001 #100002                             imp:n=0 u=    0
```

Figure 7-3: Universe 0

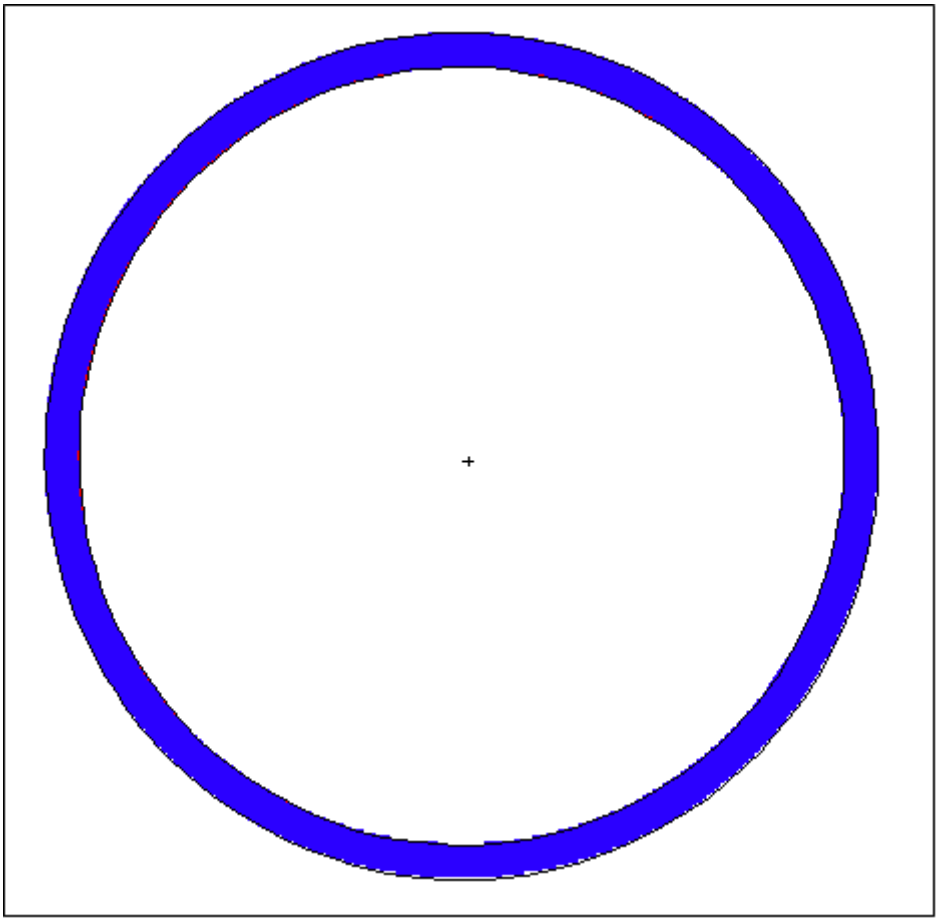

Figure 7-4: RPV only

At universe level 1, cells are defined to contain the core and reflectors which are of the lattice type. These are all separate cells and these cells are filled using the “FILL” command with the universes of level 2, as shown in Figure 7-5.

Also at universe level 1, are those reflectors which are homogenous. However, these are defined as “cells” as seen in Figure 7-6 and Figure 7-7.

```
c Universe Level 1
100004     0           (-56  -2   1)                    imp:n=1 u=    1
         fill=     2
100005     0           (-56  -3   2)                    imp:n=1 u=    1
         fill=     3
100006     0           (-56  -4   3)                    imp:n=1 u=    1
         fill=     4
100007     0           (-56  -5   4)                    imp:n=1 u=    1
         fill=     5
100008     0           (-56  -6   5)                    imp:n=1 u=    1
         fill=     6
100009     0           (-56  -7   6)                    imp:n=1 u=    1
         fill=     7
100010     0           (-56  -8   7)                    imp:n=1 u=    1
         fill=     8
100011     0           (-56  -9   8)                    imp:n=1 u=    1
         fill=     9
100012     0           (-56 -10   9)                    imp:n=1 u=    1
         fill=    10
100013     0           (-56 -11  10)                    imp:n=1 u=    1
         fill=    11
100014     0           (-56 -12  11)                    imp:n=1 u=    1
         fill=    12
100015     0           (-56 -13  12)                    imp:n=1 u=    1
         fill=    13
```

Figure 7-5: Universes of level 1

```
c bottom reflector
100016       2   0.109795  -56  -1  14                    imp:n=1 u=    1
      tmp= 2.585E-08     $   300.0000 K     26.8500 deg C
c bottom reflector
100017       3   0.109795  -56 -14  15                    imp:n=1 u=    1
      tmp= 2.585E-08     $   300.0000 K     26.8500 deg C
c bottom reflector
100018       4   0.109795  -56 -15  16                    imp:n=1 u=    1
      tmp= 2.585E-08     $   300.0000 K     26.8500 deg C
c top reflector
100019       5   0.109795  -56 -17  13                    imp:n=1 u=    1
      tmp= 2.585E-08     $   300.0000 K     26.8500 deg C
c top reflector
100020       6   0.109795  -56 -18  17                    imp:n=1 u=    1
      tmp= 2.585E-08     $   300.0000 K     26.8500 deg C
c top reflector
100021       7   0.109795  -56 -19  18                    imp:n=1 u=    1
      tmp= 2.585E-08     $   300.0000 K     26.8500 deg C
c side reflector(s)
100022       1   0.084804   -57   56  -75   74           imp:n=1 u=    1
      tmp= 2.585E-08     $   300.0000 K     26.8500 deg C
100023       8   0.171628   -58   57  -75   74           imp:n=1 u=    1
      tmp= 2.585E-08     $   300.0000 K     26.8500 deg C
100024       9   0.109795   -59   58  -75   74           imp:n=1 u=    1
      tmp= 2.585E-08     $   300.0000 K     26.8500 deg C
100025       1   0.084804   -60   59  -75   74           imp:n=1 u=    1
      tmp= 2.585E-08     $   300.0000 K     26.8500 deg C
100026       9   0.109795   -61   60  -75   74           imp:n=1 u=    1
      tmp= 2.585E-08     $   300.0000 K     26.8500 deg C
```

Figure 7-6: Reflectors

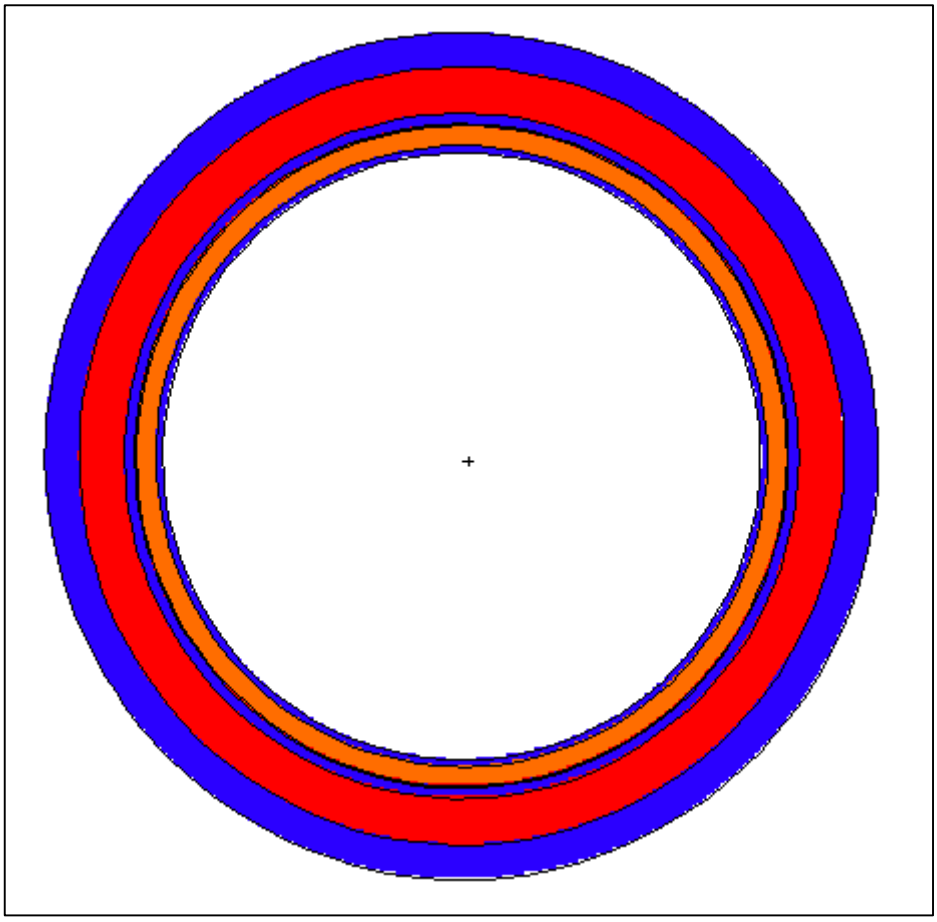

Figure 7-7: Radial view of the RPV and reflectors

The universe of level 2 contains the core layout description. The FAs in the core are not identical. The core layout description, which is a 2-D map, defines the positions of the different types of the FAs in the core, as seen in the sample input of Figure 7-8 below. The configuration of the FAs produced is given in Figure 7-9.

```
c Universe Level 2 axial level -6
100028     0            -21                                  imp:n=1 u=    2
         lat=2  fill=-10: 10 -10: 10   0:  0
          14    14    14    14    14    14    14    14   147   168
         189   210   231   252   272   291   309   326   342   357
         371
          14    14    14    14    14    14    14   127   148   169
         190   211   232   253   273   292   310   327   343   358
         372
          14    14    14    14    14    14   108   128   149   170
         191   212   233   254   274   293   311   328   344   359
         373
          14    14    14    14    14    90   109   129   150   171
         192   213   234   255   275   294   312   329   345   360
         374
          14    14    14    14    73    91   110   130   151   172
         193   214   235   256   276   295   313   330   346   361
         375
          14    14    14    57    74    92   111   131   152   173
         194   215   236   257   277   296   314   331   347   362
         376
          14    14    42    58    75    93   112   132   153   174
         195   216   237   258   278   297   315   332   348   363
         377
```

Figure 7-8: Universe level 2

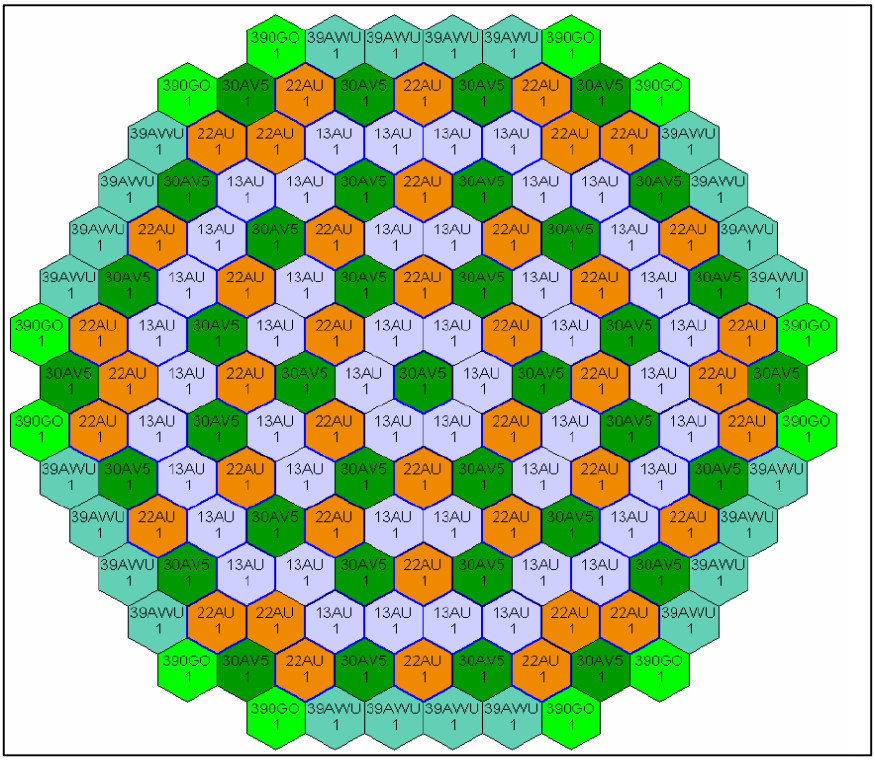

Figure 7-9: Fuel assembly layout

The universes of level 2 are filled with the “FILL” command, with universes of level 4. However, an intermediate universe of level 3 is required as a placeholder (shown in Figure 7-10) so that each universe of level 4 can be accommodated in the universes of level 2.

```
c ------------------------------------------------------------------------
c universe level 3 core node ijk  -7  1 -6
c fuel block
100201     0            -21                                imp:n=1 u=  213
       fill= 4479
100202     0
     #100201
                                                           imp:n=0 u=  213
c ------------------------------------------------------------------------
```

Figure 7-10: Universe level 3

Universe of level 4 contains the rod type layout description. In particular, the fuel assembly consists of three rod types. The rod type layout description defines the positions of the different types of rod types in the fuel assembly, as seen in Figure 7-11 and Figure 7-12

```
c universe level 4 - fuel node
100203     0             -20                    imp:n=1 u= 4479
       lat=2  fill= -11: 11 -11: 11   0:  0
      4483  4483  4483  4483  4483  4483  4483  4483  4483  4483  4483  4483  4483  4483  4483  4483  4483  4483  4483  4483  4483  4483  4483
      4483  4483  4483  4483  4483  4483  4483  4483  4483  4483  4483  4484  4484  4484  4484  4484  4484  4484  4484  4484  4484  4484  4483
      4483  4483  4483  4483  4483  4483  4483  4483  4483  4483  4484  4484  4480  4480  4480  4480  4480  4480  4480  4480  4484  4484  4483
      4483  4483  4483  4483  4483  4483  4483  4483  4483  4484  4480  4480  4480  4480  4480  4480  4480  4480  4480  4480  4480  4484  4483
      4483  4483  4483  4483  4483  4483  4483  4483  4484  4480  4480  4480  4480  4480  4480  4480  4480  4480  4480  4480  4480  4484  4483
      4483  4483  4483  4483  4483  4483  4483  4484  4480  4480  4480  4480  4480  4480  4481  4480  4480  4480  4480  4480  4480  4484  4483
      4483  4483  4483  4483  4483  4483  4484  4480  4480  4480  4480  4480  4480  4481  4480  4480  4480  4480  4481  4480  4480  4480  4483
      4483  4483  4483  4483  4483  4484  4480  4480  4480  4480  4480  4480  4480  4480  4480  4485  4480  4480  4480  4480  4480  4484  4483
      4483  4483  4483  4483  4484  4480  4480  4480  4481  4480  4485  4480  4481  4480  4480  4480  4480  4481  4480  4480  4480  4484  4483
      4483  4483  4483  4484  4480  4480  4480  4480  4480  4480  4480  4480  4480  4480  4480  4481  4480  4480  4480  4480  4480  4484  4483
      4483  4483  4484  4480  4480  4480  4480  4480  4480  4481  4480  4480  4480  4480  4480  4480  4485  4480  4480  4480  4480  4484  4483
      4483  4484  4484  4480  4480  4480  4481  4480  4480  4480  4480  4482  4480  4480  4480  4480  4481  4480  4480  4480  4484  4484  4483
      4483  4484  4480  4480  4480  4480  4480  4485  4480  4480  4480  4480  4480  4481  4480  4480  4480  4480  4480  4480  4484  4483  4483
      4483  4484  4480  4480  4480  4480  4480  4480  4481  4480  4480  4480  4480  4480  4480  4480  4480  4480  4480  4480  4484  4483  4483
      4483  4484  4480  4480  4480  4481  4480  4480  4480  4480  4481  4480  4485  4480  4481  4480  4480  4480  4484  4483  4483  4483  4483
      4483  4484  4480  4480  4480  4480  4480  4480  4485  4480  4480  4480  4480  4480  4480  4480  4480  4480  4484  4483  4483  4483  4483
      4483  4484  4480  4480  4480  4480  4481  4480  4480  4480  4480  4481  4480  4480  4480  4480  4484  4483  4483  4483  4483  4483  4483
      4483  4484  4480  4480  4480  4480  4480  4480  4481  4480  4480  4480  4480  4480  4480  4480  4484  4483  4483  4483  4483  4483  4483
      4483  4484  4480  4480  4480  4480  4480  4480  4480  4480  4480  4480  4480  4480  4480  4484  4483  4483  4483  4483  4483  4483  4483
      4483  4484  4480  4480  4480  4480  4480  4480  4480  4480  4480  4480  4480  4480  4484  4483  4483  4483  4483  4483  4483  4483  4483
      4483  4484  4484  4480  4480  4480  4480  4480  4480  4480  4480  4484  4484  4483  4483  4483  4483  4483  4483  4483  4483  4483  4483
      4483  4484  4484  4484  4484  4484  4484  4484  4484  4484  4484  4484  4483  4483  4483  4483  4483  4483  4483  4483  4483  4483  4483
      4483  4483  4483  4483  4483  4483  4483  4483  4483  4483  4483  4483  4483  4483  4483  4483  4483  4483  4483  4483  4483  4483  4483
```

Figure 7-11: Universe level 4

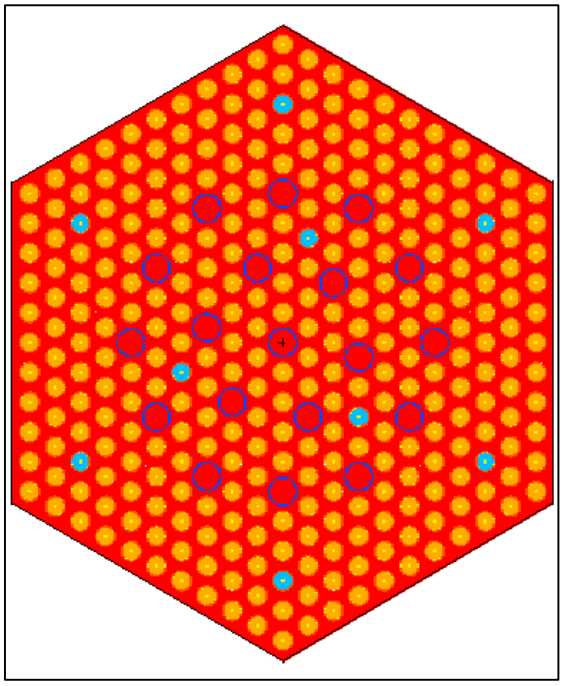

Figure 7-12: Fuel assembly

The fuel assembly consists of a lattice of fuel pins. Therefore, universes of level 4 are filled using the “FILL” command with universes of level 5. Universes of level 5 are the innermost level. These universes will contain only cell definitions. These cells are the fuel pellet, gap, cladding, water hexagons and spacer grids, as seen in Figure 7-13

```
c universe Level 5
100204      10   0.000026  -81       -77    1            imp:n=1 u= 4480
          tmp= 2.585E-08     $   300.0000 K     26.8500 deg C
100205      11   0.069459  -82   81  -77    1            imp:n=1 u= 4480
          tmp= 2.585E-08     $   300.0000 K     26.8500 deg C
100206      10   0.000026  -83   82  -77    1            imp:n=1 u= 4480
          tmp= 2.585E-08     $   300.0000 K     26.8500 deg C
100207      12   0.042589  -84   83  -77    1            imp:n=1 u= 4480
          tmp= 2.585E-08     $   300.0000 K     26.8500 deg C
100208       9   0.109795  -85   84  -77    1            imp:n=1 u= 4480
          tmp= 2.585E-08     $   300.0000 K     26.8500 deg C
100209      13   0.043264  -88   87                       imp:n=1 u= 4480
          tmp= 2.585E-08     $   300.0000 K     26.8500 deg C
100210       9   0.109795  -91   90                       imp:n=1 u= 4480
          tmp= 2.585E-08     $   300.0000 K     26.8500 deg C
100211      13   0.043264  -93   92                       imp:n=1 u= 4480
          tmp= 2.585E-08     $   300.0000 K     26.8500 deg C
100212      0
     #100204 #100205 #100206 #100207 #100208 #100209 #100210 #100211
                                                          imp:n=0 u= 4480
```

Figure 7-13: Universe level 5

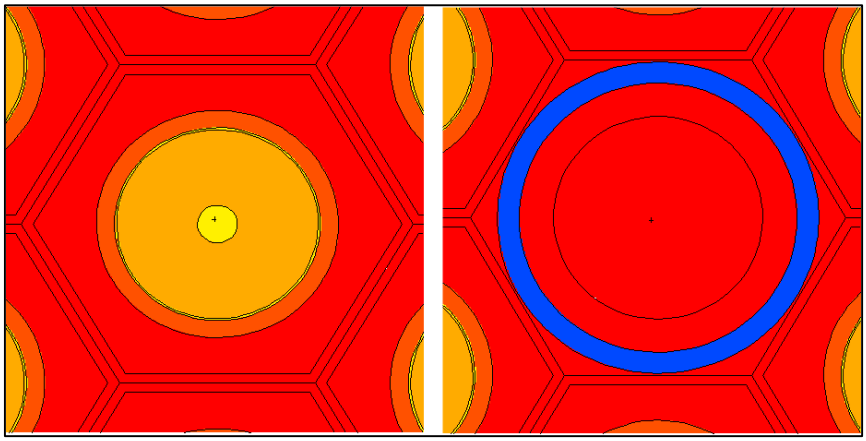

Figure 7-14: Rod type

The surfaces and material definition that are involved in the sample input as seen in Figure 7-13 are given in Figure 7-15 and Figure 7-17. Figure 7-16 contains a sample definition of the KCODE card.

```
  1 pz      -176.50000
 77 pz      -147.08300
 81 cz         0.07500
 82 cz         0.37850
 83 cz         0.38650
 84 cz         0.45500
 85 rhp        0.00000     0.00000 -176.50000
                0.00000     0.00000   29.41700
                0.60000     0.00000    0.00000
 87 rhp        0.00000     0.00000 -176.50000
                0.00000     0.00000    3.00000
                0.60000     0.00000    0.00000
 88 rhp        0.00000     0.00000 -176.50000
                0.00000     0.00000    3.00000
                0.63850     0.00000    0.00000
 90 rhp        0.00000     0.00000 -173.50000
                0.00000     0.00000   26.16700
                0.60000     0.00000    0.00000
 91 rhp        0.00000     0.00000 -173.50000
                0.00000     0.00000   26.16700
                0.63850     0.00000    0.00000
 92 rhp        0.00000     0.00000 -147.33300
                0.00000     0.00000    0.25000
                0.60000     0.00000    0.00000
 93 rhp        0.00000     0.00000 -147.33300
                0.00000     0.00000    0.25000
                0.63850     0.00000    0.00000
```

Figure 7-15: Surface definition

```
kcode  800000 1.0  300  800
ksrc            0.000      0.000   -161.792
                0.000      0.000   -132.375
                0.000      0.000   -102.958
                0.000      0.000    -73.542
                0.000      0.000    -44.125
                0.000      0.000    -14.708
                0.000      0.000     14.708
                0.000      0.000     44.125
                0.000      0.000     73.542
                0.000      0.000    102.958
                0.000      0.000    132.375
                0.000      0.000    161.792
```

Figure 7-16: KCODE card

```
c water___
m9
      1001.80c 6.6537E-01
      1002.80c 9.9820E-05
      8016.80c 3.3369E-01
      8017.80c 1.2718E-04
      5010.80c 1.4302E-04
      5011.80c 5.7568E-04
mt9      lwtr.20t
c helium__
m10
      2004.80c 1.0000E+00
c   fuel24
m11
      8016.80c 6.6641E-01
      8017.80c 2.5400E-04
     92235.80c 1.3497E-02
     92238.80c 3.1984E-01
mt11     o2/u.20t u/o2.20t
c E110
m12
     40090.80c 5.0945E-01
     40091.80c 1.1110E-01
     40092.80c 1.6981E-01
     40094.80c 1.7209E-01
     40096.80c 2.7725E-02
     41093.80c 9.8230E-03
c E635
m13
     26054.80c 8.6000E-05
     26056.80c 1.4140E-03
     26057.80c 3.5000E-05
     26058.80c 4.0000E-06
     40090.80c 5.0864E-01
     40091.80c 1.1092E-01
     40092.80c 1.6955E-01
     40094.80c 1.7182E-01
     40096.80c 2.7681E-02
     41093.80c 9.8570E-03
```

Figure 7-17: Materials definition